# Congenital learned helplessness: Synaptic protein concentrations in resilient and susceptible rats

Annika Utz

Master's thesis in Neuroscience

Supervisor: Svend Davanger

Internal supervisor: Linda White

Norwegian University of Science and Technology
Faculty of Medicine

University of Oslo
Faculty of Medicine

Trondheim, August 2017

## Acknowledgements

The present work was conducted at the Division for Anatomy, Institute of Basic Medical Sciences, Faculty of Medicine, University of Oslo (UiO).

I want to thank my supervisor Svend Davanger for his help, advice and encouragement throughout this project. I also want to thank the members of his group, Hårvard Ringsevjen, Suleman Hussain and Daniel Egbenya for helping me with the western blot technique, and for giving me advice on how to improve my western blot technique. My sincere thanks also go to Grazyna Babinska and Marianne Vaadal for their help in keeping my experiments running.

I am thankful to the nice group members of the 'neighbor' group, who gave me advice and helped me, whenever possible, Muhammad Umar Sajjad, Gro Presthus, Aram Nikolai Andersen and Katharina Dietrich.

I also want to thank Camilla Hagen, with whom I shared an office and all the ups and downs we encountered during this year. Finally, I want to thank my family and friends, for their support and help.

## Abstract

Hippocrates proposed that mental health is based on the balance of four bodily fluids, blood, black bile, yellow bile and phlegm. This theory of humorism has been discarded, but the idea, of physical changes accompanying psychological disorders still applies. Depression is fortunately no longer viewed as an excess of black bile. Nevertheless, how neurophysiology differs in depressed brains, compared to healthy ones, is still poorly investigated. Glutamatergic synapses, which provide the main excitatory input to neurons, might be implicated in depressive disorders. Ample evidence of glutamatergic dysfunction in depressed patients has been found in the hippocampus and prefrontal cortex. In addition, findings from resting state functional connectivity analyses implicate the anterior cingulate cortex (ACC) in depressive disorders. To analyze glutamatergic changes in the ACC in depression, relative concentrations of proteins with important functions in glutamatergic synapses were studied in an animal depression model. Two strains were compared, congenital helpless rats (cLH) and congenital non-helpless rats (cNLH). Additionally, the hippocampus was analyzed as a positive control, and the primary motor and somatosensory cortices as a negative controls. Surprisingly, the main difference between the two strains was found in the primary motor cortex. Here, a higher concentration of PSD95 was measured in cLH animals compared to cNLH. This increased concentration might be linked to a symptom of depressive disorders, namely psychomotor retardation.

**1 INTRODUCTION ..... 6**

1.1 Depression in humans ..... 6
1.2 The anterior cingulate cortex ..... 7
1.3 Rodent depression model: Congenital learned helplessness ..... 10
1.4 The neuroplasticity hypothesis ..... 12
1.5 Proteins of interest ..... 16
1.6 Aims ..... 17

**2 MATERIAL AND METHODS ..... 18**

2.1 Animals ..... 18
2.2 Learned Helplessness Procedure ..... 18
2.3 Dissection of Regions of Interest (ROI) ..... 20
2.4 Sample Preparation ..... 21
2.5 Immunoblotting ..... 22
2.6 Stripping of membranes ..... 25
2.7 Antibodies ..... 25
2.8 Blot design ..... 26
2.9 Analysis ..... 26
2.10 Statistics ..... 27
2.11 Linearity of protein concentration and signal detection ..... 27

**3 RESULTS ..... 28**

3.1 Latencies of learned helplessness procedure ..... 28
3.2 Main findings ..... 29
3.3 Findings from ROI differences ..... 31
3.4 Total protein concentration – signal intensity relation of antibodies ..... 32

**4 DISCUSSION ..... 34**

4.1 Findings ..... 34
*PSD95 in the motor cortex ..... 34*
*Other proteins in the primary motor cortex ..... 36*
*GluA1/GluA2 ratio in the somatosensory cortex ..... 36*
*NR2A trend in the cingulate cortex ..... 38*
4.2 Limitations ..... 40
4.3 Evaluating findings ..... 45

**5 CONCLUSION ..... 46**

**6 APPENDIX ..... 47**

Appendix A ..... 47
Appendix B ..... 50
Appendix C ..... 60

**7 REFERENCES ..... 64**

## Abbreviations

| | |
|---|---|
| ACC | anterior cingulate cortex |
| AMPAR | α-amino-3-hydroxy-5-methyl-4-isoxazolepropionic acid receptor |
| C | cingulate cortex |
| CA1 | cornu ammonis 1 |
| Cg1 | cingulate cortex, area 1 |
| Cg2 | cingulate cortex, area 2 |
| cLH | congenital learned helpless |
| cNLH | congenital non-learned helpless |
| CUMS | chronic unpredictable mild stress |
| dACC | dorsal anterior cingulate cortex |
| DG | dentate gyrus |
| dlPFC | dorsolateral prefrontal cortex |
| EAAT | excitatory amino acid transporter |
| EC | entorhinal cortex |
| EPSC | excitatory post-synaptic current |
| FC | functional connectivity |
| fMRI | functional magnetic resonance imaging |
| FRL | Flinders Resistant Line |
| FSL | Flinders Sensitive Line |
| Glx | Glutamate and glutamine |
| H | hippocampus |
| LTD | long-term depression |
| LTP | long-term potentiation |
| M1 | primary motor cortex |
| MDD | major depressive disorder |
| mPFC | medial prefrontal cortex |
| NMDAR | N-methyl-D-aspartate receptor |
| PCC | posterior cingulate cortex |
| PET | positron emission tomography |
| PPC | posterior parietal cortex |
| PSD95 | post-synaptic density 95 |
| qPCR | quantitative polymerase chain reaction |
| ROI | regions of interest |
| Rsp | retrosplenial cortex |
| S1 | primary somatosensory cortex |
| SNAP25 | Synaptosomal-associated protein 25 |
| SNARE | Soluble NSF Attachment Protein Receptors |
| TMS | transcranial magnetic stimulation |
| vACC | ventral anterior cingulate cortex |
| VAMP2 | Vesicle-associated membrane protein 2 |
| VGLUT | vesicular glutamate receptor |
| vmPFC | ventromedial prefrontal cortex |

# 1 Introduction

## 1.1 Depression in humans

Depression is the leading cause of disability worldwide[7]. The one-year prevalence of depression alone is 3.2 %[8], while the lifetime prevalence is estimated at 16.2 %[9]. Depression is often comorbid with other diseases like Parkinson's disease[10], Alzheimer's disease[11], diabetes[12] and anxiety[8, 13]. Its heritability is estimated to be 37 %[14]. Treatment outcome is still poor[9]. Diagnosing depression, and its severity, has to be based on personal interviews and questionnaires[15].

*Symptoms of depression*

Depression is seen as a disorder, as it is expressed in multiple ways and can have different causes[15]. Symptoms of a major depressive episode are depressed mood, loss of interest or pleasure in almost all activities (anhedonia), weight loss or gain, insomnia or hypersomnia, psychomotor agitation or retardation, fatigue or loss of energy, feelings of worthlessness or inappropriate guilt, concentration difficulties and suicidal thoughts. When diagnosing a person with a major depressive episode at least five of these symptoms have to apply, while one of the symptoms has to be anhedonia or depressed mood[16]. However, some of the behavioral symptoms used to define a major depressive episode are opposing, as weight loss or weight gain are both included. Biological markers for depressive disorders could help to diagnose depression more quickly and make the identification of different subtypes more precise than what is possible when relying on behavioral symptoms alone. To investigate depression, brain imaging techniques, like functional magnetic resonance imaging (fMRI) and positron emission tomography (PET), are commonly used. Differences between depressed and healthy subjects can often be seen during resting state, when analyzing functional connectivity.

*The resting-state network in depression*

The most easily accessible brain data about depressive patients are fMRI studies, which often focus on network changes, especially in resting state functional connectivity (FC). Some progress has already been made in diagnosing major depressive disorder (MDD) with the help of an FC analysis by measuring resting state activity[17, 18]. Regions consistently implicated in the resting-state network are the posterior cingulate cortex/retrosplenial cortex (PCC/Rsp), the ventromedial prefrontal cortex (vmPFC) and the hippocampal formation[19]. The ventral anterior cingulate cortex (ACC) is also often activated during resting-state, but its connectivity with other regions does not resemble the functional connectivity network of the resting state network as well as the PCC does[20]. In general, an increase in FC within the resting-state network is observable in MDD patients compared to controls[21, 22], which is also more static over time[23].

The FC between the ACC and the medial temporal lobe is increased in MDD patients and correlates with symptom severity[24]. The left ACC also shows a higher FC with the dorsolateral prefrontal cortex (dlPFC) [25], the strength of which is positively correlated with depressive symptom severity as well[26]. Decreased regional blood flow in depressed patients was measured at resting state in the right ACC[27]. While treatment of MDD normalizes FC of the PCC, the more anterior parts of the resting-state network, including the ACC, fail to normalize in their connectivity.[28] Next, I will review the ACC's implied function and structural connections to understand what its altered activity and functional connectivity implicates for depression.

## 1.2 The anterior cingulate cortex

Paxino divides the anterior part of the cingulate cortex in rats into infralimbic, prelimbic and limbic (Cg1 and Cg2) regions[29]. It comprises Brodmann Area 32, 24a, 24b and 25[30]. In more recent studies, Cg1 and Cg2 are called dorsal ACC (dACC) and ventral ACC (vACC, fig. 1.1)[31]. In MDD patients, the ACC shows decreased volume compared with healthy controls[32] and a decrease in cortical thickness of the rostral ACC[33]. Lesions of the rostral ACC also lead to depressive-like behavior in rats[34].

*Functions of the ACC*

The functions of the ACC are numerous: This region has been implicated in movement planning, decision making and memory[35]. Stimulation of the ACC in humans can lead to execution of more or less complex movements and different emotions[36]. Removal of the ACC can result in a reduction of the subjective feeling of pain in patients with chronic pain disorder[37]. In psychiatric patients, cingulectomy resulted most of the time in a reduction of anxiety and obsessiveness. Two patients also showed less interest in challenging literature, while before the surgery both had been interested readers[38]. In the light of hallmarks of depression, this could point towards the ACC being involved in hedonic behavior and motivation[35]. Depressive patients also show impairments in decision making[39], in which the ACC seems to be implicated as well[40].

The ACC is particularly implicated in decisions based on effort-reward ratio[41] and made by free will[42]. A study compared effort-reward choices in a T-maze before and after a lesion of the mPFC that included the regions Cg1 and Cg2. Before lesion, rats had mostly chosen the arm with the high effort and high reward. After the lesion, the rats changed their behavior and chose the low-effort-low-reward arm. When increasing the reward difference between the two choices and decreasing the effort, lesioned rats started to opt for the high reward again, although effort was still higher compared to the low-reward arm[41], thus showing that rats still were able to make an effort, but the reward for the same effort had to be increased. Hence,

the rat needed more motivation (the reward) to make the same effort, after the lesioning compared to before.

The ACC projects and receives projections from numerous brain regions[43, 44]. In the following, a short overview is given of the regions investigated in this thesis.

*Connections between ACC, hippocampus and primary cortices*

Structural connectivity has been analyzed in detail in rodents. The ACC has reciprocal connections to the medial agranular frontal cortex, which includes the primary motor cortex, but also parts of the secondary motor cortex[44]. More precisely, The ACC projects to forelimb and orofacial regions of the primary motor cortex[45]. The ACC receives projections from the secondary somatosensory cortex, but no direct input from the primary somatosensory cortex. A study also found afferents to the ACC from the CA1 (*cornu ammonis*) of the hippocampus[44].

Direct projections from the ACC to the hippocampal formation are not present. ACC projects mainly to subiculum and entorhinal cortex (EC). In the EC, most of the cingulate fibers terminate in deep layers, which also receive input from the hippocampal formation and project to neocortical and subcortical regions, in turn[46].

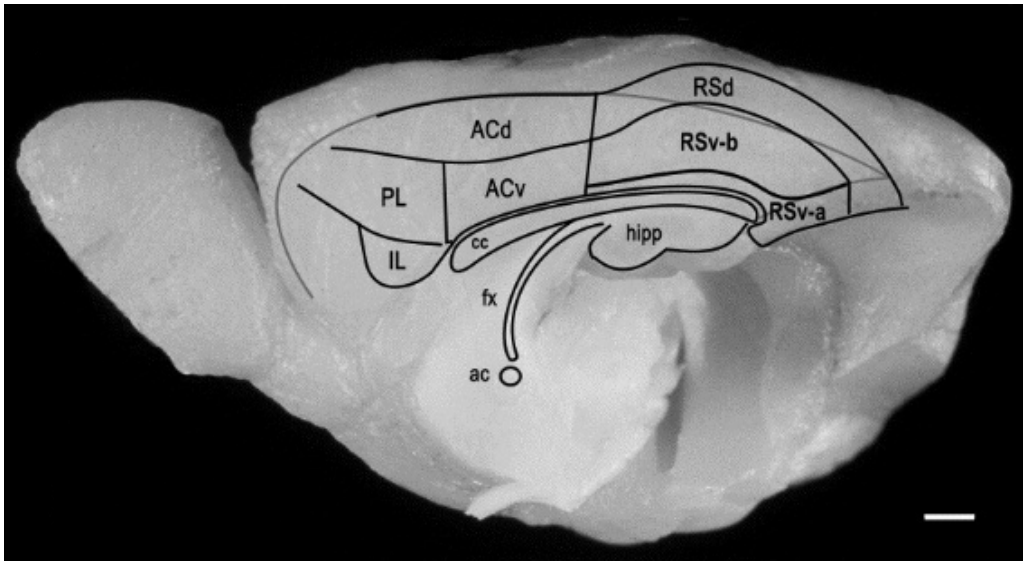


Figure 1.1 *Mid-sagittal view of the rat brain. Brain stem and cerebellum have been removed. Regions of the cingulate and retrosplenial cortex are marked. ac = anterior commissure, ACd= dorsal cingulate cortex (= dACC, Cg1), ACv = ventral cingulate cortex (= vACC, Cg2), cc = corpus callosum, fx = fornix, hipp = hippocampus, IL=infralimbic cortex, PL= pre-limbic cortex, , RSd = dorsal retrosplenial cortex, Rsv = ventral retrosplenial cortex (Scale bar 1 mm; retrieved from [47]).*

*Division of the ACC*

The ventral part of the ACC projects to the nucleus accumbens, periaqueductal gray and amygdala, while also receiving projections from the basolateral amygdala and the lateral hypothalamus[35, 43, 48]. Therefore, the ventral part is assumed to be more involved in affective functions. The dACC on the other hand is assumed to be more involved in cognitive functions. It has reciprocal connections with motor areas, the PFC and the striatum, and receives projections from the parietal cortex and midline thalamic nuclei[35, 48]. The sub-regions of the ACC are intrinsically connected, and project to the PCC[47].

Structural connectivity analyses are often done with injections of viruses. It would be unethical to do this in humans. The same holds true for stressing human subjects until they shows depression-like symptoms. Therefore, rats were used, as a model for depression. In the next section I will discuss the specifics of this model.

## 1.3 Rodent depression model: Congenital learned helplessness

There are several models of depression in animals. The congenital learned helplessness paradigm uses inescapable random shocks, which are applied to the animal from a metal grid floor, mostly rats or mice. To assess whether the rodent is helpless after the procedure, it is put back in the cage after 24 h. This time, the rodent has the possibility to end the shock by pressing a lever. In general, the animal is considered helpless if it does not press the lever in time to escape the shock. If the animal presses the lever quickly for a specific number of trials, it is considered resilient or non-helpless[49]. Mating the helpless rats with each other, as well as the non -helpless rats, for several generations, resulted in two strains: one which is more stress susceptible (congenital learned helpless = cLH) and one which is more stress resilient (congenital non-learned helpless = cNLH)[50]. They have been compared in several depression and anxiety tests to validate whether they can be used as a model for depression.

*Testing anhedonia*

Postulating that a rodent has a depressive disorder is not possible. However, depression symptoms can be deduced from behavioral tests. To test anhedonia, a central symptom of MDD, an animal's preference for sucrose over water is assessed. A control animal would prefer sucrose over water, as drinking a sucrose solution is more enjoyable than drinking water. Another sucrose test is how much effort an animal would make to get a pleasurable reward. In a progressive reward schedule animals have to press a lever to obtain a reward. The number of lever presses needed to obtain a reward increases over time. The final ratio of the number of lever presses and the amount of reward obtained is compared. The ratio was lower for cLH than cNLH rats, indicating that cLH rats gave up earlier than cNLH. With a fixed ratio schedule, where one drop of sucrose was given for each lever press, the number of lever presses was similar between the groups. Moreover, all rats had a reduction of 10 % in body weight prior to the experiments[51]. Food deprivation seems to be necessary for showing a significant difference between rats with depression-like symptoms and control rats in saccharin intake[52]. This makes it questionable, whether a lower ratio value represents anhedonic tendencies at all or whether this is a motivational issue. However, motivational deficits, called anergia, are also a key symptom of depression.

*Classifying the depressive disorder*

For the aforementioned study, rats showed depression symptoms, although no inescapable shock was applied. Showing symptoms without a stressor, resembles a model of chronic mild depression rather than major depressive disorder[51, 53]. However, increased resting-state network activity has also been found in patients with chronic mild depression, while antidepressant treatment could normalize the connectivity[54]. As this seems to be a consistent finding in depression it is worth looking at the resting-state network activity in rats, and changes in functional connectivity in the learned helpless model of depression.

*Resting-state network activity in rats*

In anesthetized rats a network resembling the human resting-state network has been found. Structures included the ACC, PCC, and hippocampal formation, as well as other regions implied in the human resting-state network. However, contrary to findings in humans[19], the whole of the cingulate cortex was active in rats, including the medial part[55]. Another study, investigating the resting-state network in rats, took the time to habituate the animal to the fMRI machine and measured FC at resting state in awake animals. They used the ACC as a seed region and found that it was functionally connected to the retrosplenial cortex, parietal cortex, temporal association cortex and hippocampus, while no activity in the medial part of the cingulate cortex was found[56]. Thus, a similar resting-state network seems to be present in rats. It can therefore be investigated whether animals with depression-like behavior show the same changes as patients with MDD.

*Resting-state network activity in rat depression models*

In a genetic animal model of depression, alterations in connectivity were found, resembling those found in MDD patients. FC analyses showed a higher FC of the hippocampus with the left frontal association cortex/dorsolateral orbital cortex, while decreased connectivity was found with the cingulate cortex (Cg1/Cg2)[57]. In cLH rats, connectivity in the hippocampal-frontal cortex network is enhanced. Cg1 showed lower connectivity with visceral motor structures, while Cg2 showed increased FC with the secondary motor cortex[58]. Changes in FC of the resting-state network are a consistent phenomenon in depressive patients, thus making it necessary to ensure that animal models of depression show a similar change. This will also make it easier to establish whether drugs tested for their anti-depressant effect in animal models will also work in humans. But to understand the changes seen in FC and how to normalize them, more knowledge about the molecular changes in depression are needed, as well as knowledge about how these changes might underlie depressive symptoms.

## 1.4 The neuroplasticity hypothesis

Iproniazid and imipramine were the first anti-depressants to be discovered. As these drugs manipulate the serotonergic and dopaminergic system in the brain, research on depression focused primarily on these systems, although treatment success remained poor[59]. New hypotheses have emerged, one of them being neuroplasticity hypothesis[60]. Naturally, changes in the depressed brain are not just restricted to serotonergic and dopaminergic neuronal populations and synapses. Changes in the glutamatergic system, which entails the majority of excitatory synapses in the brain, have been found consistently, as well[61, 62]. This change in synaptic plasticity can be a result of long-term potentiation (LTP), long-term depression (LTD; s. fig. 1.2) or homeostatic plasticity (s. fig. 1.3). There are, however, many other ways of changing a neuron's functioning and activity.

First, changes in humans with depressive disorders will be discussed. Then, congenital learned helpless rats as well as other learned helplessness models of depression will be discussed with a focus on glutamatergic changes.

*Glutamatergic synapses in the ACC of humans*

Glutamate serum levels are higher in depressed patients compared to healthy participants[63, 64], while treatment with anti-depressants decreases glutamate levels in serum[65].

However, the picture looks different in the ACC. Here, a decrease in glutamate levels has been shown in several studies[66, 67]. Another study, investigating expression levels of several proteins involved in glutamate signaling found decreased levels of post-synaptic density 95 (PSD95), a postsynaptic anchoring protein at excitatory synapses, in the ACC[68]. This decrease could be a result of a decrease in neuronal number in depression. However, studies about neuronal number are inconsistent. A post-mortem study found a decrease in density of pyramidal neurons in layer Vb of the ACC, while size was increased in layers V and VI[69]. Other studies found an increase in the number of neurons in layer 5, but with smaller somata[70], or no significant change in neuronal number[71]. The decrease in glutamatergic proteins could be due to a decrease in synaptic strength. Expression levels of α-amino-3-hydroxy-5-methyl-4-isoxazolepropionic acid receptor (AMPAR) subunits did not differ in MDD patients compared with controls[68], and increased AMPAR binding has been found in the ACC of depressed patients[72]. In summary, the ACC in depression is still an incomplete picture.

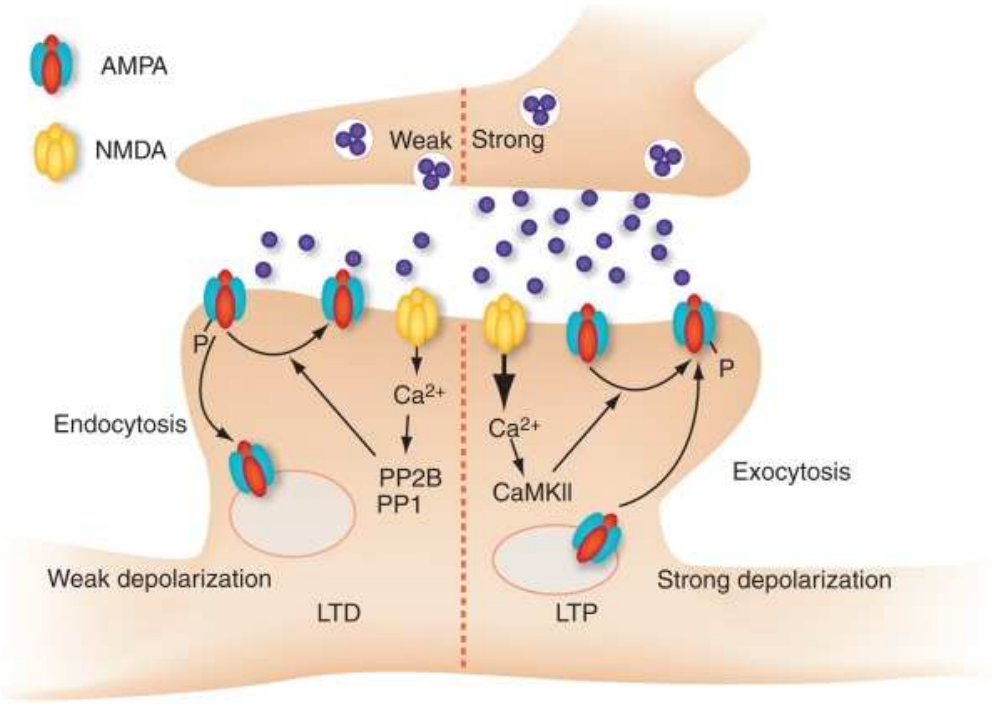


Figure 1.2 *(left side) LTD results in long-lasting weakening of synaptic connections. LTD can be induced artificially by long but low frequency stimulation (1-3 Hz for 5-15 minutes) of the presynaptic terminals. Stimulation of the presynaptic terminal, resembles action potentials arriving at the presynaptic terminal. This leads to an influx of calcium into the presynaptic terminal, which in turn, leads to exocytosis of presynaptic vesicles. Vesicles of glutamatergic neurons contain glutamate, which will be released into the synaptic cleft and can now bind to post-synaptic glutamate receptors. This leads to an influx of sodium through AMPARs, and of small amounts of calcium into the cell at the post-synaptic membrane due to NMDARs, which are not entirely blocked by magnesium[1]. Therefore, a small amount of calcium can pass the membrane through the NMDARs. Low calcium levels activate a phosphatase, calcineurin. Calcineurin has a relatively high affinity for calcium. Protein phosphatase 1 (PP1) is also activated due to a low influx of calcium. Both phosphatases can de-phosphorylate AMPAR subunits. This leads to a decrease in receptor conductance and AMPAR density at the post-synaptic membrane. AMPAR density at the post-synaptic membrane determines synaptic strength. A reduction in AMPARs therefore leads to weakening of the synapse[2, 3]. (right side) LTP on the other hand results in a strengthening of synapses. At resting potential of the post-synaptic membrane, NMDARs are blocked by magnesium. Binding of glutamate alone will not open NMDARs. However, depolarization of the membrane leads to release of the magnesium ion. If the depolarization of the post-synaptic membrane sustains, while enough glutamate is in the synaptic cleft, and can bind to NMDARs, NMDARs will open. NMDAR are calcium permeable. Opening of NMDARs will result in an increase in intracellular calcium concentration at the post-synaptic site. The rise of the calcium level activates calmodulin and subsequently calcium/calmodulin-dependent (CaM) kinase II. CaMKII phosphorylates AMPAR, leading to a higher density of AMPAR at the post-synaptic membrane as well as a higher permeability to sodium of those receptors. This is an immediate strengthening of the synaptic connection[5, 6].( AMPAR = α-amino-3-hydroxy-5-methyl-4-isoxazolepropionic acid receptor; NMDAR = N-methyl-D-aspartate receptor)(figure retrieved from [5]).*

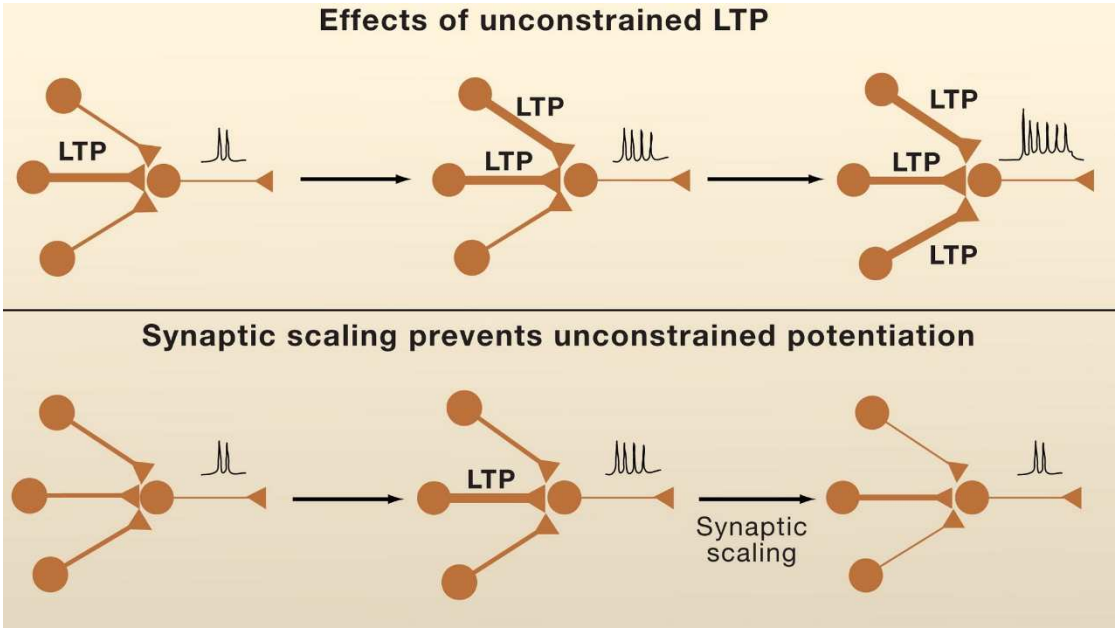


Fig. 1.3 *Homeostatic plasticity is a process for maintaining the overall activity of a neuron or a network. Synaptic scaling is a form of homeostatic plasticity. It is described as an up or down scaling of neuronal connections to stabilize firing of the neuron. Synapses that were strengthened due to LTP are more likely to be depolarized again, thus resulting in further strengthening of the synapse. This would eventually lead to a rigid network of neuronal connections, unable to adjust to new input. Another issue is the false correlation of unrelated events. The ease with which a weak presynaptic terminal can lead to a strong response in the post-synaptic neuron will lead to a strengthening of the pre-synapse as well, although the incoming signal was weak. To avoid this, neurons seem to be able to find their way back to a 'default' firing rate.[4] (figure retrieved from [4])*

*Glutamatergic synapses in the hippocampus of humans*

In the hippocampus, lower Glx (glutamate + glutamine) levels are associated with MDD[73], while administration of ketamine, an NMDAR antagonist, leads to an increase in glutamate concentration[74]. In the dentate gyrus (DG) and CA1, a decrease in pre-synaptic proteins has been found, including synaptosomal-associated protein 25 (SNAP25), which is involved in exocytosis of presynaptic vesicles[75]. GluA1 and GluA4, subunits of AMPARs, were downregulated as well[61]. Besides the decrease in AMPAR subunits, NMDAR subunits also seem to be implicated. A study found hypermethylation of the gene body encoding NR2A in the hippocampus[76], which in general would result in a higher expression level of the gene[77]. Incorporation of NR2A containing NMDAR leads to a higher peak currency, while shortening the opening period of the receptor[78]. This would alter neuronal activity. Gene expression of glial glutamate transporters (EAAT1 and EAAT2; EAAT = excitatory amino acid transporter), important for uptake of glutamate from the synaptic cleft, are decreased in the hippocampus, while expression of a vesicular glutamate transporter (VGLUT) was upregulated in MDD[62].

The mentioned findings show that glutamate signaling seems to be disturbed in MDD patients in both the ACC and the hippocampus. Several of these findings can also be detected in rat

models of depression. Several animal models of depression have been employed. As congenital learned helpless (cLH) and non-learned helpless (cNLH) rats were used in this thesis, the focus will be on this model. Findings in other learned helplessness models will be discussed as well. The ACC in congenital learned helpless rats in regard to glutamatergic changes has rarely been investigated. Therefore, studies discussed here are mostly limited to the hippocampus.

*Changes in congenital learned helpless rats*

A study found decreased absolute glutamate concentrations in the hippocampus of cLH[79], which is in compliance with findings in human depression[73]. A decrease in synaptic vesicle proteins complexin I and II was found, which are important for pre-synaptic vesicle release into the synaptic cleft[80], similar to SNAP25, which is downregulated in human depression[61]. No change in the ACC has been found[80]. Another study found a reduced expression of EAAT1 and EAAT5, which are glutamate transporters at astrocytes, in the hippocampus and cerebral cortex[81], which might result in the decreased glutamate uptake observed[82]. In other depression models, which show helplessness, similar changes can be observed.

*Changes in other learned helpless models of depression*

Another animal model for depression uses chronic unpredictable mild stress (CUMS). After a CUMS paradigm, rats showed depressive behavior. Expression of EAAT2 and EAAT3 was decreased in the hippocampus, but glutamate concentration was increased in the hippocampus. Ketamine administration led to an increase in EAAT2 and EAAT3 expression and a decrease in glutamate concentration in the hippocampus, while decreasing depression-like symptoms[83]. The increased glutamate concentration in the hippocampus of rats with depression-like symptoms is contradictory to what is found in humans[73, 74]. AMPARs and NMDARs seem to undergo changes as well, although, they do not manifest as simple down-regulations, but rather changes in subunit composition. Flinders Sensitive Line (FSL) rats showed a lower ratio of NR2A/NR2B in hippocampal post-synaptic fractions compared to Flinders Resistant Line (FRL) rats, as well as a lower GluA2/GluA3 ratio. Expression of individual GluA1, GluA2 and GluA3 subunits showed no change between the two strains[84].

FSL and FRL rats resemble the same principle as the congenital helpless and non-helpless rats used here. They focus on differences that can be observed between resilient and susceptible rats, rather than rats that underwent a stressful paradigm to develop depression-like symptoms and rats that did not. This sets more focus on the specific differences observed in resilient and susceptible rats, and cancels out the influence of stress alone.

Here, cLH and cNLH rats are used. The relative concentrations of several proteins have been measured in this project: NMDAR subunits NR1, NR2A, NR2B, the AMPAR subunits GluA1 and

GluA2, as well as PSD95, and vesicle-associated membrane protein 2 (VAMP2). In the following section, I will present a short overview of these proteins.

## 1.5 Proteins of interest

*AMPARs*

AMPARs are sodium permeable, upon binding of glutamate. AMPARs consist of different combinations of four different subunits: GluA1, GluA2, GluA3 and GluA4. In the cortex, GluA2 has a higher expression level than GluA1. Antibody binding to GluA2/3 is also higher than to GluA1[85]. During development a switch from GluA2-lacking to GluA2-containing AMPARs occurs. This is important, because GluA2-lacking AMPAR are calcium permeable[86] and can thus contribute to LTP and LTD at synapses[87].

*NMDARs*

NMDARs are both sodium and calcium permeable[88] and can consist of different subunits, NR1, NR2 and NR3[89, 90]. NR1 has to be present in the NMDAR. In addition, NR2 or NR3 subunits form one tetramer together with one or two NR1 subunits[91]. NR1 is broadly distributed, while the other subunits have distinct localizations in the brain and during development. NR2B starts being expressed prenatally and peaks postnatally, while NR2A expression starts around birth[92]. NMDARs with NR2B subunits are especially abundant at growth cones and thus might be important for the elongation of neurons[93]. NR2B and NR2A are both found in the cortex and hippocampus[94, 95], although NR2B to a lesser extent[96]. Higher NR2A levels in cortical neurons lead to shorter, but stronger excitatory post-synaptic currents (EPSCs)[78, 97]. The ratio of NR2A to NR2B might therefore be implicated in regulating the threshold for changes in synaptic strength[98].

*PSD95*

PSD95 is an anchoring protein located at spines[99-101]. It anchors NR2 subunits of the NMDAR[101], as well as AMPARs indirectly[102, 103], and may help clustering receptors at the post-synaptic density[104]. Moreover, PSD95 is implied in synaptic plasticity[105].

*VAMP2*

Vesicle-associated membrane protein 2 (VAMP2) is part of the soluble NSF attachment protein receptors (SNARE) complex[75]. It is assumed to be involved in the fusion of vesicles at the presynaptic terminal with the pre-synaptic membrane to release neurotransmitters into the synaptic cleft[106]. Additionally, VAMP2 has been found at the post-synapse, and is involved in AMPAR trafficking in post - synaptic spines[107]. The SNARE complex might also be involved in neural growth, at the growth cone[108].

## 1.6 Aims

The biological differences underlying resilience and susceptibility to stress are still poorly understood. Functional imaging studies show that the ACC seems to be implicated in depression. The neuroplasticity hypothesis states that glutamatergic synapses are affected in depression. Therefore, relative protein concentrations of congenital learned helpless rats and congenital non-learned helpless rats have been compared in this project, using western blot. The proteins analyzed are constituents of glutamatergic synapses (NR1, NR2A, NR2B, GluA1, GluA2, PSD95 and VAMP2). Regions analyzed were the cingulate cortex (Cg1 and Cg2 in Paxinos' rat brain atlas[29]), hippocampus, primary motor cortex and primary somatosensory cortex. The hypotheses are:

1) Differences in synaptic protein concentrations are expected in the cingulate cortex and hippocampus between cLH and cNLH.
2) No difference in protein concentrations is expected in the primary cortices.

# 2 Material and Methods

## 2.1 Animals

Ten male Sprague-Dawley rats (Janvier France), weighing between 200 and 240 g, were housed in 38 x 20 x 59 cm plastic cages. Up to four animals were housed in one cage at 22°C with a 12 hour light-dark rhythm. Food and water were supplied *ad libidum*. Animals were handled in accordance with the European Communities Council Directive of 24th November, 1986. The experimental procedure was approved by Regierungspraesidium Karlsruhe.

## 2.2 Learned Helplessness Procedure

Rats underwent the learned helplessness procedure, using the Operant Behavior System Mannheim Type 259900 (TSE, Saalburgstrasse 157, D-61350 Bad Homburg, Germany). The Operant Behavior System consisted of an operant conditioning chamber, to which electrical current could be applied. The walls were made of steel with one Plexiglas front covered by a metal grid to make observation possible. The floor was covered with rods (6mm diameter) every 20 mm. During the first session, the rat was exposed to inescapable random foot shocks (8 mA). Shocks and inter-shock intervals were of variable duration (5-15 sec) and were applied randomly by a computer. The session lasted for 40 min and the total shock period was 20 min. 24 hours later, rats were put into the same cage but with a lever, as well as a lamp located over the lever. A pulsating current (0.8 mA, 200 ms) was applied for 60 sec. The light over the lever was turned on during the shock periods. Fifteen shocks were applied, each followed by a pause of 24 seconds. Pressing the lever stopped the current prematurely. Failing to press the lever more than ten out of 15 times was considered as helpless behavior. A rat failing to press the lever less than five times was considered as resilient. The helpless rats and the resilient rats have been bred separately for 40 generations. The ten rats used for this project, were only put in the box with the lever and light, and therefore could escape the electrical shock by pressing the lever (fig. 2.1). Five of the ten rats were considered as resilient, pressing the lever more than ten times. Four rats failed to press the lever more than ten times and were considered as helpless. One rat failing to press the lever nine times was nonetheless included in the helpless group. Latencies for each trial and rat were measured. The described procedure was conducted by Barbara Vollmayr and colleagues in Mannheim.

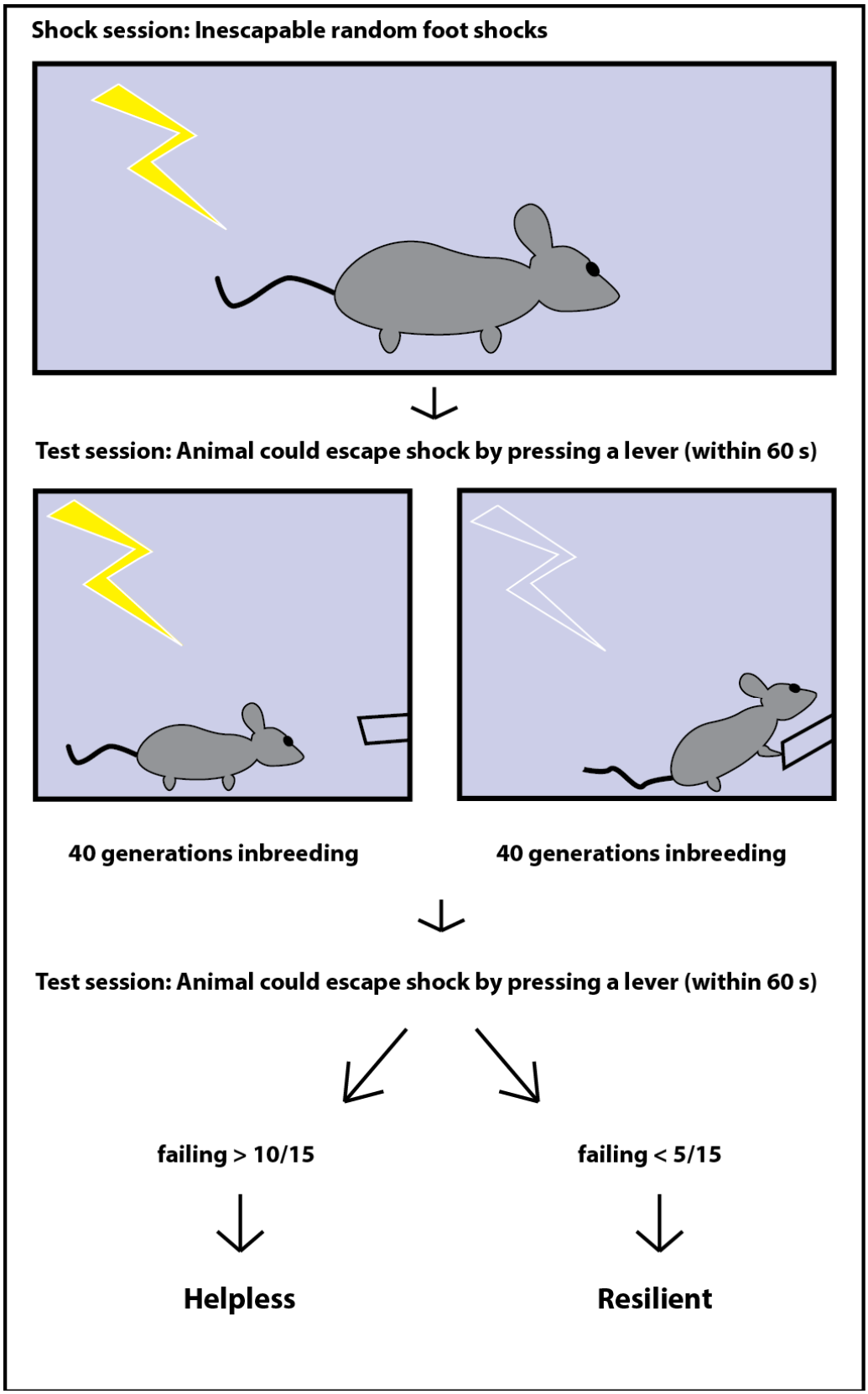


Figure 2.1 *Learned helplessness procedure done in Mannheim. Animals were put into a chamber, in which they were exposed to inescapable random foot shocks. After this, the animals were put in the same cage, this time including a lever to stop the foot shock. Depending on the number of failed trials, animals were divided into two groups, and inbred for at least 40 generations. The animals used here, have been exposed to foot shocks, they could escape from, and depending on their number of failed trials, divided up into helpless and resilient rats.*

## 2.3 Dissection of Regions of Interest (ROI)

Rats were anaesthetized with Equithesin (0.4 ml/100 g body weight) and decapitated with a guillotine, approximately eleven months after the stress procedure. After removing the brain from the cranium, the ROIs were carefully dissected. ROIs included the primary somatosensory cortex (S1), primary motor cortex (M1), cingulate cortex (C) and hippocampus (H) of both hemispheres. A 3D rat brain atlas[109] with marked ROIs was used for orientation. The areas have been marked with the help of ITK-SNAP (3.0) and Paxinos' rat brain atlas[29] by Laura Marian Valencia Pesqueira (fig. 2.2). Each sample contained ROIs of both hemispheres of either S1, M1, C or H of one rat. In total 40 samples (10 animals, 4 ROIs) were collected and stored at -80 °C for two years. The described procedure was conducted by Svend Davanger in Mannheim.

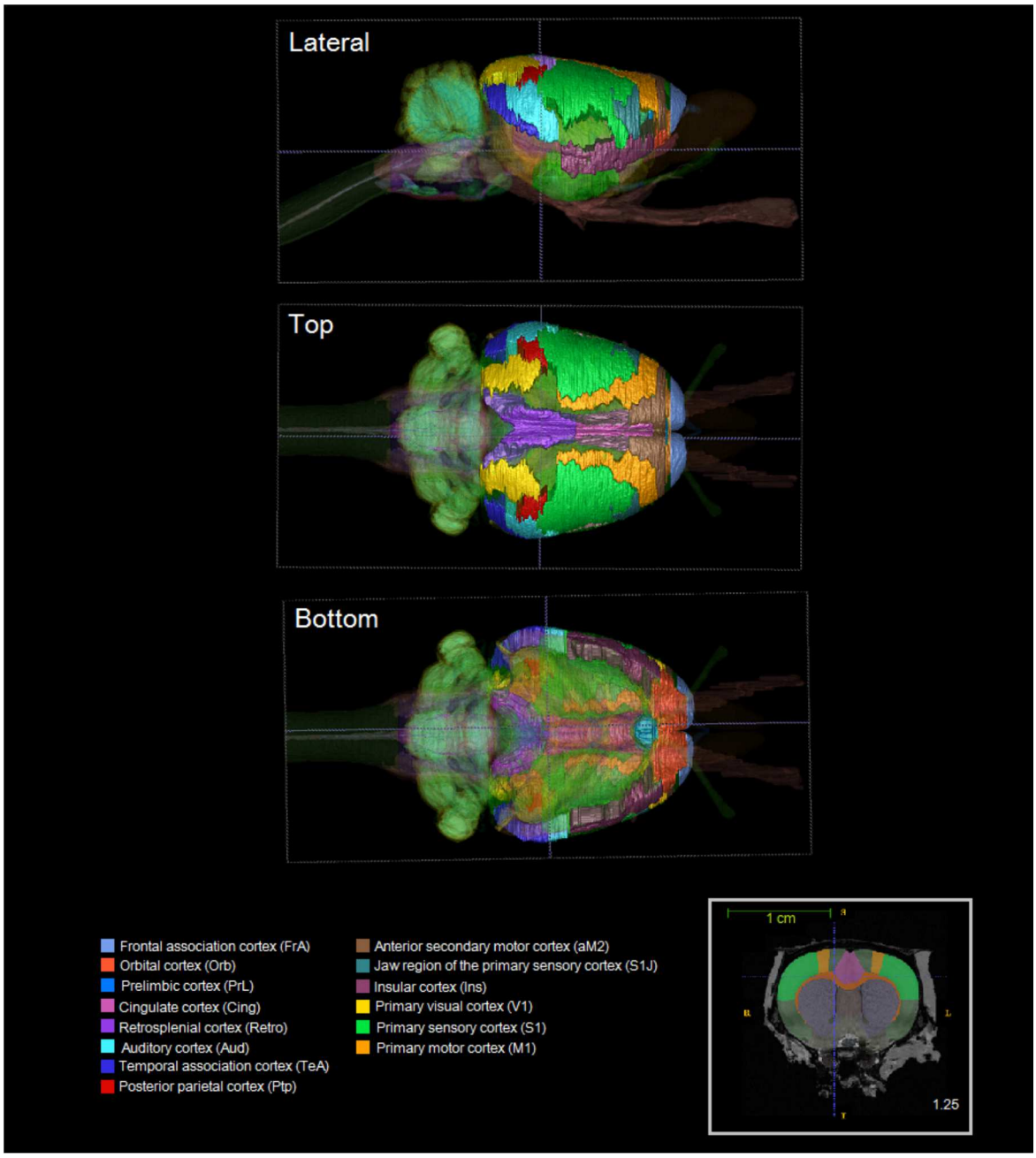


Figure 2.2 *3D atlas of a rat brain with the marked ROIs, cingulate cortex (light pink), primary motor cortex (orange) and primary somatosensory cortex (green). Taken from Laura Marian Valencia Pesqueira's master's thesis, fig.5.2. ([110]).*

## 2.4 Sample Preparation

The ROI samples were homogenized in 1.2 ml ice cold 4 mM Hepes-buffered sucrose (0.32 mM sucrose, pH 7.36) and protease inhibitor cocktail (cOmplete ULTRA Tablets, Mini, *EASYpack,* Roche, 05 892 970 001) with nine strokes in a 2 $cm^3$ tissue grinder (VWR 432-0208) on ice. All subsequent steps were carried out at 4 °C and samples were kept on ice. The homogenate was centrifuged at 1 060g (Eppendorf centrifuge, 5417C) for 15 minutes. The supernatant S1 was collected while the pellet P1 was resuspended in 0.3 ml of buffer and

centrifuged at 1060g for 15 minutes. The supernatant was collected again and added to S1. P1 was resuspended in 0.3 ml of buffer and stored. S1' was then centrifuged at 11 700g for 15 minutes and the supernatant S2 was removed. The pellet P2 was washed (resuspended in 0.3 ml buffer, centrifuged at 11 700 g, the supernatant was removed) and then resuspended in 0.3 ml buffer. P2' was the washed crude synaptosomal fraction (fig. 2.3). The protein concentrations were measured with a Bradford Protein Assay from BioRad (see Appendix A.1).

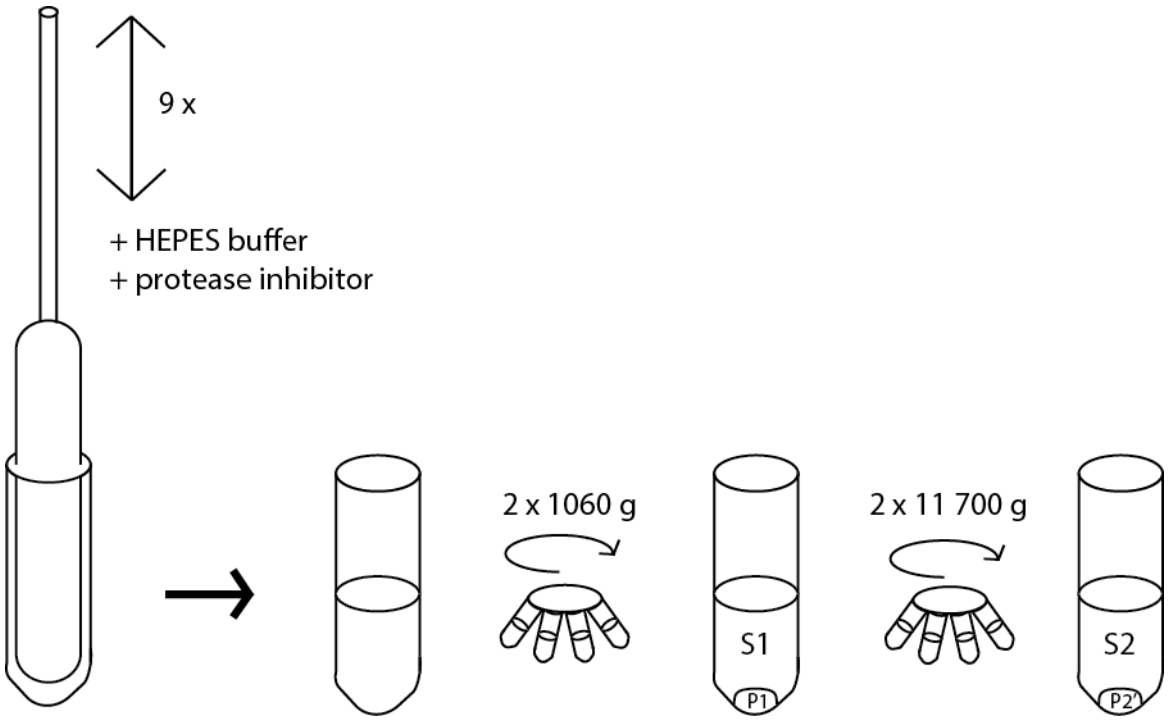


Figure 2.3 *Preparation of washed crude synaptosomal fraction P2'.*

## 2.5 Immunoblotting

A mixture of SDS-containing loading buffer (5.25 % sodium dodecyl sulfate w/v) and the crude synaptosomal fractions was incubated at 70 °C for 20 minutes. Fifteen microliters of the mixtures (4 µg protein, 1:6 loading buffer) were loaded into the wells of the gel (4–20 % Criterion™ TGX™ Precast Midi Protein Gel, 26 well, 15 µl #5671095). Empty wells were loaded with 7.5 µl Precision Plus Protein Dual Color Standard (BioRad, 161-0374). The gel was run at 180 V for 50 minutes in Læmli buffer (250 mM Trizma base, 1.92 M glycine, 1 % w/v SDS; pH = 8.3). After the electrophoresis, the gel was adjusted to the Towbin buffer (250 mM Trizma base, 1.92 M glycine, pH = 8.3) for 10 minutes. For semi-dry blotting the Trans-Blot® Turbo™Blotting System (BioRad 1704150) was used. The blotting sandwich was constructed as follows: One sheet of precut extra thick blot filter paper (BioRad, 1703969) was soaked in Towbin buffer containing 20% v/v methanol and put into the cast. The PVDF membrane

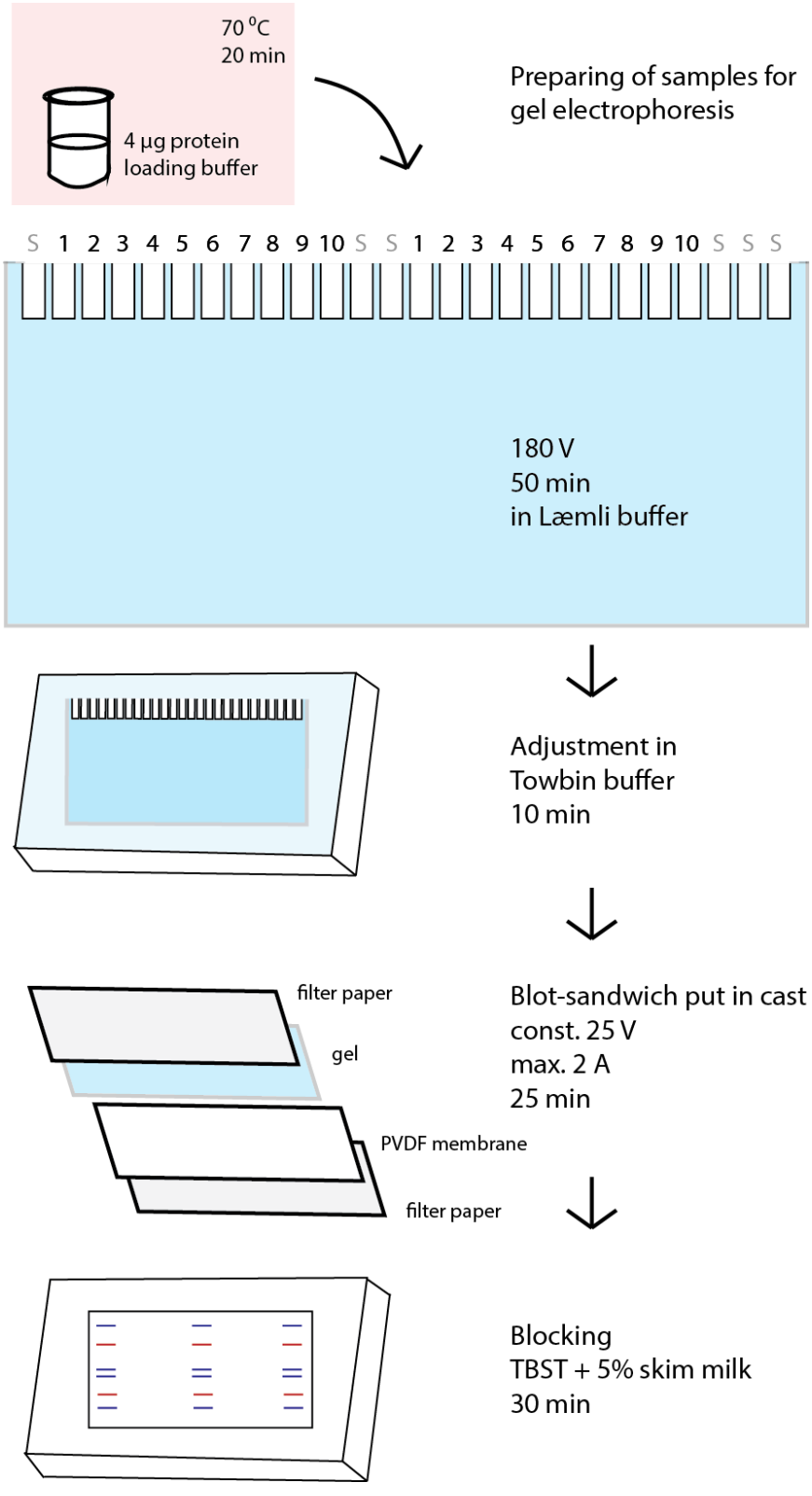


Figure 2.4 *Gel electrophresis and blotting*

(BioRad Immun-Blot® Low Fluorescence PVDF membrane, 1620264) was cut into size and soaked in pure methanol for 30 seconds. Subsequently, the membrane was soaked in Towbin

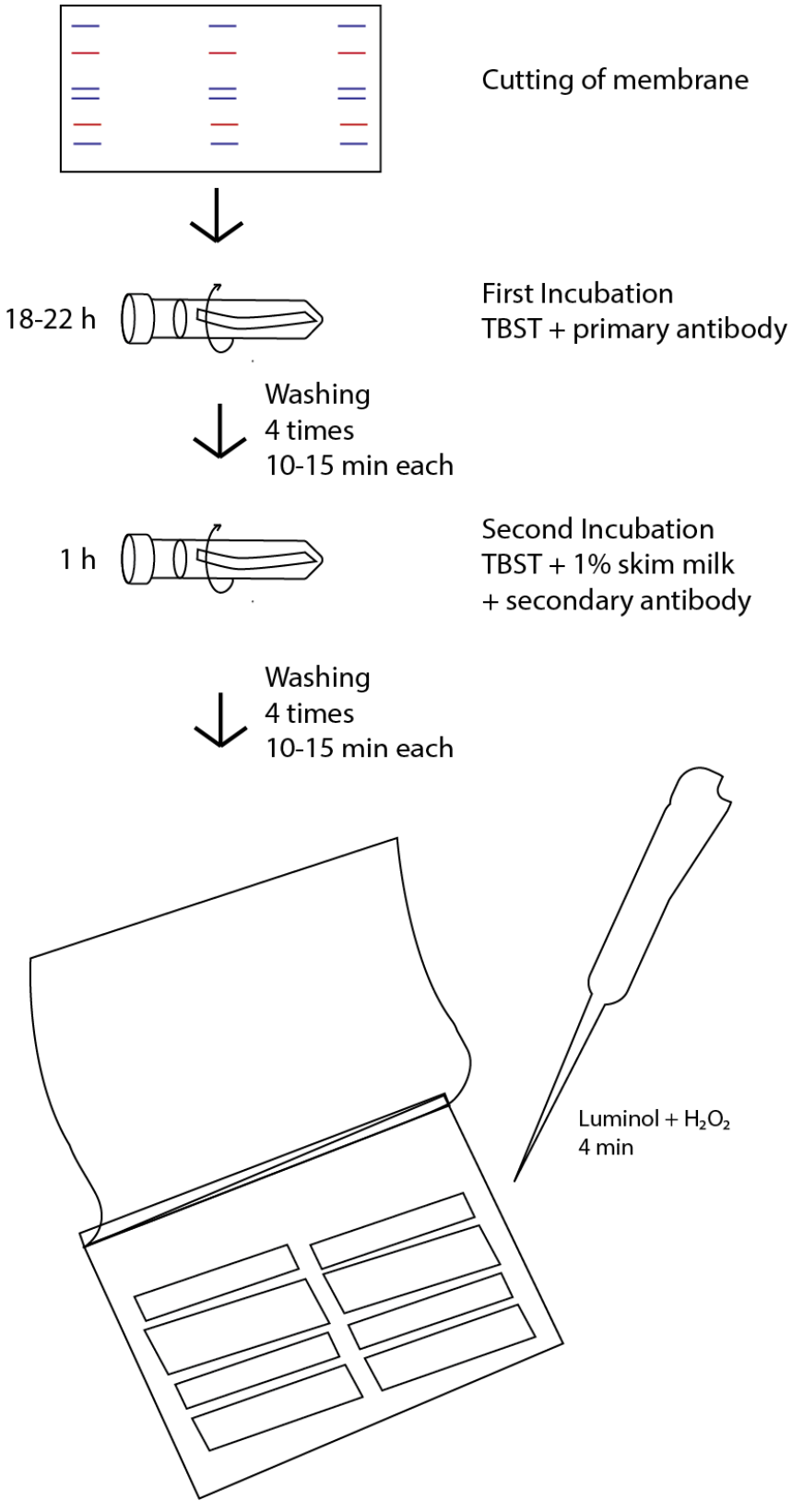


Figure 2.5 *Incubation, washing, and preparing the membrane for taking images*

buffer with 20 % methanol for one minute. The gel was layered on top of the membrane. Air bubbles were pressed out carefully with a roller. On top of the gel another extra thick filter paper soaked in buffer containing 20 % methanol was layered. After putting on the lid, the cast was put into the Trans-Blot® Turbo™ (Program: 25 minutes, maximal 2.0 Ampère,

constant 25 Volt). After blotting, the membrane was reactivated with methanol. The PVDF membrane was then incubated in 5 % skim milk in TBST buffer (0.4 M Trizma base, 2.74 M NaCl, 10 % v/v Tween, pH = 7.6) for 30 minutes and subsequently washed quickly four times. After washing, the membrane was incubated in TBST buffer with the primary antibody overnight (12-24 h) at 4 °C in 15 ml tubes (VWR, 89401-566). The next day the PVDF membrane was transferred into new tubes with TBST buffer and washed four times for 10-15 minutes as well as quickly washed in between the washing steps. Incubation with secondary antibodies in 1 % skim milk TBST for one hour at room temperature followed. The membrane was washed as described before. $H_2O_2$ and luminol (Super Signal West Pico Chemiluminescent Substrate, Thermo Fisher, 34078) were mixed in a one-to-one ratio and applied to the membrane for 4 minutes before the membrane was put between two plastic foils and the remaining liquid was pressed out with a roller (fig. 2.5). The membrane was immediately scanned with the BioRad ChemiDoc (BioRad ChemiDoc Touch Imaging System, chemiluminescence, exposure time: 10-2000 seconds). The blot was exposed until the bands became saturated. The image before saturation was chosen for analysis. All samples were run four times for each antibody.

## 2.6 Stripping of membranes

Some membranes have been stripped and reincubated with another antibody (C and H of PSD95). For this, the needed membrane stripes, which correspond to the molecular weight of PSD95, were incubated in stripping buffer (pH = 6.8) for 40 min at approximately 50 °C. Membranes were washed three times within 1 h. Afterwards, a 1:1 mixture of luminol and $H_2O_2$ was applied as described above. Images were taken with an exposure time of 2000 sec, to check for binding residues of antibodies. If binding was detected, membranes were incubated at 50 °C in stripping buffer for another 30 minutes. If no binding was detected, membranes were shortly reactivated in methanol and incubated in the needed primary antibody solution. It was proceeded as described above.

## 2.7 Antibodies

For primary incubation anti-NMDAR2A (Abcam), anti-NMDAR2B (Abcam), anti-GluA1 (Abcam), anti-GluA2 (extracellular) (Alomone labs), anti-NMDAR1 (Abcam), anti-GluN1 (Abcam), anti-PSD95 (Abcam), anti-VAMP2 (Abcam), anti-Actin (Millipore) and anti-Histone H3 (CST) antibodies were used. Anti-histone antibodies were kindly provided by Mahmood Reza Amiry-Moghaddam and Nadia Skauli. For secondary incubation anti-rabbit (Thermo) and anti-mouse (Thermo Fisher) antibodies were used. (For details, A.2.)

## 2.8 Blot design

Each gel was loaded with the same ten samples twice. Thus, two replicates for one of the four areas were run on one blot. The empty wells were loaded with protein standard. The order of samples was changed for several blots in order to control for differences in staining due to different locations of the sample. For incubation, the blot was cut horizontally (to enable incubation in different antibody solutions, due to their difference in molecular weight and so different location on the blot) and vertically (to ensure equal incubation condition for the whole strip) (fig. 2.6).

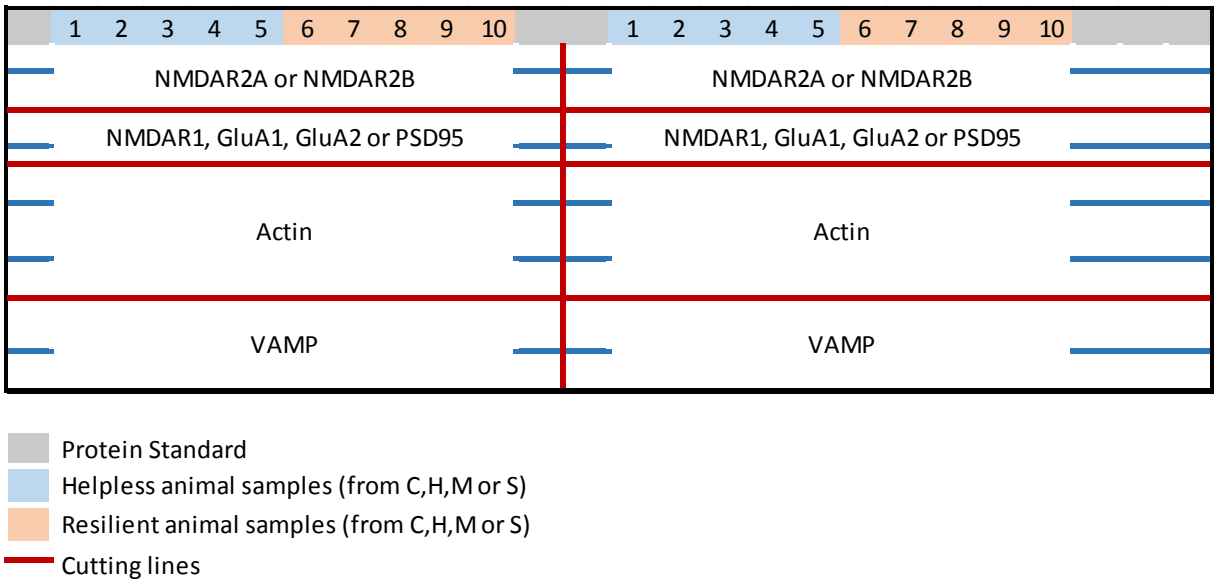


Figure 2.6 *Blot design. Loading of the gel for all ten samples of one area and cutting of the membrane for optimal incubation. Wells with protein standard show molecular weight lines, indicated by the blue and red lines. This blot had to be run two times, to yield the four runs for one protein in one of the areas.*

## 2.9 Analysis

The images were cut, resulting in single images for each antibody of the blot. The images were analyzed using Image Lab (version 5.2.1, fig. A.3). A multichannel image was created, one of the channels being the image of actin. Lanes were generated manually, and bands, which matched the molecular weight of the protein, were detected semi-manually. For blots with high background, the automatic background subtraction was increased. The lane profile of each band was inspected and, if necessary, its boundaries were adjusted manually. By clicking on the normalization button, the actin image could be chosen as housekeeping protein bands, using them as the normalization channel. The normalized values could subsequently be exported as an Excel table. As outlined before, ten samples were run twice on two blots (so two times the blot, illustrated in fig. 2.6), resulting in four replicates. The three best runs were chosen for analysis. Criteria for this were sufficient signal (i.e., blots that showed stronger binding of the antibody were chosen over blots that showed weak binding), low background signal and crisp single bands (A.4). This was done before the closer analysis and statistical tests

to avoid bias. Some deviations in overall staining of the different replicates became obvious. Thus, the measured values were normalized to sample 1 of each replicate using Matlab R2015b. Sample 1 was selected, as it had the smallest standard deviation over all measurements for every protein. This was calculated using Matlab.

## 2.10 Statistics

The mean of the three measurements of the bands were calculated for each sample and each protein using Matlab R2015b. Ratios of the mean of GluA1/GluA2 and NMDAR2A/NMDAR2B were calculated using Excel. A Shapiro-Wilk test was conducted to test for normality separately for each group for every protein and every area. When possible, a two-tailed independent samples t-test was conducted, otherwise the independent samples Mann-Whitney U test was conducted, also two-tailed. The exact significance was used, as sample size was small. Differences of relative protein concentrations between the ROIs were calculated using Matlab and analyzed with a non-parametric Mann-Whitney U test, as data were not normally distributed. In addition, the latency values from the behavioral tests were analyzed. Because the data were normally distributed in the helpless and the resilient group, a repeated two-way ANOVA was conducted. These tests were conducted with IBM SPSS Statistics (Version 24).

## 2.11 Linearity of protein concentration and signal detection

For each antibody the linearity of its signal towards the protein concentration in each well was determined. Wells were loaded with 2, 3, 4, 5 and 7.5 µg of synaptosomal fraction of whole rat brain, provided by Suleman Hussain. The following procedure of gel electrophoresis and blotting was the same as described before. The measured values of each concentration were plotted with Excel. Only one run was carried out for each antibody. Kendall's tau and Pearson correlation coefficients were calculated for each antibody and its concentration, as well as each antibody and the actin antibody binding intensity. This was done with IBM SPSS Statistics (Version 24).

# 3 Results

## 3.1 Latencies of learned helplessness procedure

Latencies differed significantly between the resilient rats, and the helpless rats as seen in a two-way repeated measurement ANOVA (F (1.7) = 11.803, p=0.011, mean (helpless) = 42.63, mean (resilient) = 6.82, fig. 3.1; for raw data see Appendix B.1).

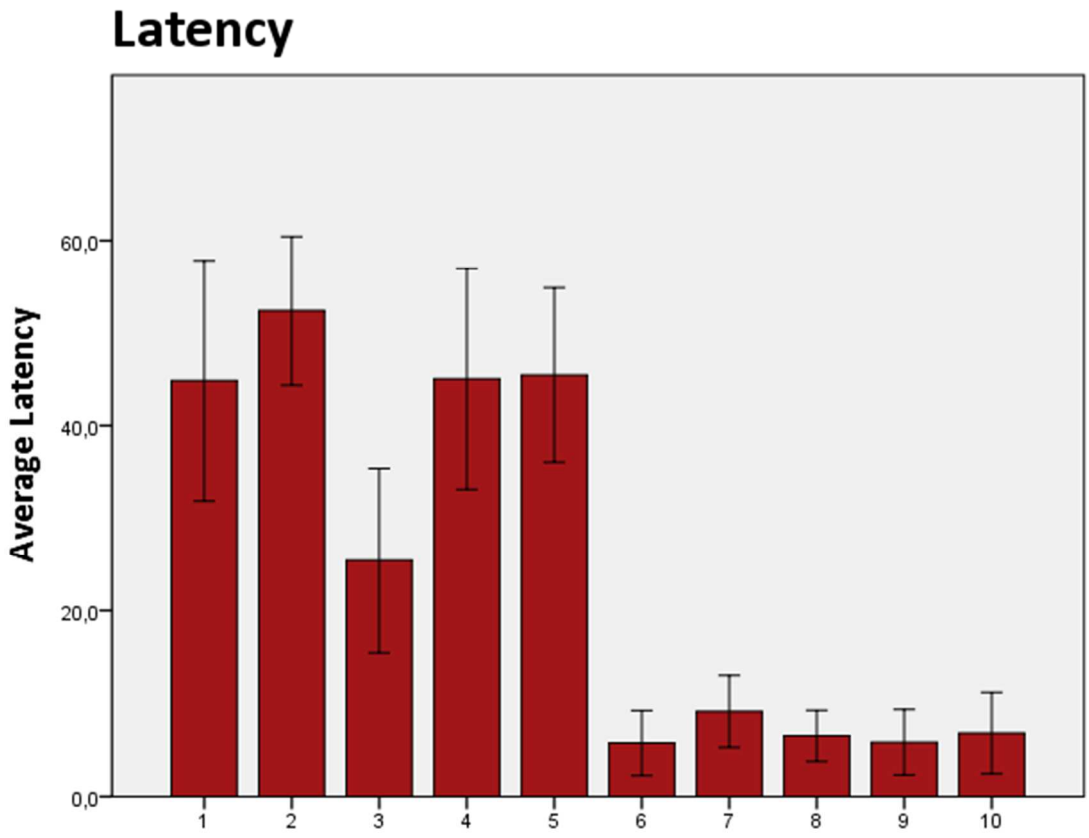


*Figure 3.1* Averaged latencies over 15 trials of helpless (1 - 5) and resilient (6 - 10) animals. All helpless animals, except for rat 3, failed the behavioral test at least 10 times. Rat 3 failed 9 times. All resilient animals failed less than 5 times out of fifteen. Mean ± 2SE is shown.

## 3.2 Main findings

In the motor cortex, the PSD95 protein concentration was significantly lower in resilient (Mdn = 3) animals compared to helpless (Mdn = 8) ones (U = 0, z = -2.611, p = 0.008) (fig. 3.2; see Appendix B.2 for blot). In the somatosensory cortex, the GluR1/GluR2 ratio was significantly lower in resilient (Mdn = 3.4) compared to helpless (Mdn = 7.6) animals (U = 2, z = -2.193, p = 0.032) (fig. 3.3; see Appendix B.2-6).

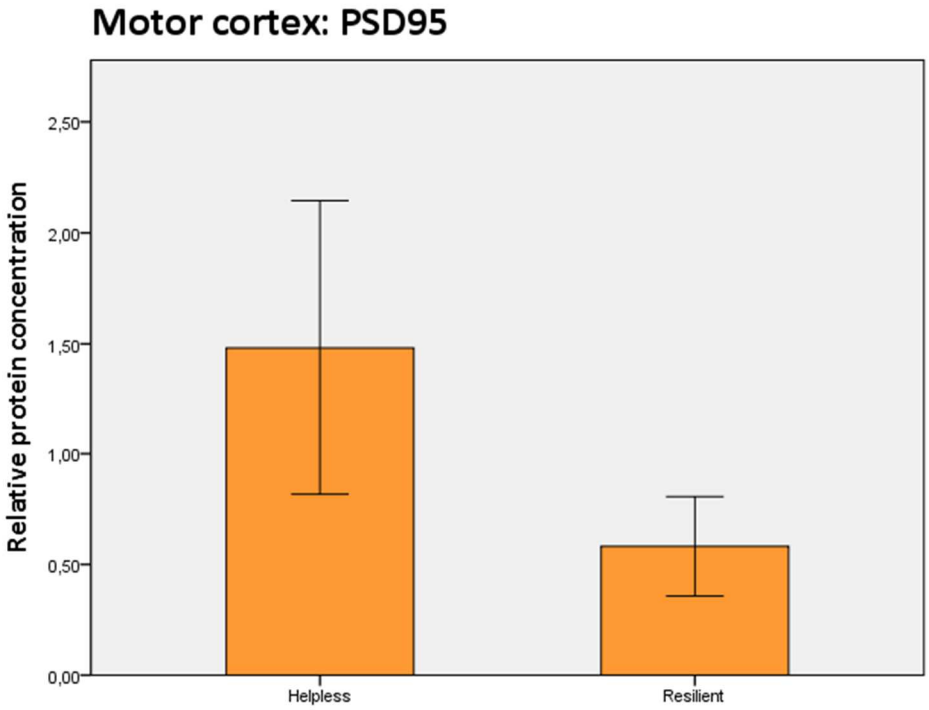


Figure 3.2 *Mean of relative protein concentration of PSD95 in the primary motor cortex of helpless and resilient rats. There was a significant higher relative concentration of PSD95 in the primary motor cortex of helpless animals compared to resilient animals. Data are shown as mean ± 2 SE.*

In the cingulate cortex, a trend of a lower protein level of NMDAR2A was found in resilient (Mdn = 3.4) compared to helpless (Mdn = 7.6) animals (U = 3, z = -1.984, p = 0.056) (fig. 3.4; see Appendix B.6). All results, including the non-significant ones, are stated in the appendix (B.7, B.8, B.9).

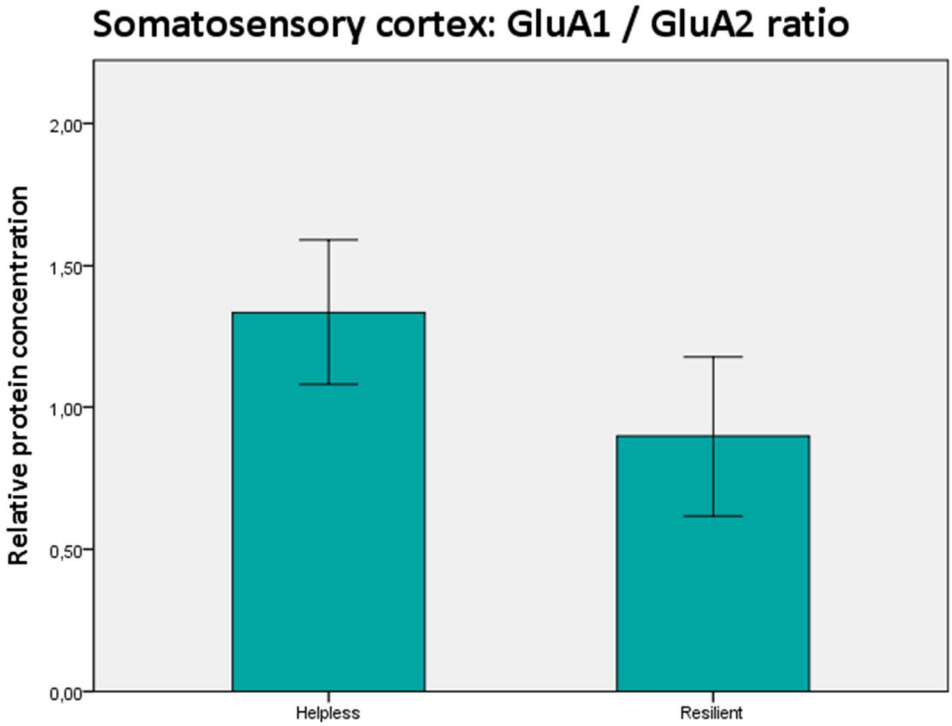


Figure 3.3 *Mean of relative protein concentration ratio of GluA1/GluA2 in the primary somatosensory cortex of helpless and resilient rats. There was a significant higher GluA1/GluA2 ratio in the primary somatosensory cortex of helpless animals compared to resilient animals. Data are shown as mean ± 2 SE.*

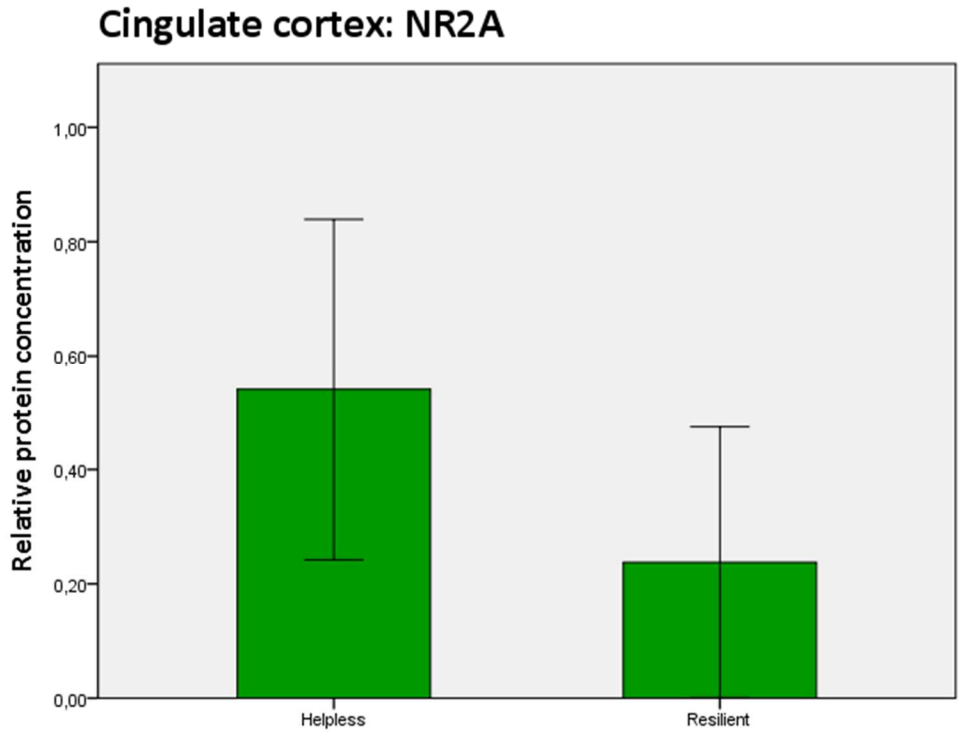


Figure 3.4 *Mean of relative protein concentration of NR2A in the cingulate cortex of helpless and resilient rats. There was a trend of higher relative concentration of NR2A in the cortex of helpless animals compared to resilient animals. Data are shown as mean ± 2 SE.*

## 3.3 Findings from ROI differences

The analysis of differences between ROIs, showed that the PSD95 concentration difference between the primary cortex and the hippocampus in helpless rats (Mdn = 3) is significantly different from the ones of resilient rats (Mdn = 8; U = 25, z = 2.611, p = 0.008). The PSD95 concentration was higher in the primary motor cortex compared to the hippocampus in helpless rats. In resilient rats, the PSD95 concentration was lower in the primary motor cortex than the hippocampus. The PSD95 concentration was also higher in the primary motor cortex in helpless rats (Mdn = 7.6) compared to resilient ones (Mdn = 3.4) when compared to the somatosensory cortex (U = 2; z = -2.193; p = 0.032). GluA2 concentration differences between primary motor and primary somatosensory cortex differed significantly between resilient (Mdn = 3.2) and helpless rats (Mdn = 7.8; U = 1, z = -2.402, p = 0.016) (fig. 3.5). The concentration of GluA2 in the primary somatosensory cortex was higher in the helpless group compared to the resilient group (see Appendix Table B.10 for all results).

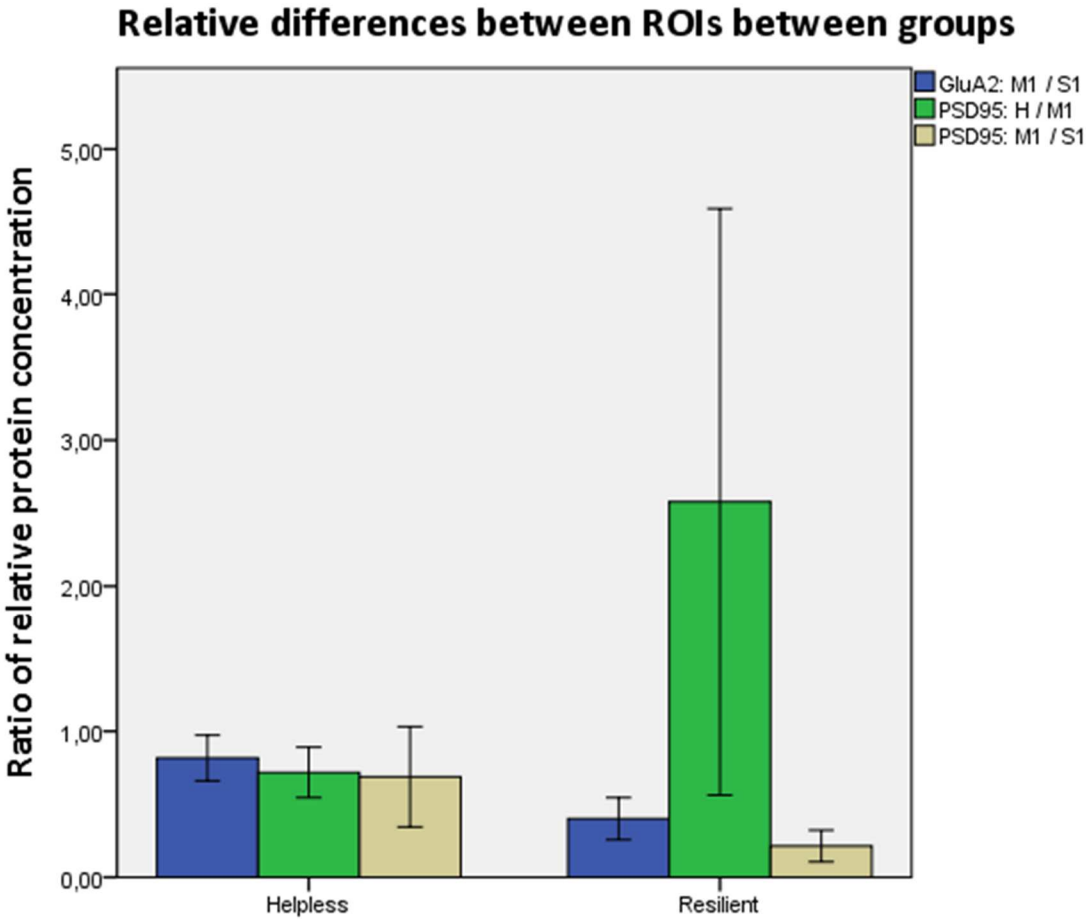


Figure 3.5 *Bar plot shows differences in relative protein concentration of GluA2 between primary motor cortex and primary somatosensory cortex (blue), and the differences of PSD95 between hippocampus and primary motor cortex (green), and primary motor cortex and primary somatosensory cortex (grey). Bar shows mean ± 2SE.*

## 3.4 Total protein concentration – signal intensity relation of antibodies

Actin, GluA1 and NR2B antibodies began to saturate at 5 µg. Other antibodies approximately followed linearity with single outliers (fig. 3.6). Pearson's correlations showed that the protein concentration correlated well with signal intensity for all antibodies. The protein concentration/signal intensity relation of the actin antibody correlated worse with that of NR2A and GluA2, than other antibodies, and the one-tailed significance level is not reached. The data were not normally distributed, though, so whether the correlations, calculated by the Pearson's correlation test were significant can actually not be concluded from this test. The non-parametric Kendall's tau test showed significant correlations for all antibodies (tab. 3.1).

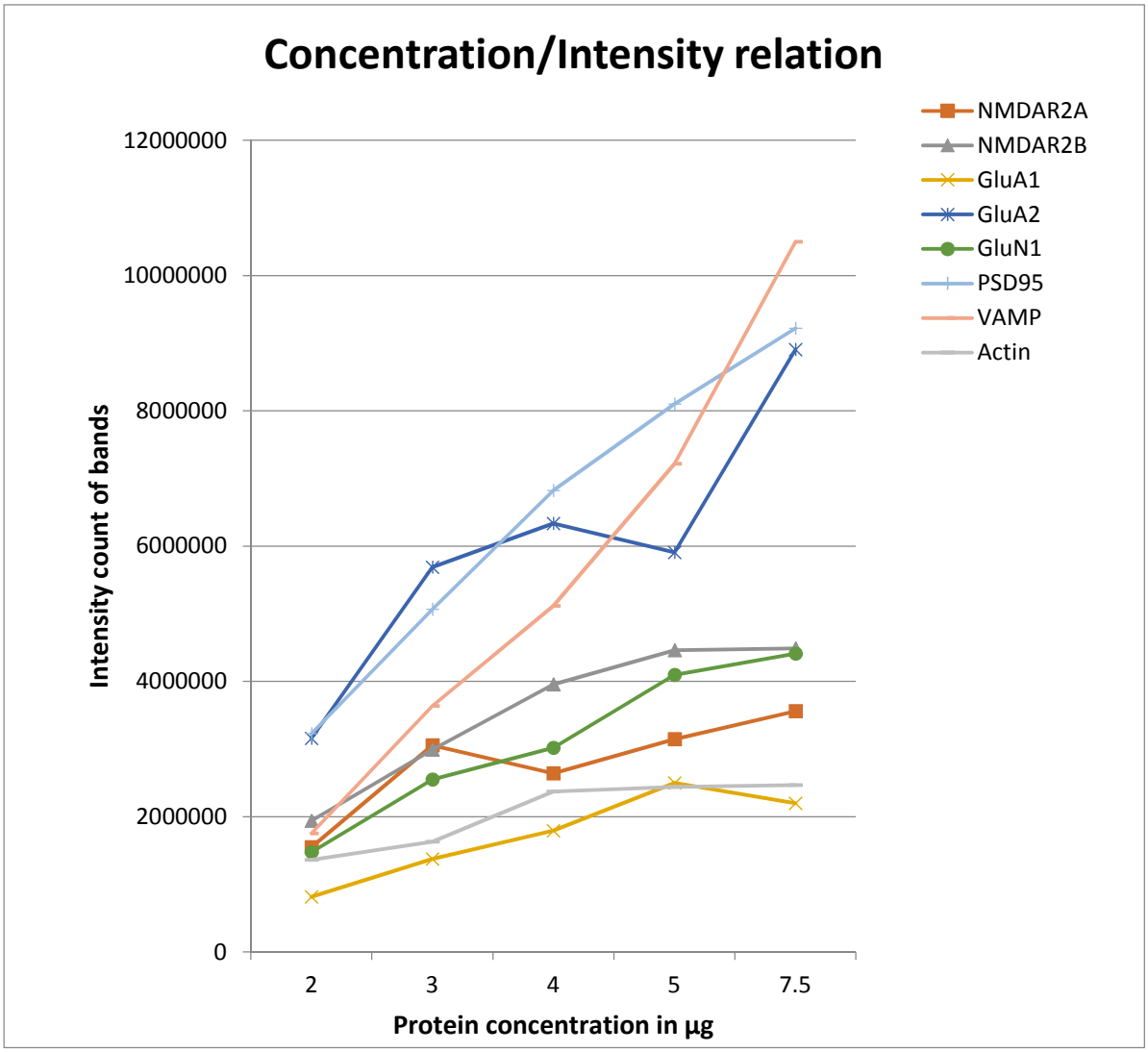


Figure 3.6 *Relation of signal intensity of antibody binding, and protein concentration in the well. Points are connected for illustration of the dynamic, the curve does not resemble a trendline.*

Table 3.1 *Pearson Correlation and significance values for a 1-tailed bivariate Pearson's correlation, and Kendall's tau correlation coefficient. (* p < 0.05; ** p < 0.001)(Conc. = concentration).*

| Pearson | | NR2A | NR2B | GluA1 | GluA2 | NR1 | PSD95 | VAMP | Actin |
|---|---|---|---|---|---|---|---|---|---|
| Conc. | Pearson Correlation | 0.815* | 0.862* | 0.815* | 0.931* | 0.933* | 0.949** | 0.996** | 0.830* |
| | Sig. (1-tailed) | 0.047 | 0.030 | 0.047 | 0.011 | 0.010 | 0.007 | 0.000 | 0.041 |
| Actin | Pearson Correlation | 0.724 | 0.977** | 0.934* | 0.792 | 0.913* | 0.950** | 0.854* | 1.000 |
| | Sig. (1-tailed) | 0.083 | 0.002 | 0.010 | 0.055 | 0.015 | 0.007 | 0.033 | |

| Kendall's tau | | NR2A | NR2B | GluA1 | GluA2 | NR1 | PSD95 | VAMP | Actin |
|---|---|---|---|---|---|---|---|---|---|
| Conc. | Correlation Coefficient | 0.800* | 1.000** | 0.800* | 0.800* | 1.000** | 1.000** | 1.000** | 1.000** |
| | Sig. (1-tailed) | 0.025 | 0.000 | 0.025 | 0.025 | 0.000 | 0.000 | 0.000 | 0.000 |
| Actin | Correlation Coefficient | 0.800* | 1.000** | 0.800* | 0.800* | 1.000** | 1.000** | 1.000** | 1.000 |
| | Sig. (1-tailed) | 0.025 | 0.000 | 0.025 | 0.025 | 0.000 | 0.000 | 0.000 | 0.000 |

# 4 Discussion

The main findings of this thesis are as follows: Congenital helpless rats showed significant differences of relative protein concentrations in the primary motor cortex and primary somatosensory cortex compared to congenital non-helpless rats. Although not significant, a trend was also present in the cingulate cortex. In the following sections, the possible implications of these differences are discussed, followed by assessing the limitations of the current study.

## 4.1 Findings

*PSD95 in the motor cortex*

In this thesis, a significantly higher concentration of PSD95 has been found in the primary motor cortex of helpless rats compared to non-helpless rats. This might be linked to the motoric activity of the animal. In a social stress depression model in mice a decrease of motor activity was found[111]. Another mouse depression model, using light deprivation, found decreased connectivity in the motor cortex, while synapse strength increased[112]. The light deprivation model of depression also shows impairment of locomotor activity[112]. How synaptic proteins differed has not been investigated. Synaptic changes in the primary motor cortex in animal models of depression are rarely investigated in general. Hence, how upregulation of PSD95 in the primary motor cortex affects behavior is not known.

***PSD95 at synapses.*** The function of PSD95 at synaptic sites has mainly been investigated at hippocampal synapses. In this region, PSD95 is important for the delivery of AMPAR to post-synaptic membranes and LTP induction[102]. PSD95 is implied in anchoring AMPARs[103], and binds to NR2 subunits of NMDARs[100, 101] and voltage-gated potassium channels[99]. Mutation of NMDAR and AMPAR binding sites of PSD95 resulted in increased anxiety-like behavior and hypoactivity in a novel environment[113]. This shows that PSD95 can alter behavior due to its anchoring function for glutamate receptors. However, no difference in AMPAR or NMDAR subunit concentration has been found in addition to the PSD95 increase. Reasons for this could be that the increase of AMPARs and NMDARs separately are not as easily detectable with the western blot technique. Besides its anchoring function, PSD95 is also necessary for regulation of plasticity.

***PSD95 has regulatory functions.*** Mutation of binding sites, which are not implicated in NMDAR or AMPAR binding, lead to an impairment of LTD and a high increase in LTP in the hippocampus of rats. NMDAR-currents at the post-synapse did not differ, neither did NMDAR expression. This points to a regulatory property of PSD95[105], at least at hippocampal synapses.

***Overexpression of PSD95.*** PSD95 overexpression in pyramidal neurons of the rat cortex leads to increased AMPAR-mediated EPSCs and a higher probability for LTD. This increase in AMPAR-mediated EPSCs is due to an increase in synapse number, and not an increase in receptor number[114]. PSD95 is also important for the balance of inhibitory and excitatory synapses. A study found that overexpression of PSD95 leads to an increase in the number and strength of excitatory synapses[115]. The heightened concentration of PSD95 in the primary motor cortex of helpless rats could indicate an increased number and strength of excitatory synapses.

***Excitatory activity of the motor cortex.*** A short-term increase in synapses[116], and strengthening of synaptic connections[117], has been detected after learning of new motor skills. How long-lasting increases of excitability influence motor cortex functioning and behavior in depressive disorders is less well established. Findings of transcranial magnetic stimulation (TMS) studies in depressed subjects show asymmetric excitability of the motor cortices of the two hemispheres[118], as well as a decrease in interaction between the two hemispheres[119]. However, in this thesis the two motor hemispheres have been pooled. Therefore, no conclusions can be drawn about hemispheric differences. Nevertheless, the findings of the TMS studies underscore the global changes within the brain in depression, and an influence of the disorder on the motor cortex.

***The motor cortex in depressed patients***. In depressed patients, post-exercise facilitation is decreased[120], possibly pointing towards an inability to strengthen synaptic connections further[121]. Moreover, a reduction of LTP-like plasticity was found when using a paired association stimulation protocol[122, 123]. Additionally, a shorter cortical silent period at the motor cortex of MDD patients has been measured, which is a sign of less inhibitory activity in the network[124]. In atypical depression, a reduction of inhibition in the motor cortex was found as well[125]. Summarizing these findings, it seems probable, that helpless rats have a higher number of synapses and/or greater strengthening of those, resulting in more excitatory activity in the motor cortex. This is either accompanied by, or a result of, less inhibition. Synapses are, as a result, unable to strengthen themselves further. However, the consequences of this are uncertain.

***Locomotion of depressed patients.*** Depressed patients show diminished strength and a different gait than controls[126]. Whether this is a direct result of changes in the primary motor cortex is questionable. It is often proposed that the decrease in motivation, accompanying depressed patients[127], underlies this decrease in strength. Motor deficits, called psychomotor retardation, and anhedonia are correlated and it is therefore difficult to distinguish between the two[128-130]. However, this has been attempted, finding assumingly solely sensorimotor impairments, which are probably only marginally influenced by the motivational drive of the patient[131].

***Locomotion of depressive-like rats.*** The Wistar-Kyoto rat, a depression model which shows learned helplessness, is symptomized by psychomotor retardation[132]. PSD95 differences in the Wistar-Kyoto rat have not been studied in the motor cortex, but a significantly higher concentration of neuroligin1, which binds to PSD95[133], has been found in the motor cortex of these rats[134]. However, congenital learned helpless rats, from the same research group as the rats used here, did not show any hypoactivity in the open field test. On the contrary, at the beginning of the session, locomotion was increased compared to control[51]. It would be interesting to test the cLH rats for other motoric abilities, to check more specifically for signs of psychomotor retardation, one of the symptoms of major depressive episodes.

***A possible mechanism.*** The increased concentration of PSD95, and the assumingly increased strength of synapses, might be an impairment in the down-scaling of the synaptic input, by homeostatic plasticity mechanisms. Artificial stimulation of neurons in the motor cortex results in an upregulation of GABARs three weeks after stimulation[135]. This might be a natural mechanism to down-scale synaptic strength and might be impaired in helpless animals.

*Other proteins in the primary motor cortex*

Concentrations between the two groups have been normalized to different regions to cancel out any individual differences in the whole brain. Compared to the primary somatosensory cortex and the hippocampus, PSD95 concentration in the motor cortex was significantly higher in the helpless group compared to the resilient one. Therefore, this result seems quite robust. GluA2 concentration in the motor cortex normalized to the somatosensory cortex showed a higher concentration in the helpless group as well. This is supported by the overall small trend of GluA2 concentration being higher in the primary motor cortex of the helpless animals.

***GluA2 in synaptic plasticity.*** GluA2 is mostly found at excitatory synapses in the motor cortex[136]. AMPARs are anchored indirectly by PSD95[103]. Consequently, the increased concentration of PSD95 and the one of GluA2 might be causally connected. GluA2 knock-out in mice results in locomotor abnormalities. They showed both increased locomotion, and stayed still for an increased amount of time. The overall strength of muscles was not altered[137]. This implicates the GluA2 subunit in motor behavior. Overexpression of GluA2 in the hippocampus leads to an increase in spine size and spine density[138]. The increased concentration of GluA2 might therefor be linked to an increase in synaptic strength and number, as proposed above.

*GluA1/GluA2 ratio in the somatosensory cortex*

A significantly higher GluA1/GluA2 ratio has been measured in the somatosensory cortex of helpless rats compared to non-helpless rats. Studies found an involvement of AMPARs in depressive disorder in several brain areas[61, 139]. However, a study investigating resilience and

vulnerability in a chronic social stress model found the opposite, a lower GluA1/GluA2 ratio, in vulnerable rats, and an overall higher AMPAR density[140]. In this study, only the hippocampus was investigated, not the somatosensory cortex. A brain wide deletion of the GluR1 subunit results in a depressive-like phenotype with increased helplessness[141], and a more anhedonic response towards sucrose[142]. Another study deleting the GluR1 subunit found no increase in anxiety-related behavior[143].

***AMPAR and depression.*** Treatment with anti-depressants leads to an increase in AMPAR subunits in the frontal cortex and hippocampus[144]. An AMPAR potentiator helped to reduce some symptoms of depression in rats, such as immobility in the tail suspension test and weight loss, but an anxiety test and the sucrose preference test showed no difference[140]. However, it is not only the amount of AMPARs that can change single cell and network properties; the subunit composition of AMPARs also plays an important role for a neuron's electrophysiological properties, and thus for its excitability as well.

***AMPAR and plasticity.*** GluA2-lacking AMPAR are calcium permeable[145]. Knock-out of GluA2 leads to an increase in LTP in the hippocampus[146] and a number of behavioral abnormalities, such as motor and learning deficits[137]. The authors of the study conclude that these deficits are due to the higher excitability in the brain. As there is a higher GluA1/GluA2 ratio in helpless rats, this would point to a decrease in excitatory activity in the somatosensory cortex in helpless animals.

***The somatosensory cortex in learned helpless animals.*** The somatosensory cortex is not often investigated in depression research. In this project, no difference was expected, as this area was supposed to serve as a control. However, a study that also used the somatosensory cortex as a control found a smaller density of PSD95 in the somatosensory cortex of learned helpless rats compared to naïve rats[147], underscoring that changes in the primary somatosensory cortex can occur in helpless rats. Additionally, a decreased concentration of PSD95 in helpless rats might reflect a decrease in excitatory activity in the somatosensory cortex.

***The somatosensory cortex in depressed patients.*** Similarly to rats, the human somatosensory cortex has not been the center of attention in research of depression. There are no obvious differences in the number of neurons and glial cells in the somatosensory cortex between depressed patients and controls[71]. However, increased internal connectivity has been found in the somatosensory cortex of late life depressed people[148] and a decrease in interhemispheric connectivity has been found in the sensory system[149]. Depressed patients with anxiety have shown more gray matter volume in the primary somatosensory compared to control[150]. Thus, together with the presented findings, the role of the somatosensory cortex involvement in depression is inconclusive.

*NR2A trend in the cingulate cortex*

A trend of a higher concentration of the NMDAR subunit NR2A was found in the helpless rats compared to the non-helpless rats in the cingulate cortex. This is in accordance with a study showing a decrease in anxiety- and depressive-related behavior in NR2A knock-out mice[151]. Whether this decrease in anxiety and depressive behavior is due to changes in the cingulate cortex is, however, unclear.

***NR2A in animals with depression-like symptoms.*** In accordance with resilient animals having lower levels of NR2A in the cingulate cortex, functional uncoupling of NR2A from PSD95 in the PFC of rats maternally separated led to a decrease in anxiety[152], which is highly comorbid with depression[8, 13]. Contrary to these findings, a decrease in the NR2A subunit concentration was found in prenatally stressed rats. However, the whole of the PFC and the hippocampus have been investigated[153, 154]. Although NR2A subunit concentrations are downregulated in some areas of the brain in animals with depression-like symptoms, a complete knock-out of NR2A helps to avert depression-like symptoms. How NR2A upregulation in the cingulate cortex affects behavior is not known, but a study has investigated overexpression in forebrain regions.

***Memory function in depression.*** Overexpression of NR2A in forebrain regions, including most likely the anterior parts of the cingulate cortex, impairs social recognition, olfactory memory[155], and long-term memory[156]. However, patients with MDD do not show strong impairments of memory function, especially not long-term memory. Impairments measured are more often attributed to attention deficits and lack of motivation[157]. In congenital helpless rats, learning deficits are not observed[51]. A lesion of the ACC alone does not impair spatial memory performance[158], nor discrimination learning in rats[159]. The observed impairments in memory function might therefore stem from other forebrain regions, not necessarily the ACC. Nevertheless, NR2A is implicated in behavioral mechanisms, and changes in its concentration can alter brain functioning.

***NR2A and information processing.*** In general, an increase in NR2A could either be due to an increase in NMDARs, or a different subunit composition of NMDARs in helpless animals. Because no significant difference was detected in NR1 concentrations, a change in subunit composition seems more plausible. NMDARs with different subunit compositions have different electrophysiological characteristics. Higher NR2A levels in cortical neurons lead to shorter, but stronger EPSCs[78]. This decreases the neuron's ability for temporal integration of incoming signals[160]. A higher concentration of NR2A, as measured here, might therefore alter information processing within the ACC.

***Connectivity and function of the ACC.*** The ACC receives input from both the posterior parietal cortex (PPC) and the dlPFC. Interestingly, they project in alternating columns to the layers of the ACC[161]. An impairment in temporal integration of signals might therefore impair integration of information from the PPC, implicated in spatial perception of oneself, and the dlPFC, implicated in working memory. Considering the ACC's role in decision making, problems in integrating internal and external information could contribute to the increased decision latencies found in depressed patients[162]. Another connection of the ACC is the one projecting to motor areas[44]. The dACC is implicated in action initiation[163], and a positive correlation between the activity of the dACC and psychometric retardation has been found in depressed patients[164]. Hence, increased NR2A levels in the ACC might contribute to the symptom of psychomotor retardation.

The discussed findings implicate glutamatergic synapses in the primary motor cortex, somatosensory cortex and possibly the cingulate cortex in depression. This interpretation is discussed in the next section with regards to limitations in the study design and methodology.

## 4.2 Limitations

### 4.2.1 Study design

*Learned helplessness procedure*

Research on learned helplessness is commonly done with animals. However, using an animal model presents some issues that will now be discussed. Depression in humans is defined in very broad terms and characteristics of depression include contrary symptoms, such as weight loss and weight gain. Because the disease pattern of depressive disorders is not very coherent, applying such a diagnosis to an animal is problematic, especially as the main symptoms, depressed mood and anhedonia, are difficult to test for in animals. Sucrose tests with animals, which underwent weight loss beforehand, are suboptimal to prove anhedonic behavior in rodents. Nevertheless, cLH rats show other symptoms of depression and biological changes similar to those found in humans[50].

The rats used for this project were only tested for their helplessness and based on these results, divided into two groups. Although other symptoms of depression could have been present, this was not assessed. Taking into account that these animals also have a genetic background, which is more stress resilient or more stress susceptible as they were bred for at least 40 generations, the probability for the rats having other symptoms of depression is high. Nevertheless, it would have been preferable to test for anhedonia in all animals used in this project to support the assumption that the rats can be regarded as modelling depression.

Another drawback of the current study was that the criteria of helplessness was not fulfilled for one of the rats. The cut-off for helpless animals was set to failing to press the lever for more than 10 out of 15 times, while one of the rats put into the helpless group (rat number 3) failed only 9 out of 15 times. Although it is only a slight deviation, it might have increased variability in the helpless group. To test this, the standard deviation of the helpless group has been calculated several times, each time removing one of the samples and calculating the change in standard deviation compared to all of the samples included. Removing sample 3 from standard deviation calculations, decreased the standard deviation in the cingulate cortex by around 12 %, and in the hippocampus by around 11 %. Compared to the removal of other samples, these values did not stand out. An increase in variability due to rat 3's insufficient compliance with the criteria is therefore less likely (see Appendix C.1 for details).

*Missing control group*

All rats used in this project underwent the learned helplessness procedure, meaning inescapable random foot shocks were applied to all of them. Because all animals were exposed to stress, changes in the brain due to the stress cannot be investigated here, and have not been in the focus of this study. Rather, the different coping mechanisms of the animals, and

the underlying neurological changes are of interest. Not all humans exposed to extreme stress will develop depression, just as not all rats undergoing the learned helplessness procedure will develop depressive symptoms. Stress itself has been shown to lead to synaptic changes in different brain areas[165-168], but the question is, whether synapses change differently in helpless compared to non-helpless animals. Additionally, prior to the stress procedure, the neurological architecture might already show differences between the two groups. As another study stated[140], resilience and susceptibility to stress can be seen as a strain, and control animals cannot be checked for this. Many studies investigating depression in animal models compare 'depressed' animals with controls. It is therefore difficult to distinguish changes due to stress in general and changes due to a depressive syndrome. Here, control animals have not been included as no information would be gained regarding stress resilience and susceptibility.

*Diversity of the cingulate cortex*

The ACC has been in focus for this thesis, but significant differences in protein concentrations in this region could not be found. The reason for this could be that there are no differences to be found, or at least not for the proteins tested. However, the ACC shows changes in functional connectivity as well as regional blood flow in imaging studies. Glutamatergic synapses are highly abundant in the cortex[169], and changes in PSD95, an anchoring protein at excitatory synapses, have been found in depressed patients[68]. However, it might be helpful to look at the sub-regions of the cingulate cortex in more detail in further experiments due to their diversity. The Cg1 and Cg2, which were dissected for the study, correspond to Brodmann area 24a and 24b. Distinctions between the caudal and the rostral part of these areas have been found. Therefore, the caudal part, 24a' and 24b', are now considered as being part of the midcingulate cortex, while 24a and 24b are considered as part of the ACC. In addition, a dorsal and a ventral distinction of the ACC has been found, with distinct connections and functions. Using sub-regions of the ACC for western blots could make it easier to detect differences.

*Ventral and dorsal hippocampus*

No differences in the hippocampus have been found between the resilient and susceptible rats. The same logic applies here as for the ACC. In a study comparing resilient with stress susceptible mice, changes in AMPAR subunits in the hippocampus have been found. The stress paradigm consisted of social stress in mice, not inescapable random shocks in rats. Another difference was how the mice were divided into the groups. As opposed to using a behavioral test, corticosterone levels have been measured. Mice with persistent high corticosterone levels in the morning, five weeks after the stress procedure, were considered as stress susceptible animals. Mice with baseline corticosteroid levels were, on the other hand, viewed as stress resilient[140]. This approach makes sure that some neurobiological changes took place,

but whether this is a better indicator for a depressive disorder is questionable. In the mentioned study, hippocampal areas (CA1, CA2, CA3, DG) were tested separately, opposed to the whole hippocampus, as hippocampal subareas often respond differently to stress. The same is true for the ventral-dorsal axis of the hippocampus. Under normal conditions, the probability for LTP is higher in the dorsal part of the hippocampus, which is more associated with cognition, than in the ventral part, which is more associated with emotions. Acute stress exposure facilitates LTP in the ventral hippocampus, while decreasing the probability of LTP in the dorsal part[170]. If the hippocampus reacts differently in different regions to stress, depression might also manifest itself differently along the ventral-dorsal axis.

### 4.2.1 Methodology

*Sample preparation*

The protein yield was very low in most of the samples. This could be due to hand homogenization, which results in relatively inefficient protein yield, when compared to other methods[171]. In addition, protein concentrations varied considerably across samples (see Appendix C.2). The high variability of protein concentrations of the different samples, despite being adjusted according to the measured values of the Bradford protein assay, made it difficult to find the best antibody concentration. While some of the samples show almost oversaturation, others are very weak, and have a decreased signal-to-noise ratio.

In other studies, tissue of small areas of one experimental group are sometimes pooled, to yield a higher protein concentration. The drawback of this is a loss of information, as the variability within each group cannot be detected. Running the samples of each rat separately proved to be very important here as the variability in concentration of tested proteins within each group was so high. It should be noted, that the inability to detect a difference between the two groups was not due to overall similar concentrations, but were due to the differences in concentrations found between each of the samples. Pooling the samples might therefore have led to a loss of information.

To load the wells of the gels with the same amount of protein, protein concentrations of the 40 samples were measured with a Bradford protein assay. The absolute protein concentration was considered as the average of two measurements. Thus, all measurements could be done on the same titer plate and calculated with the same standard curve. Still, more replicates of measurement would have improved accuracy of the calculated protein concentrations.

*Actin as a loading control*

To ensure that an actual difference in the concentration of a specific protein is being detected, and not the loaded amount of sample, loading controls are a necessity in western blots. Here, anti-actin antibodies were used. Actin is a so-called housekeeping gene (HKG), being abundant and assumedly stable for different tissues and conditions. It is therefore commonly used as a loading control in western blot.

However, it has been shown that there is a high variability in actin concentration in different tissues[172], and between different brain regions[173]. The actin concentration differs during development and in different experimental conditions[173]. β-tubulin, another common loading control, shows different concentrations in post-mortem samples of schizophrenic patients, most notably in the ACC[174]. Therefore, changes in cytoskeletal structures in mood disorders are possible. However, a post-mortem study in schizophrenia found no significant difference of actin in the ACC, dlPFC, hippocampus and primary visual cortex[175]. In depressed human patients, blood plasma analysis showed no significant difference in actin concentration compared to controls[176]. Whether there is a change in protein levels within the brain has not been established.

When compared with other, common loading controls, actin proved to be one of the most stable ones[177], especially in hippocampal and striatal tissue[178]. Conversely, in a study analyzing the accuracy and precision of several different loading controls for quantitative polymerase chain reaction (qPCR), actin performed as one of the worst, together with other common loading controls. The expression level of actin had one of the highest variabilities, and when analyzing measurements, different significant results were obtained, depending on which loading control was used for normalization[179]. In qPCR, expression levels are of interest, not the actual protein levels, so translatability to western blots is questionable. Nevertheless, western blot studies have found a high coefficient of variation with actin-binding, and a low coefficient of correlation with the actual protein concentration[180]. Analyzes showed a high variability of actin binding in this thesis, as well (see Appendix C.3)

Other questions concerning loading controls, are when the signal saturates and how long the linear range of the housekeeping protein is. Actin is very abundant, while proteins of interest like PSD95 are less abundant. Thus, the linear range of the two, might not be around the same total protein load. Depending on the type of tissue, different ranges of linearity have been found. The cytosolic fraction of HzAm1 cells (which are cells from the cotton bollworm, *Helicoverpa zea*) had a linearity range of actin between 0.7 and 1.9 µg of total protein[181]. Monoclonal β-actin antibody-binding to the cytosolic fraction breast cancer cells saturated at 0.47 µg of total protein[182].

For this study, the linearity of protein concentration and signal intensity for each antibody has been determined as well. Actin seems to become saturated at 4 µg. It has to be taken into consideration that the graph (fig. 3.6) only depicts values of one measurement, so no replicates have been done. Additionally, due to a limitation in sample volume, the original samples have not been used for this analysis. Instead, practice material consisting of the synaptosomal fraction of whole rat brains was used.

*The issue of normalization*

Incubating the membrane in separate tubes was necessary to ensure an accessibility of the membrane for the antibody solution. Although membrane stripes have been treated the same way, with the same antibody solutions, the same washing procedure and the same exposure time, overall staining differences were evident. All measured values have therefore been normalized to sample 1 on the same membrane stripe. Sample 1 was chosen as it showed strong staining and the smallest standard deviation, though it has to be noted that too high measurements outside the linear range can increase variability after normalization as well. Fixed point normalization increases specificity, but decreases sensitivity. This increases the number of false negatives[183].

## 4.3 Evaluating findings

Differences have been found in several areas of the helpless rats compared to resilient rats. Whether these results are valid has to be considered in more depth. The blots obtained for the significant results and for the trend show some flaws, which could alter the mean in each group. Especially, GluA1 staining of the S1 samples is highly irregular, and results for the difference in GluA1/GluA2 ratio of S1 should therefore not be relied on. The correlation of GluA2 and actin was relatively low as well, thus making it more probable that normalization skewed the relative protein concentration. The same is true for the correlation between NR2A and actin. Hence, the NR2A trend within the cingulate cortex should be considered carefully. The third run shows a difference in the staining pattern of actin, which could increase the relative concentration in the helpless group, and decrease the one in the resilient group. In general, actin showed very weak staining, and as the signal-to-noise ratio decreases with weaker staining, variability increases[183]. For PSD95 in the motor cortex, actin staining is strong, but might be oversaturated. However, when normalizing the PSD95 concentration to other regions of interest, such as the somatosensory cortex and hippocampus, a significantly higher concentration in cLH compared to cNLH rats was still obtained.

# 5 Conclusion

In this project, increased concentrations of PSD95 in the primary motor cortex of an animal model of depression have been found. This change might underlie the depression symptom of psychomotor retardation found in depressed humans. A mechanism that could have led to this increased concentration is an impairment of synaptic scaling. A trend of increased NMDAR subunit NR2A concentration in the Cg1 and Cg2 region of the rat has been found as well. Considering the connectivity between these two regions, a causal relation between these two results might exist, but awaits to be tested.

# 6 Appendix

## Appendix A

A.1 Bradford Protein Assay

A protein BSA (bovine serum albumin) standard with known concentration was diluted 1:2 with distilled water in five steps for the protein standard curve. Samples were diluted 1:10 with distilled water. Ten µl of each standard and sample as well as a blank were pipetted into the wells of a 96 well microplate, as shown in tab. 5.1. A mixture of 250 µl Solution A and 5 µl Solution S was prepared. In each well, 25 µl of the mixture was added. Subsequently, 200 µl of Solution B was added in each well with a mulitpipet. The microplate was mixed on a plate rocker for 15 minutes and bubbles were destroyed with pipet tips. Absorbance was measured at 750nm. The blank was subtracted from each measurement and the average was calculated for each standard and sample. A linear trendline was generated using the standard protein concentrations and the measured absorption after subtraction of the blank (fig. 5.2). The formula of the linear trendline was used for calculating the protein concentration of the samples. This was done in Excel.

*Table 6.2* Pipetting of standards and samples into the wells. Standard 2 was a dilution of Standard 1 with an equal part of water, Standard 3 a dilution of Standard 2 with an equal part of water, etc. S1 = Crude synaptosomal fraction of somatosensory cortex of rat 1, M = Motor cortex, H = Hippocampus, C = Cingulate Cortex; 1-10: rats (1-5 helpless, 6-10 resilient).

| | 1 | 2 | 3 | 4 | 5 | 6 | 7 | 8 | 9 | 10 | 11 | 12 |
|---|---|---|---|---|---|---|---|---|---|---|---|---|
| **A** | Blank | Blank | S1 | S2 | S3 | S4 | S5 | S6 | S7 | S8 | S9 | S10 |
| **B** | Standard 1 | Standard 1 | S1 | S2 | S3 | S4 | S5 | S6 | S7 | S8 | S9 | S10 |
| **C** | Standard 2 | Standard 2 | M1 | M2 | M3 | M4 | M5 | M6 | M7 | M8 | M9 | M10 |
| **D** | Standard 3 | Standard 3 | M1 | M2 | M3 | M4 | M5 | M6 | M7 | M8 | M9 | M10 |
| **E** | Standard 4 | Standard 4 | H1 | H2 | H3 | H4 | H5 | H6 | H7 | H8 | H9 | H10 |
| **F** | Standard 5 | Standard 5 | H1 | H2 | H3 | H4 | H5 | H6 | H7 | H8 | H9 | H10 |
| **G** | Standard 5 | Standard 6 | C1 | C2 | C3 | C4 | C5 | C6 | C7 | C8 | C9 | C10 |
| **H** | Standard 6 | Standard 6 | C1 | C2 | C3 | C4 | C5 | C6 | C7 | C8 | C9 | C10 |

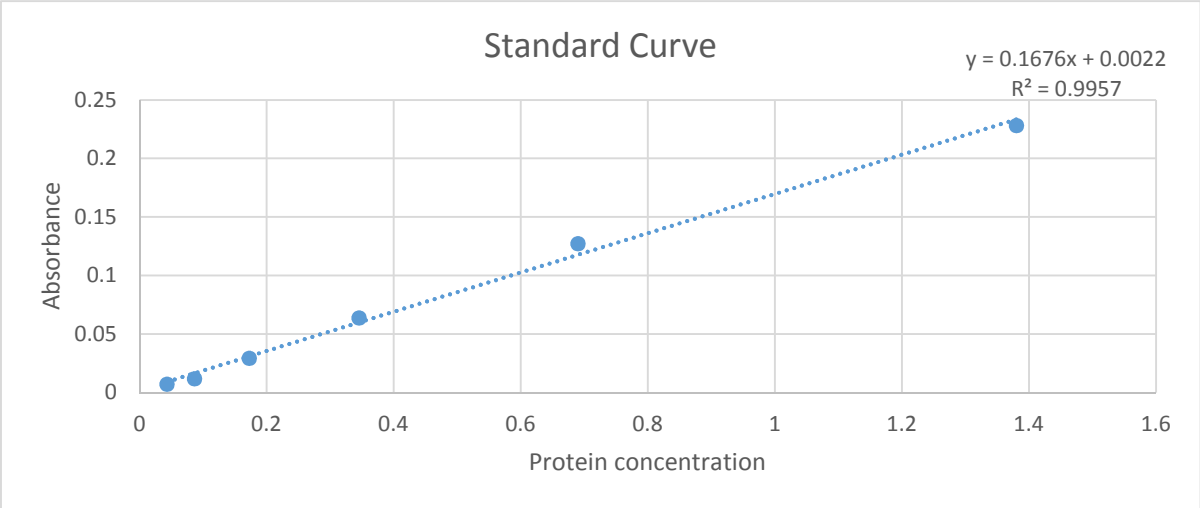


*Figure 6.1* Plot of the standard curve with linear trendline, formula for trendline and $R^2$ of the Bradford Protein Assay. Absorbance was measured at 750nm. Absorbance values were subtracted by blank, mean of subtracted absorbance was plotted against known protein concentration.

A.2 *Details of antibodies used. Mol.w. = molecular weight (in kilodalton).*

| Protein | Type | Dilution | Mol.w. | Producer | Product# | Lot# |
|---|---|---|---|---|---|---|
| **NMDAR2A** | Rabbit monoclonal | 1:500 | 165 | Abcam | ab133265 | GR88453-12 |
| **NMDAR2B** | Rabbit polyclonal | 1:1 500 | 166 | Abcam | ab65783 | GR310911-1 |
| **GluA1** | Rabbit polyclonal | 1:1 000 | 102 | Abcam | ab31232 | GR231799-1 |
| **GluA2** | Rabbit polyclonal | 1:1 000 | 100 | Alomone labs | AGC-005 | AN0302 |
| **NMDAR1** | Rabbit monoclonal | 1:1 000 | 105 | Abcam | ab109182 | GR207980-19 |
| **PSD95** | Rabbit polyclonal | 1:1 000 | 95 | Abcam | ab18258 | GR295786-1 |
| **Actin** | Mouse monoclonal | 1:1 000 | 43 | Millipore | MAB1501 | 25088783 |
| **VAMP2** | Rabbit polyclonal | 1:1 000 000 | 19 | Abcam | ab3347 | GR280715-3 |
| **Histone H3** | Rabbit monoclonal | 1:5 000 | 17 | Cell Signaling Technology | 4499 | 9 |
| **anti-rabbit peroxidase conjugated** | Goat polyclonal | 1:15 000 | --------- | Thermo Fisher | 31460 | SA245916 |
| **anti-mouse peroxidase conjugated** | Goat polyclonal | 1:20 000 | --------- | Thermo Fisher | 31430 | SA245916 |

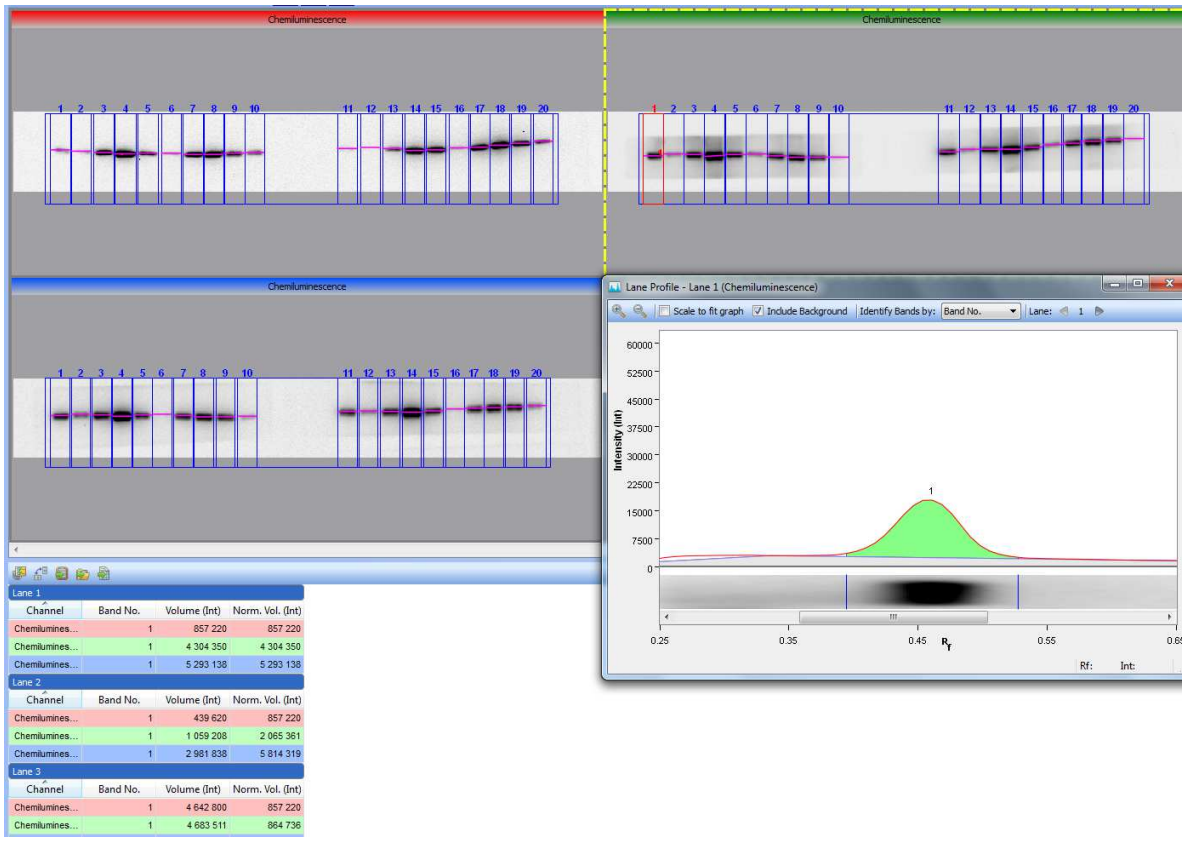


A.3 *Image Lab software. Red channel (upper left corner) is actin and chosen as normalization channel.*

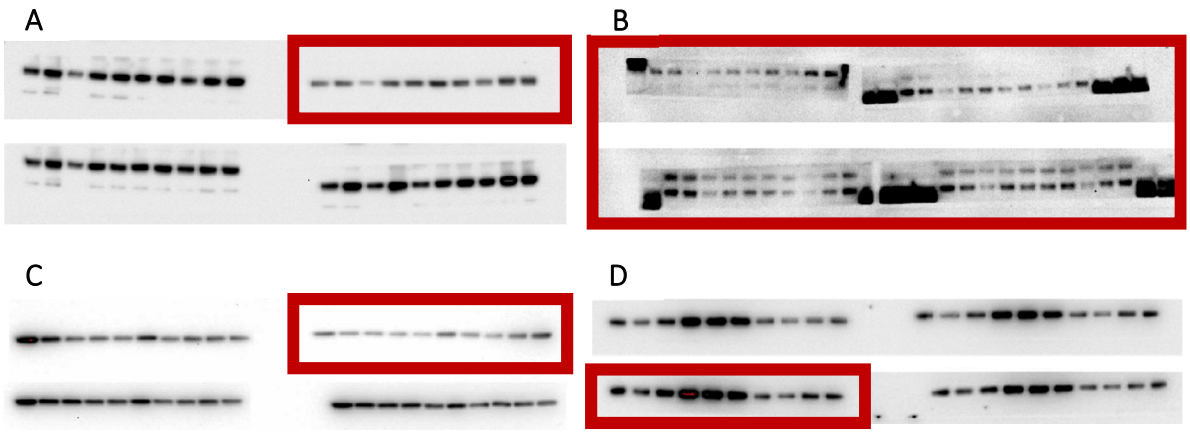


A.4 *Examples of selection of the best three runs. Red boxes indicate which run was kicked out. A run 2 is weaker than the other three. B Unstable staining and different staining of the different runs. Redo of 4 runs. C weak staining, and different staining pattern. D slightly oversaturated.*

# Appendix B

B.1 *Latencies of learned helpless test in seconds. Each column is a different animal (1-5 helpless, 6-10 resilient). Provided by Barbara Vollmayr.*

| | **1** | **2** | **3** | **4** | **5** | **6** | **7** | **8** | **9** | **10** |
|---|---|---|---|---|---|---|---|---|---|---|
| **Trial 1** | 2.1 | 45.8 | 5.8 | 3.5 | 17.2 | 8.1 | 12.2 | 17.3 | 5.1 | 20.8 |
| **Trial 2** | 1.7 | 60 | 60 | 8.9 | 24.3 | 0.6 | 16.3 | 14.9 | 2.1 | 28.4 |
| **Trial 3** | 4.9 | 60 | 32.1 | 7.8 | 60 | 1.5 | 4.5 | 0.7 | 10.6 | 1.9 |
| **Trial 4** | 60 | 60 | 0.5 | 55.7 | 60 | 2 | 21.9 | 12.9 | 0.3 | 7.8 |
| **Trial 5** | 60 | 23 | 21.9 | 60 | 54 | 0.1 | 0.9 | 3.3 | 11.8 | 5.6 |
| **Trial 6** | 53.5 | 9.6 | 15 | 60 | 60 | 8.7 | 19.2 | 5.4 | 0.5 | 2.1 |
| **Trial 7** | 60 | 47.4 | 40.8 | 60 | 23.2 | 1 | 19.5 | 10.5 | 0.5 | 0.2 |
| **Trial 8** | 60 | 60 | 29.8 | 60 | 26.4 | 0.2 | 15.3 | 8.4 | 0.8 | 6.8 |
| **Trial 9** | 10.5 | 60 | 5.2 | 60 | 60 | 3.2 | 3.2 | 3.7 | 11.9 | 1.3 |
| **Trial 10** | 60 | 60 | 22.5 | 60 | 60 | 12.6 | 6.7 | 0.8 | 7.3 | 1.2 |
| **Trial 11** | 60 | 60 | 60 | 60 | 60 | 25.1 | 2 | 1.8 | 25.5 | 9.3 |
| **Trial 12** | 60 | 60 | 42.1 | 44.9 | 60 | 7.9 | 3.7 | 6.5 | 2.1 | 15.2 |
| **Trial 13** | 60 | 60 | 0.4 | 14.7 | 15.7 | 10.5 | 3.8 | 6.9 | 1.5 | 0.8 |
| **Trial 14** | 60 | 60 | 27.7 | 60 | 55.3 | 4 | 7.8 | 0.3 | 4.3 | 0.3 |
| **Trial 15** | 60 | 60 | 17.5 | 60 | 45.8 | 0.8 | 0.4 | 4.5 | 3.4 | 0.6 |
| **Sum Latency** | 672.7 | 785.8 | 381.3 | 675.5 | 681.9 | 86.3 | 137.4 | 97.9 | 87.7 | 102.3 |
| **Failed trials** | 11 | 14 | 9 | 11 | 13 | 1 | 1 | 0 | 1 | 2 |

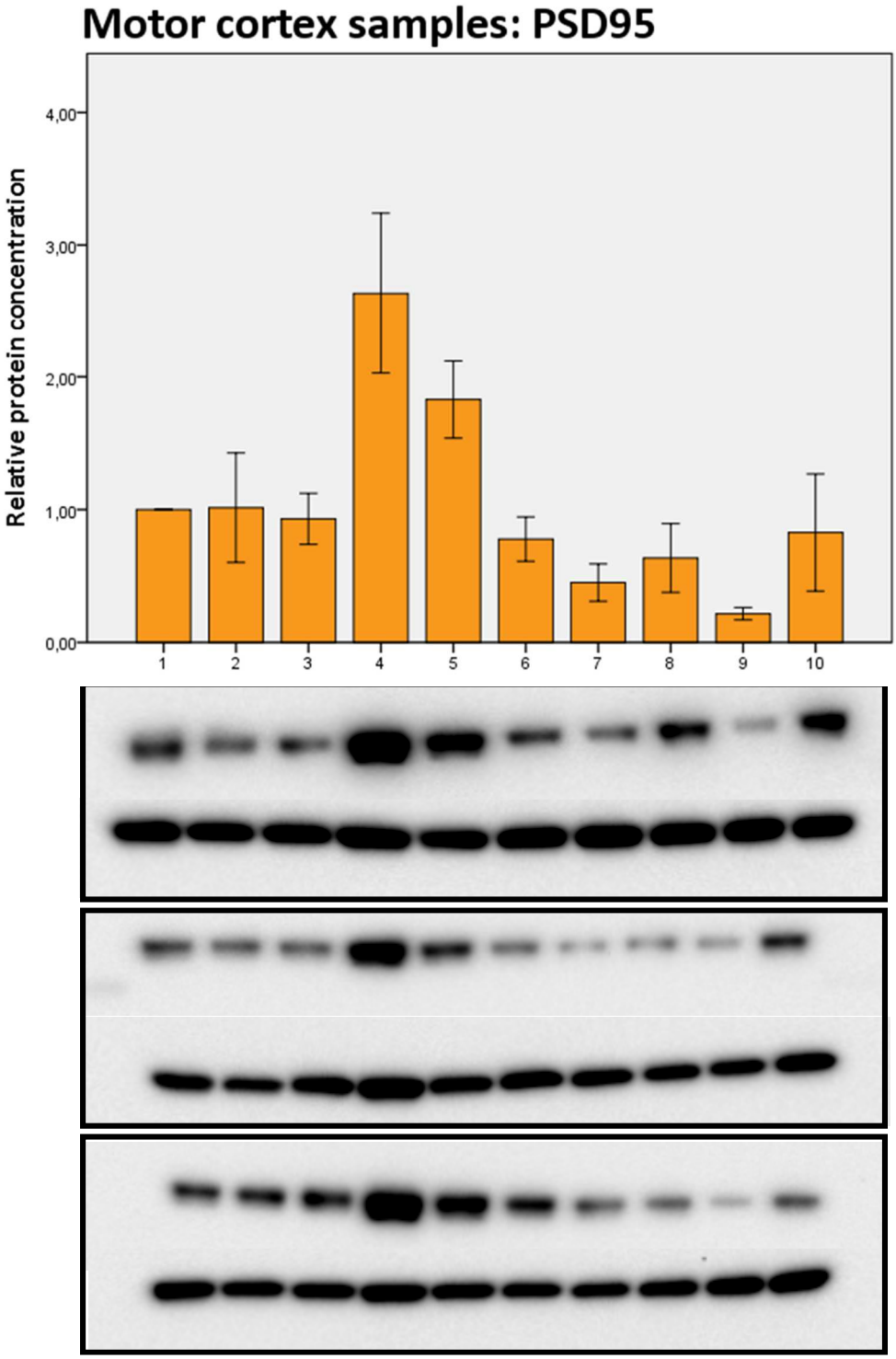


B.2 *Bar plot shows relative PSD95 protein concentrations in the primary motor cortex. (1-5: helpless; 6-10: resilient). Error bars show mean of the three runs ± 2 SE. Images below show the three separate runs, indicated as boxes. The first is from a separate blot, the last two from the same one, but they were incubated separately. The first stripe in each box is PSD95 antibody binding, the second stripe is actin binding. The binding pattern is relatively equal, and actin bands are strong. (Exposure time: 172.270 sec)*

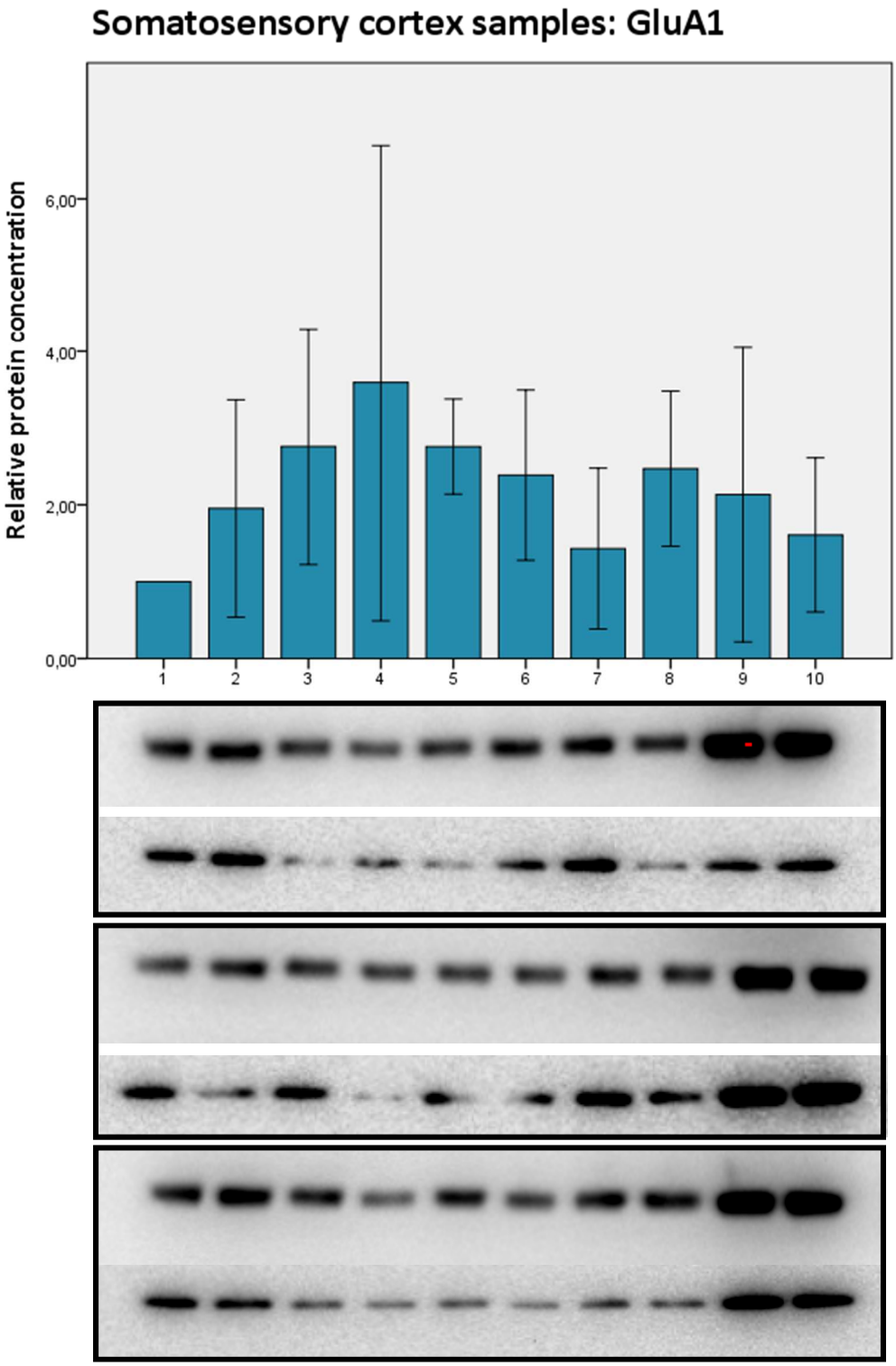


B.3 *Bar plot shows relative GluA1 protein concentrations in the primary somatosensory cortex. (1-5: helpless; 6-10: resilient). Error bars show mean of the three runs ± 2 SE. Images below show the three separate runs, indicated as boxes. The first two are from the same blot, but incubated separately, while the third box is from another blot. The first stripe in each box is GluA1 antibody binding, the second stripe is actin binding. Binding of actin is weak, and unsteady across blots. (Exposure time: 341.659 sec)*

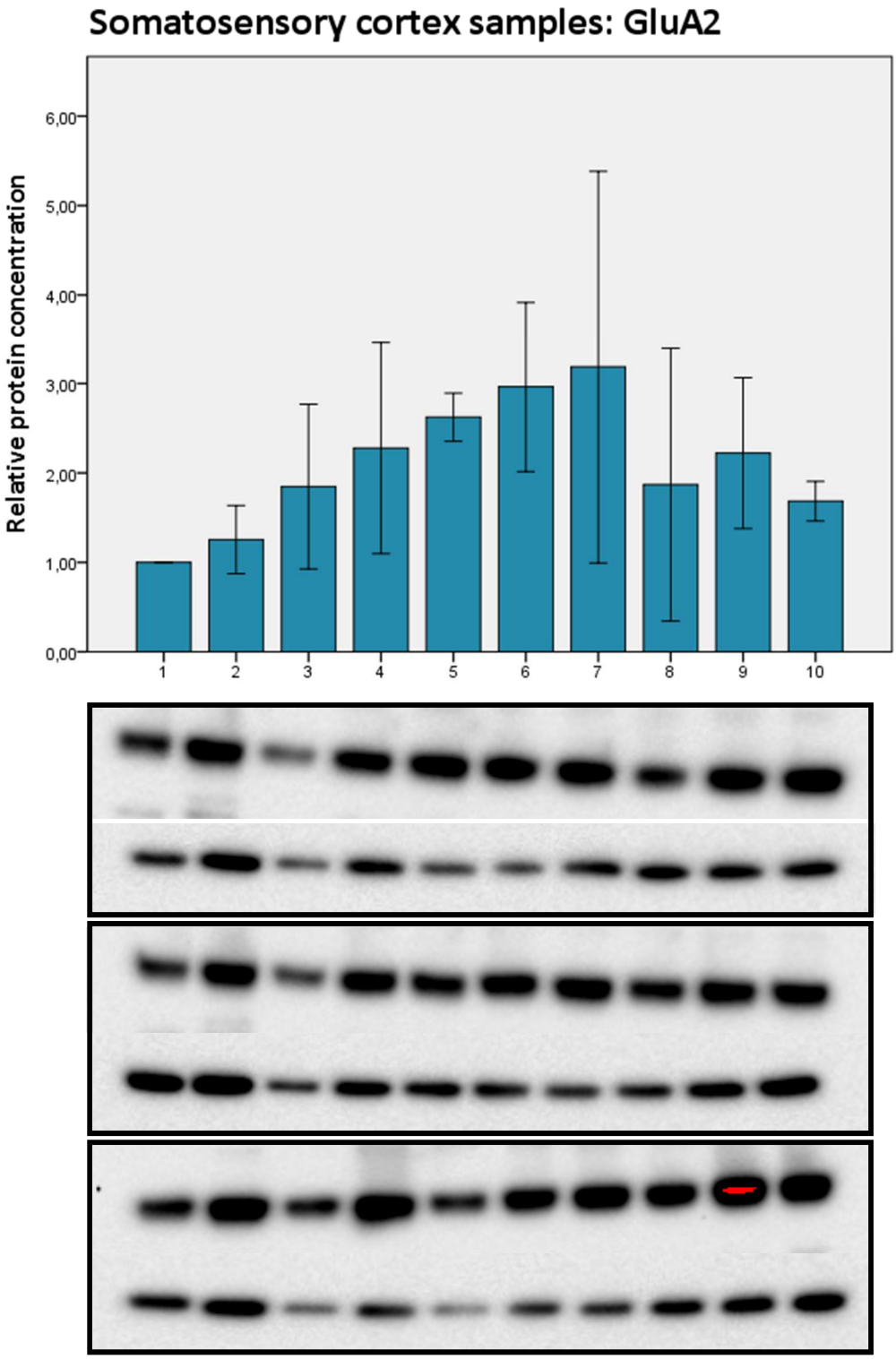


B.4 *Bar plot shows relative GluA2 protein concentrations in the primary somatosensory cortex. (1-5: helpless; 6-10: resilient). Error bars show mean of the three runs ± 2 SE. Images below show the three separate runs, indicated as boxes. The first box is from a separate blot, the other two boxes are from the same blot, but incubated separately. The first stripe in each box is GluA2 antibody binding, the second stripe is actin binding. The binding pattern of actin is unsteady across blots. In the last blot, sample 9 is oversaturated. (Exposure time: 254.096 sec)*

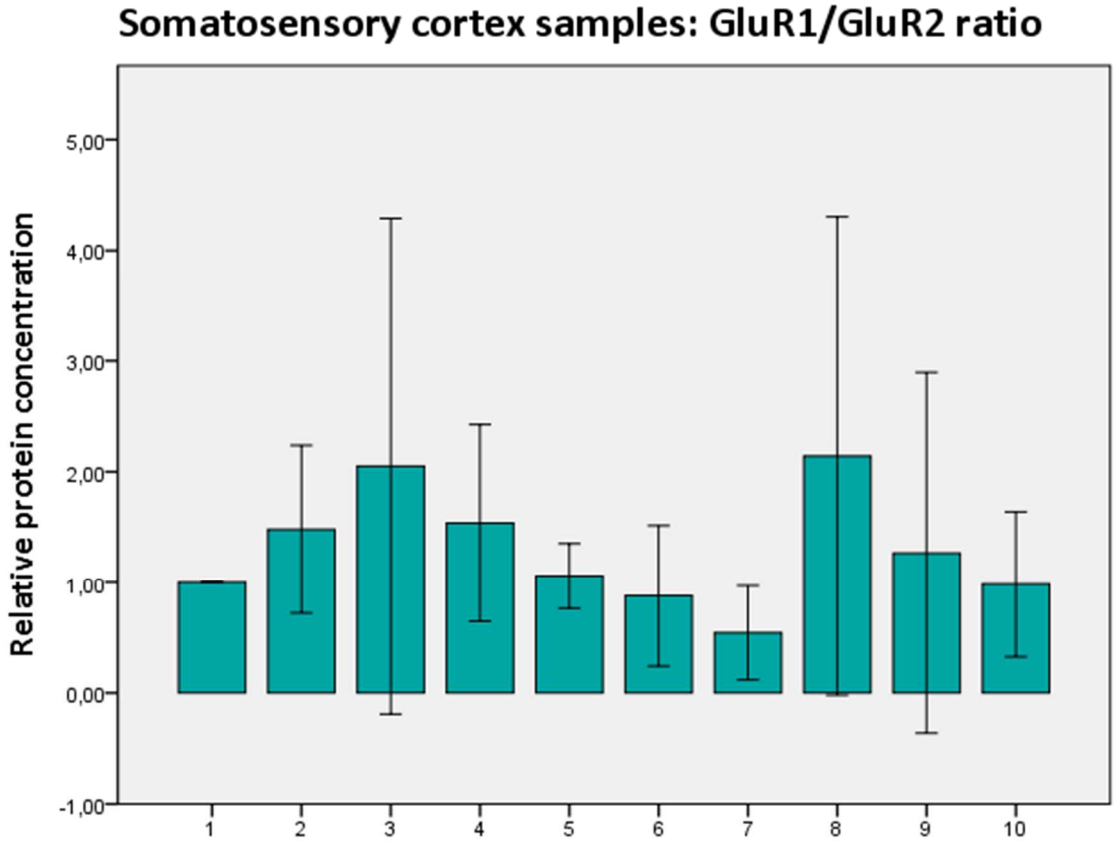


B.5 *Bar plot shows GluA1/GluA2 ratio of primary somatosensory cortex samples. (1-5: helpless; 6-10: resilient). Error bars show mean ± 2 SE.*

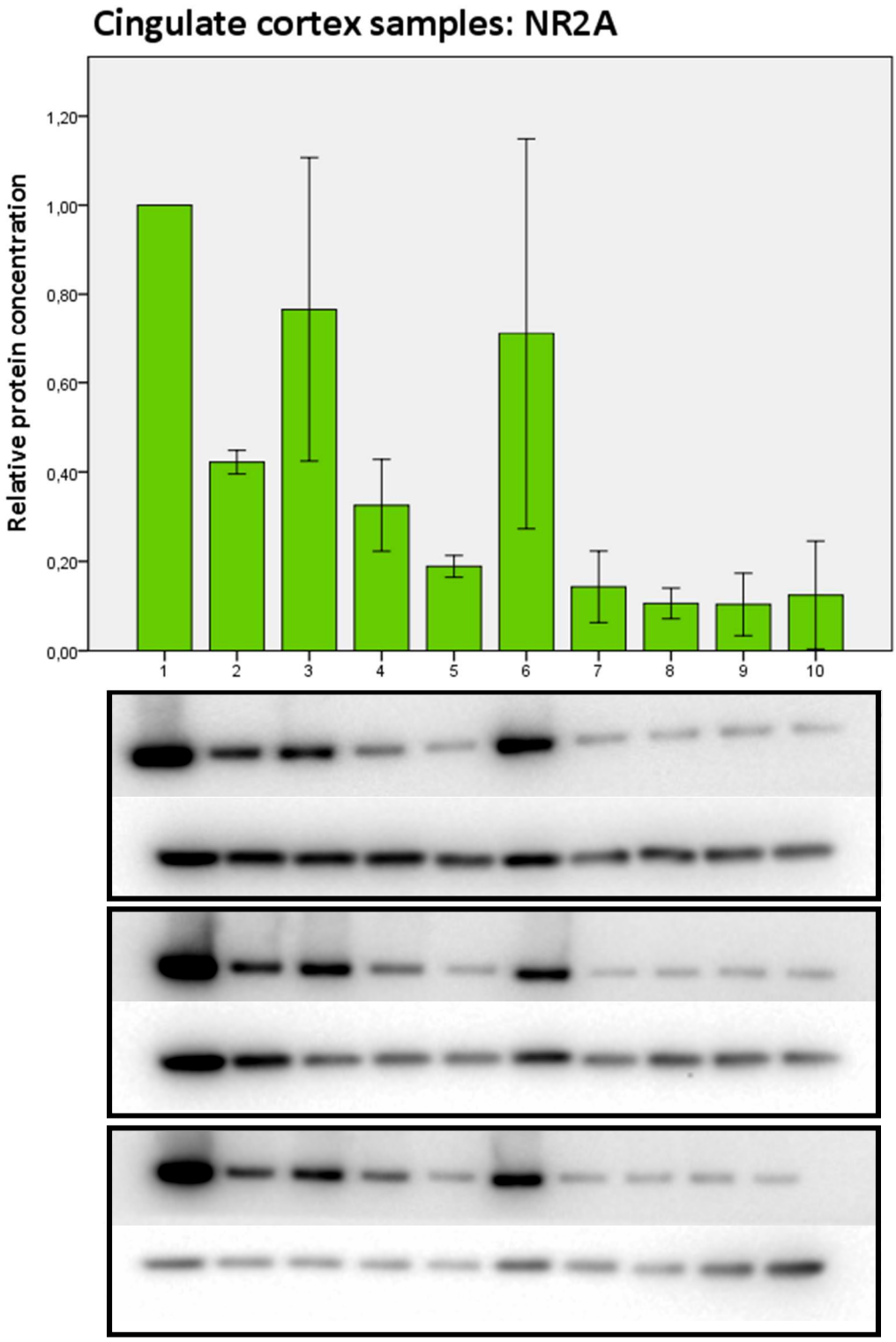


B.6 *Bar plot shows relative NR2A protein concentrations in the cingulate cortex. (1-5: helpless; 6-10: resilient). Error bars show mean of the three runs ± 2 SE. Images below show the three separate runs, indicated as boxes. The first two are from the same blot, but were incubated separately. The first stripe in each box is NR2A antibody binding, the second stripe is actin binding. Note the different binding pattern of actin for the last run. (Exposure time: 213.178 sec)*

B.7 *Non-significant results of statistical analysis using the means of three measurements. Samples of helpless (n=5) and resilient (n=5) animals, of each area separately, were analyzed for each protein and several ratios of proteins were analyzed. h=helpless, r=resilient, mdn=median. P = exact significance of Mann-Whitney U test*

| Area | Protein | h (mdn) | r (mdn) | U | z | p |
|---|---|---|---|---|---|---|
| **Cingulate** | NMDAR2A | 7.4 | 3.6 | 3 | -1.984 | 0.056 |
| **Cingulate** | NMDAR2B | 5.4 | 5.6 | 13 | 1.104 | 1.000 |
| **Cingulate** | NMDAR1 | 5.6 | 5.4 | 12 | -0.104 | 1.000 |
| **Cingulate** | GluA1 | 4.6 | 6.4 | 17 | 0.940 | 0.421 |
| **Cingulate** | GluA2 | 6.6 | 4.4 | 7 | -1.149 | 0.310 |
| **Cingulate** | PSD95 | 6.8 | 4.2 | 6 | -1.358 | 0.222 |
| **Cingulate** | VAMP | 4.2 | 6.8 | 19 | 1.358 | 0.222 |
| **Cingulate** | GluA1/GluA2 | 4 | 7 | 20 | 1.567 | 0.151 |
| **Cingulate** | NMDAR2A/NMDAR2B | 7.2 | 3.8 | 4 | -1.776 | 0.095 |
| **Hippocampus** | NMDAR2A | 6.8 | 5.2 | 11 | -0.313 | 0.841 |
| **Hippocampus** | NMDAR2B | 6.6 | 4.4 | 7 | -1.149 | 0.310 |
| **Hippocampus** | NMDAR1 | 4.8 | 6.2 | 16 | 0.731 | 0.548 |
| **Hippocampus** | GluA1 | 5.8 | 5.2 | 11 | -0.313 | 0.841 |
| **Hippocampus** | GluA2 | 6.8 | 4.2 | 6 | -1.358 | 0.222 |
| **Hippocampus** | PSD95 | 5.4 | 5.6 | 13 | 0.104 | 1.000 |
| **Hippocampus** | VAMP | 5.4 | 5.6 | 13 | 0.104 | 1.000 |
| **Hippocampus** | GluA1/GluA2 | 5 | 6 | 15 | 0.522 | 0.690 |
| **Hippocampus** | NMDAR2A/NMDAR2B | 5.8 | 5.2 | 11 | -0.313 | 0.841 |
| **Motor*** | NMDAR2A* | 0.9092* | 0.8993* | t(7.997)=0.018* | | 0.986* |
| **Motor** | NMDAR2B | 5 | 6 | 15 | 0.522 | 0.690 |
| **Motor** | NMDAR1 | 4.4 | 6.6 | 18 | 1.149 | 0.310 |
| **Motor** | GluA1 | 5.2 | 5.8 | 14 | 0.313 | 0.841 |
| **Motor** | GluA2 | 7.2 | 3.8 | 4 | -1.776 | 0.095 |
| **Motor** | PSD95 | 8 | 3 | 0 | -2.611 | **0.008** |
| **Motor** | VAMP | 4.2 | 6.8 | 19 | 1.358 | 0.222 |
| **Motor** | GluA1/GluA2 | 4.6 | 6.4 | 17 | 0.940 | 0.421 |
| **Motor** | NMDAR2A/NMDAR2B | 5.4 | 5.6 | 13 | 0.104 | 1.000 |
| **Somatosensory** | NMDAR2A | 6 | 5 | 10 | -0.522 | 0.690 |
| **Somatosensory** | NMDAR2B | 6.8 | 4.2 | 6 | -1.358 | 0.222 |
| **Somatosensory** | NMDAR1 | 5 | 6 | 10 | 0.522 | 0.690 |
| **Somatosensory** | GluA1 | 6.4 | 4.6 | 10 | -0.940 | 0.421 |
| **Somatosensory** | GluA2 | 4.4 | 6.6 | 18 | 1.149 | 0.310 |
| **Somatosensory** | PSD95 | 5.8 | 5.2 | 11 | -0.313 | 0.841 |
| **Somatosensory** | VAMP | 4.6 | 6.4 | 17 | 0.940 | 0.421 |
| **Somatosensory** | GluA1/GluA2 | 7.6 | 3.4 | 2 | -2.193 | **0.032** |
| **Somatosensory** | NMDAR2A/NMDAR2B | 5.8 | 5.2 | 11 | -0.313 | 0.841 |

*Samples of each group (helpless, resilient) were normally distributed. Values show results of an independent samples t-test, two-tailed

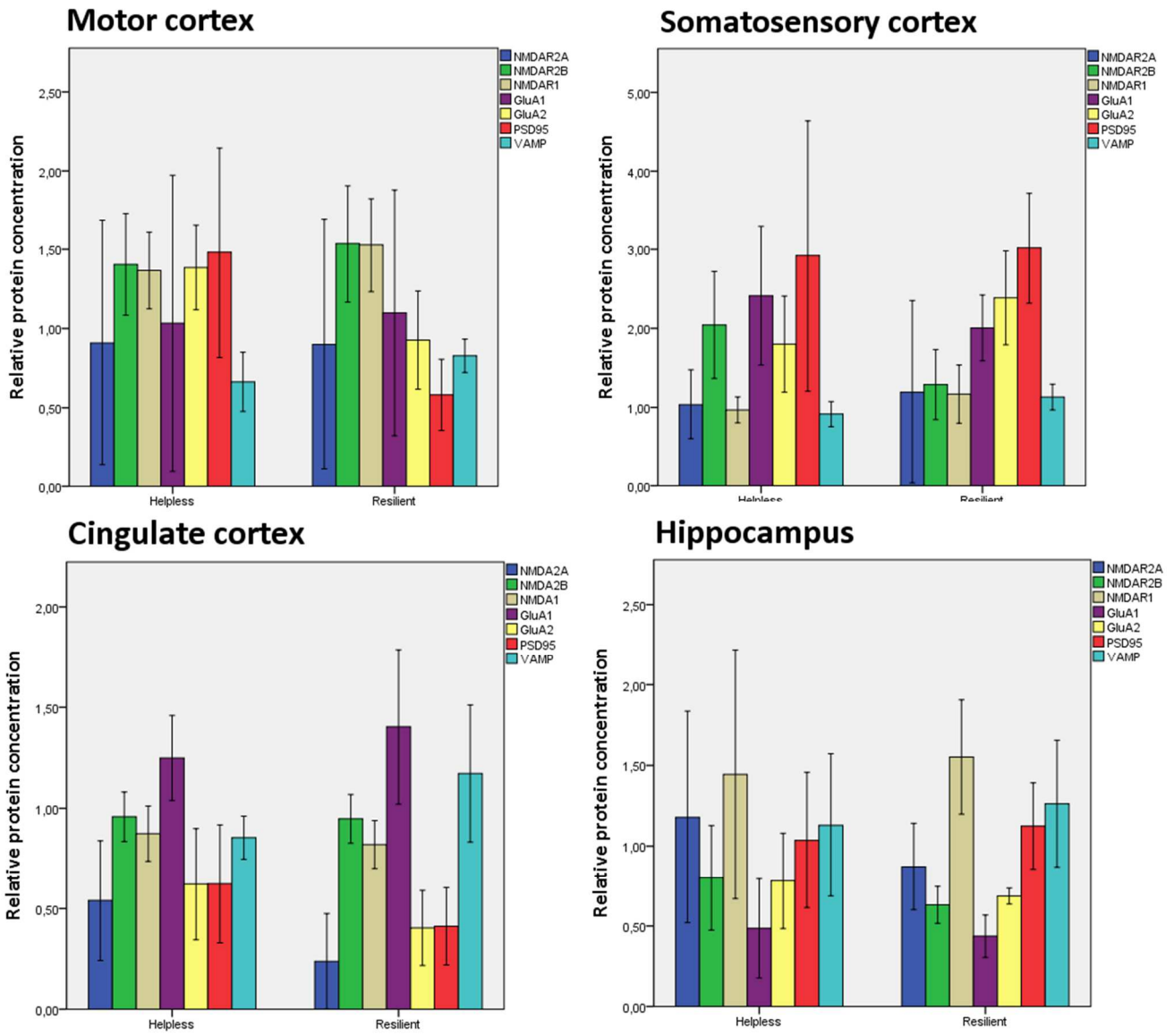


B.8 *Bar plots of all results except ratios. Bars show mean ± 2SE*

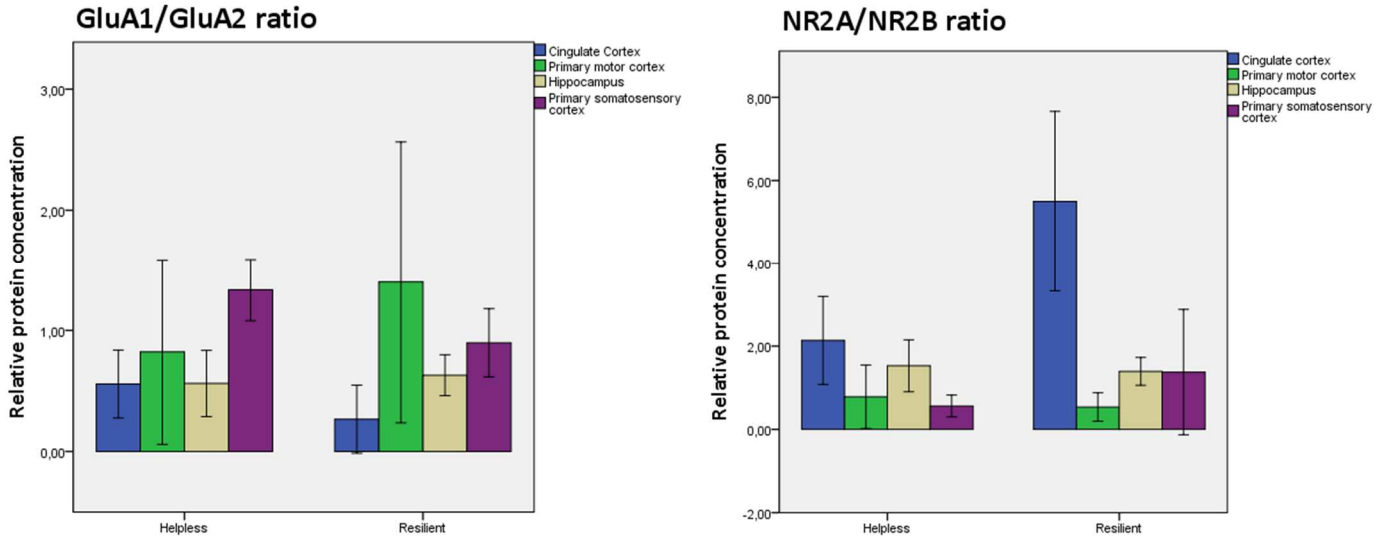


B.9 *Bar plots of all results except ratios. Bars show mean ± 2SE*

B.10 *All results of statistical analysis of differences between regions of interest. h=helpless, r=resilient, mdn=median. P = exact significance of Mann-Whitney U test.*

| Protein | Area ratio | h (mdn) | r (mdn) | U | z | p |
|---|---|---|---|---|---|---|
| **NR2A** | C/H | 6.6 | 4.4 | 7 | -1.149 | 0.31 |
| **NR2A** | C/M1 | 7.2 | 3.8 | 4 | -1.776 | 0.095 |
| **NR2A** | C/S1 | 6.2 | 4.8 | 9 | -0.731 | 0.548 |
| **NR2A** | H/M1 | 6.6 | 4.4 | 12 | -0.104 | 1 |
| **NR2A** | H/S1 | 5 | 6 | 15 | 0.522 | 0.69 |
| **NR2A** | M1/S1 | 5.4 | 5.6 | 13 | 0.104 | 1 |
| **NR2B** | C/H | 4.2 | 6.8 | 19 | 1.358 | 0.222 |
| **NR2B** | C/M1 | 6 | 5 | 10 | -0.522 | 0.69 |
| **NR2B** | C/S1 | 4.2 | 6.8 | 19 | 1.358 | 0.222 |
| **NR2B** | H/M1 | 6.8 | 4.2 | 6 | -1.358 | 0.222 |
| **NR2B** | H/S1 | 4.8 | 6.2 | 16 | 0.731 | 0.548 |
| **NR2B** | M1/S1 | 3.6 | 7.4 | 22 | 1.984 | 0.056 |
| **NR1** | C/H | 6.6 | 4.4 | 7 | -1.149 | 0.31 |
| **NR1** | C/M1 | 6.4 | 4.6 | 8 | -0.94 | 0.421 |
| **NR1** | C/S1 | 6.4 | 4.6 | 8 | -0.94 | 0.421 |
| **NR1** | H/M1 | 5.2 | 5.8 | 14 | 0.313 | 0.841 |
| **NR1** | H/S1 | 5.8 | 5.2 | 11 | -0.313 | 0.841 |
| **NR1** | M1/S1 | 5.4 | 5.6 | 13 | 0.104 | 1 |
| **GluA1** | C/H | 4.8 | 6.2 | 16 | 0.731 | 0.548 |
| **GluA1** | C/M1 | 6.6 | 4.4 | 12 | -0.104 | 1 |
| **GluA1** | C/S1 | 4.8 | 6.2 | 16 | 0.731 | 0.548 |
| **GluA1** | H/M1 | 6.6 | 4.4 | 12 | -0.104 | 1 |
| **GluA1** | H/S1 | 5.2 | 5.8 | 14 | 0.313 | 0.841 |
| **GluA1** | M1/S1 | 4.8 | 6.2 | 16 | 0.731 | 0.548 |
| **GluA2** | C/H | 6.2 | 4.8 | 9 | -0.731 | 0.548 |
| **GluA2** | C/M1 | 6.6 | 4.4 | 12 | -0.104 | 1 |
| **GluA2** | C/S1 | 7 | 4 | 5 | -1.567 | 0.151 |
| **GluA2** | H/M1 | 4.8 | 6.2 | 16 | 0.731 | 0.548 |
| **GluA2** | H/S1 | 6.8 | 4.2 | 6 | -1.358 | 0.222 |
| **GluA2** | M1/S1 | 8 | 3 | 8 | -2.611 | **0.008** |
| **PSD95** | C/H | 6.8 | 4.2 | 6 | -1.358 | 0.222 |
| **PSD95** | C/M1 | 4.8 | 6.2 | 16 | 0.731 | 0.548 |
| **PSD95** | C/S1 | 6.2 | 4.8 | 9 | -0.731 | 0.548 |
| **PSD95** | H/M1 | 3 | 8 | 25 | 2.611 | **0.008** |
| **PSD95** | H/S1 | 6.6 | 4.4 | 12 | -0.104 | 1 |
| **PSD95** | M1/S1 | 7.6 | 3.4 | 2 | -2.193 | **0.032** |
| **VAMP** | C/H | 5.4 | 5.6 | 13 | 0.104 | 1 |
| **VAMP** | C/M1 | 5 | 6 | 15 | 0.522 | 0.69 |
| **VAMP** | C/S1 | 5 | 6 | 15 | 0.522 | 0.69 |
| **VAMP** | H/M1 | 5.6 | 5.4 | 12 | -0.104 | 1 |
| **VAMP** | H/S1 | 6.4 | 4.6 | 8 | -0.94 | 0.421 |

| | | | | | | |
|---|---|---|---|---|---|---|
| **VAMP** | M1/S1 | 5.4 | 5.6 | 13 | 0.104 | 1 |
| **NR2A/NR2B** | C/H | 7 | 4 | 5 | -1.567 | 0.151 |
| **NR2A/NR2B** | C/M1 | 7.2 | 3.8 | 4 | -1.776 | 0.095 |
| **NR2A/NR2B** | C/S1 | 6 | 5 | 10 | -0.522 | 0.69 |
| **NR2A/NR2B** | H/M1 | 5.8 | 5.2 | 11 | -0.313 | 0.841 |
| **NR2A/NR2B** | H/S1 | 5.4 | 5.6 | 13 | 0.104 | 1 |
| **NR2A/NR2B** | M1/S1 | 5.6 | 5.4 | 12 | -0.104 | 1 |
| **GluA1/GluA2** | C/H | 4.4 | 6.6 | 18 | 1.149 | 0.31 |
| **GluA1/GluA3** | C/M1 | 5.8 | 5.2 | 11 | -0.313 | 0.841 |
| **GluA1/GluA4** | C/S1 | 4 | 7 | 20 | 1.567 | 0.151 |
| **GluA1/GluA5** | H/M1 | 6.2 | 4.8 | 9 | -0.731 | 0.548 |
| **GluA1/GluA6** | H/S1 | 4 | 7 | 20 | 1.567 | 0.151 |
| **GluA1/GluA7** | M1/S1 | 3.8 | 7.2 | 21 | 1.776 | 0.095 |

# Appendix C

C.1 *Does sample 3 make the helpless group data more variable?*

One of the rats did not meet the requirements for helplessness, failing the test only 9 times, while the criteria was more than 10 times. Nevertheless the rat was added to the helpless group for increasing the sample size. To determine whether this increased the variability of the results, the standard deviation for all samples of the helpless groups in each area were calculated. Additionally, the standard deviation of all samples except one of them were calculated as well. For example, the standard deviation of samples 2-5 were calculated. This standard deviation was then compared to the standard deviation of all samples, by subtracting the standard deviation of all samples except sample 1 from the one of all samples. The percentual decrease of the standard deviation was then calculated.

C.1 *Percentual decrease of the standard deviation of the samples of helpless animals (sample 1-5), if one of the samples is taken out. E.g., Missing 1 row values show percental decrease of standard deviation, if sample 1 is not taken into the calculation, compared to, if all samples are taken into the calculation.*

| | Cingulate cortex | Hippocampus | Primary somatosensory cortex | Primary motor cortex | All |
|---|---|---|---|---|---|
| Missing 1 | 1.92 | -8.60 | -3.73 | -7.61 | -5.33 |
| Missing 2 | -1.77 | -7.83 | -1.70 | 29.27 | 4.37 |
| Missing 3 | 12.06 | 11.33 | -5.86 | -4.31 | 0.73 |
| Missing 4 | -3.55 | 16.53 | 4.27 | 1.59 | 5.90 |
| Missing 5 | -0.49 | -1.93 | 14.14 | -0.60 | 4.92 |

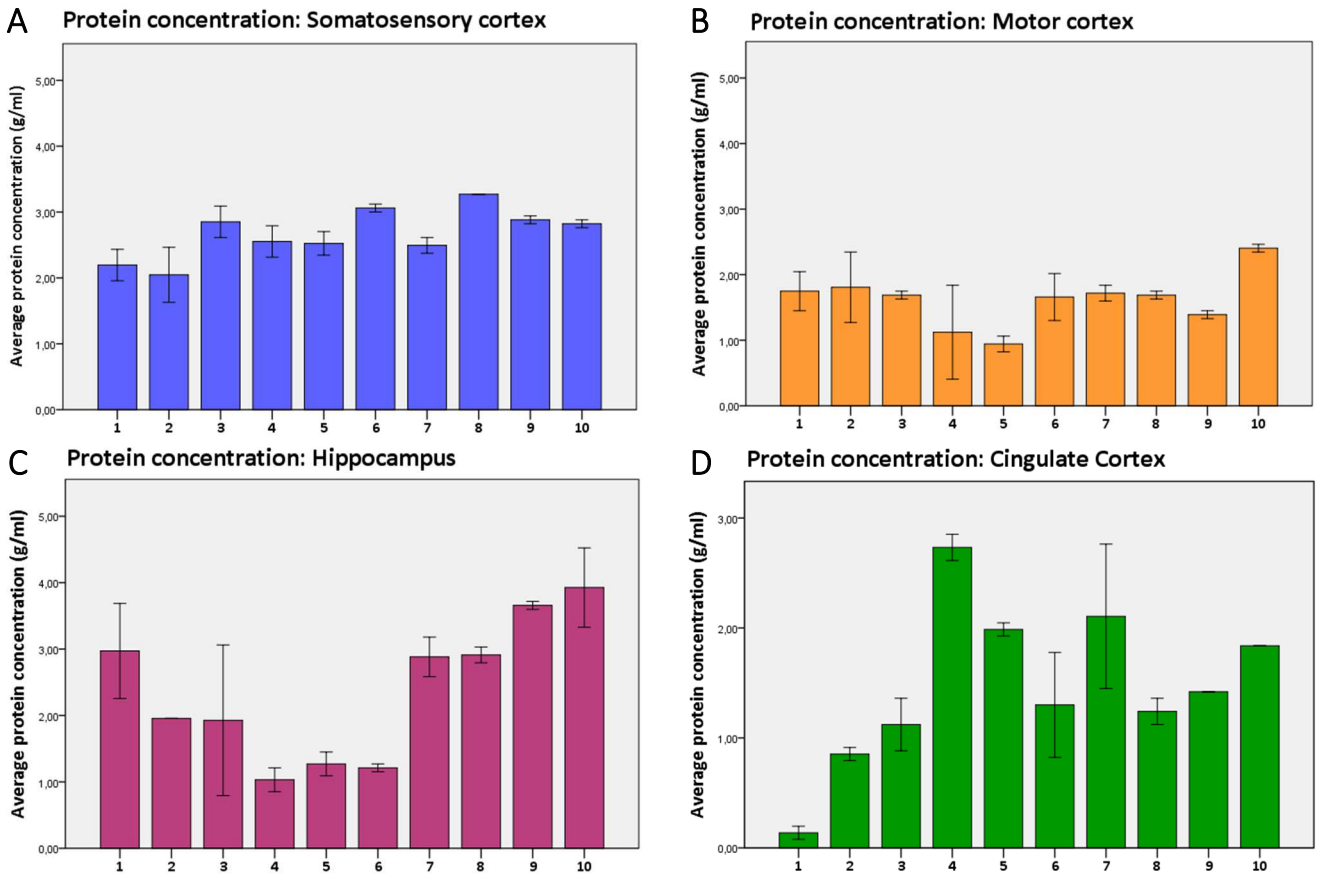


C.2 *Protein concentrations of samples. Note the relatively high variation in concentration, and the high standard deviation of the measurements. (helpless: 1-5; resilient: 6-10) Mean of two measurements ± 2 SE is shown.*

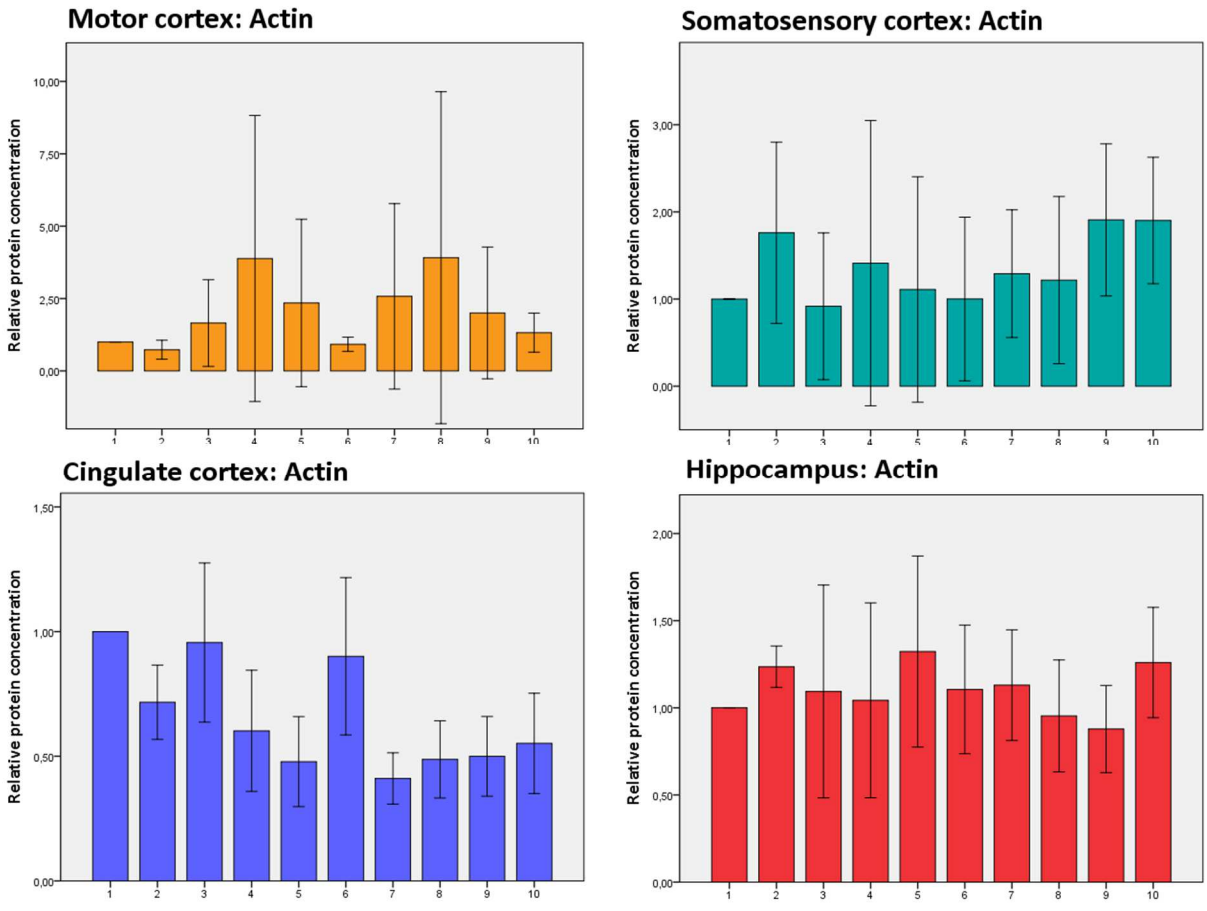


C.3 *The mean of the measured relative actin concentration of all western blots is plotted. Note the high standard deviation of the measurements. (helpless: 1-5; resilient: 6-10) Mean of two measurements ± 2 SE is shown.*

**Buffers and Solutions used**

10x Læmli buffer

To 800 ml of $dH_2O$ add:

30.3 g Trizma® base (T1503 Sigma-Aldrich)
144.1 g Glycine (G8898 Sigma-Aldrich)
10.0 g SDS (Sodium Dodecyl Sulfat ???)

Add $dH_2O$ to a final volume of 1000 ml.
pH should be 8.3-8.9 without adjustment.
Stored at 4 °C.

10x Towbin buffer

To 800 ml of $dH_2O$ add:

30.3 g Trizma® base (T1503 Sigma-Aldrich)
144.1 g Glycine (G8898 Sigma-Aldrich)

Add $dH_2O$ to a final volume of 1000 ml.
pH should be 8.3-8.9 without adjustment.
Stored at 4 °C.

20x Tris-buffered saline (TBS)

48.5 g Trizma® base (T1503 Sigma-Aldrich)
160.1 g NaCl (Natrium Chloride; S7653 Sigma-Aldrich)

Adjust pH to 7.6 with concentrated HCl (Hydrochloric acid; 20252.290 VWR Chemicals).
Add $dH_2O$ to a final volume of 1000 ml.

Tween Tris-buffered saline (TBST)

400 ml 20x TBS buffer
40 ml 10% v/v Tween (P2287 Sigma-Aldrich)
7560 ml $dH_2O$

Tris-HCl 1.5 M

To 170 ml of $dH_2O$ add:

36.3 g Trizma® base (T1503 Sigma-Aldrich)

Adjust pH to 6.8 with concentrated HCl (Hydrochloric acid; 20252.290 VWR Chemicals) at room temperature. Add $dH_2O$ to a final volume of 200 ml.

6x Loading buffer

3.6 ml $dH_2O$
1.6 ml Tris-HCl 1.5 M (pH 6.8)
0.42 g SDS (Sodium Dodecyl Sulfat; L3771 Simga-Aldrich)
2.4 ml Glycerol (G5561 Sigma-Aldrich)
0.4 ml 2-mercaptoethanol (M7154 Sigma-Aldrich)
Trace amount of bromphenol blue-xylene cyanole dye solution (B3269 Sigma-Aldrich)

# 7 References


1. Jahr CE, Stevens CF. Calcium permeability of the N-methyl-D-aspartate receptor channel in hippocampal neurons in culture. Proceedings of the National Academy of Sciences of the United States of America. 1993;90(24):11573-7.
2. Lisman J. A mechanism for the Hebb and the anti-Hebb processes underlying learning and memory. Proceedings of the National Academy of Sciences of the United States of America. 1989;86(23):9574-8.
3. Santos SD, Carvalho AL, Caldeira MV, Duarte CB. Regulation of AMPA receptors and synaptic plasticity. Neuroscience. 2009;158(1):105-25.
4. Turrigiano GG. The Self-Tuning Neuron: Synaptic Scaling of Excitatory Synapses. Cell. 2008;135(3):422-35.
5. Lüscher C, Malenka RC. NMDA Receptor-Dependent Long-Term Potentiation and Long-Term Depression (LTP/LTD). Cold Spring Harbor Perspectives in Biology. 2012;4(6):a005710.
6. Lisman J, Schulman H, Cline H. The molecular basis of CaMKII function in synaptic and behavioural memory. Nature reviews Neuroscience. 2002;3(3):175-90.
7. Lopez AD, Murray CCJL. The global burden of disease, 1990-2020. Nature medicine. 1998;4(11):1241-3.
8. Moussavi S, Chatterji S, Verdes E, Tandon A, Patel V, Ustun B. Depression, chronic diseases, and decrements in health: results from the World Health Surveys. Lancet (London, England). 2007;370(9590):851-8.
9. A. John Rush MD, Madhukar H. Trivedi MD, Stephen R. Wisniewski PD, Andrew A. Nierenberg MD, Jonathan W. Stewart MD, Diane Warden PD, M.B.A. ,, et al. Acute and Longer-Term Outcomes in Depressed Outpatients Requiring One or Several Treatment Steps: A STAR*D Report. American Journal of Psychiatry. 2006;163(11):1905-17.
10. Cummings JL. Depression and Parkinson's disease: a review. Am J Psychiatry. 1992;149(4):443-54.
11. Lee HB, Lyketsos CG. Depression in Alzheimer's disease: heterogeneity and related issues. Biol Psychiatry. 2003;54(3):353-62.
12. Tu H-P, Hsieh H-M, Liu T-L, Jiang H-J, Wang P-W, Huang C-J. Prevalence of Depressive Disorder in Persons With Type 2 Diabetes: A National Population-Based Cohort Study 2000–2010. Psychosomatics. 2017;58(2):151-63.
13. Judd LL, Kessler RC, Paulus MP, Zeller PV, Wittchen HU, Kunovac JL. Comorbidity as a fundamental feature of generalized anxiety disorders: results from the National Comorbidity Study (NCS). Acta psychiatrica Scandinavica Supplementum. 1998;393:6-11.
14. Bienvenu OJ, Davydow DS, Kendler KS. Psychiatric 'diseases' versus behavioral disorders and degree of genetic influence. Psychological medicine. 2011;41(1):33-40.
15. McCarron RM, Vanderlip ER, Rado J. DEpression. Annals of Internal Medicine. 2016;165(7):ITC49-ITC64.
16. American Psychiatric A. Diagnostic and statistical manual of mental disorders : DSM-5. 5th ed. ed. Washington, D.C: American Psychiatric Association; 2013.
17. Zeng LL, Shen H, Liu L, Wang L, Li B, Fang P, et al. Identifying major depression using whole-brain functional connectivity: a multivariate pattern analysis. Brain : a journal of neurology. 2012;135(Pt 5):1498-507.
18. Zeng LL, Shen H, Liu L, Hu D. Unsupervised classification of major depression using functional connectivity MRI. Hum Brain Mapp. 2014;35(4):1630-41.
19. Buckner RL, Andrews-hanna JR, Schacter DL. The Brain's Default Network. Annals of the New York Academy of Sciences. 2008;1124(1):1-38.
20. Greicius MD, Krasnow B, Reiss AL, Menon V. Functional connectivity in the resting brain: A network analysis of the default mode hypothesis. Proceedings of the National Academy of Sciences. 2003;100(1):253-8.

21. Dichter GS, Gibbs D, Smoski MJ. A systematic review of relations between resting-state functional-MRI and treatment response in major depressive disorder. Journal of affective disorders. 2015;172:8-17.
22. Greicius MD, Flores BH, Menon V, Glover GH, Solvason HB, Kenna H, et al. Resting-state functional connectivity in major depression: abnormally increased contributions from subgenual cingulate cortex and thalamus. Biol Psychiatry. 2007;62(5):429-37.
23. Demirtas M, Tornador C, Falcon C, Lopez-Sola M, Hernandez-Ribas R, Pujol J, et al. Dynamic functional connectivity reveals altered variability in functional connectivity among patients with major depressive disorder. Hum Brain Mapp. 2016;37(8):2918-30.
24. de Kwaasteniet B, Ruhe E, Caan M, Rive M, Olabarriaga S, Groefsema M, et al. Relation between structural and functional connectivity in major depressive disorder. Biol Psychiatry. 2013;74(1):40-7.
25. Ye T, Peng J, Nie B, Gao J, Liu J, Li Y, et al. Altered functional connectivity of the dorsolateral prefrontal cortex in first-episode patients with major depressive disorder. European journal of radiology. 2012;81(12):4035-40.
26. Davey CG, Harrison BJ, Yucel M, Allen NB. Regionally specific alterations in functional connectivity of the anterior cingulate cortex in major depressive disorder. Psychological medicine. 2012;42(10):2071-81.
27. Monkul ES, Silva LAP, Narayana S, Peluso MAM, Zamarripa F, Nery FG, et al. Abnormal Resting State Corticolimbic Blood Flow in Depressed Unmedicated Patients With Major Depression: A (15)O-H(2)O PET Study. Human brain mapping. 2012;33(2):272-9.
28. Li B, Liu L, Friston KJ, Shen H, Wang L, Zeng L-L, et al. A Treatment-Resistant Default Mode Subnetwork in Major Depression. Biological Psychiatry. 2013;74(1):48-54.
29. Paxinos G, Watson C. The rat brain in stereotaxic coordinates. Elsevier Academic Press. 2005.
30. Brodmann K, Gary LJ, SpringerLink. Brodmann's : Localisation in the Cerebral Cortex: Springer US; 2006.
31. Vogt BA, Paxinos G. Cytoarchitecture of mouse and rat cingulate cortex with human homologies. Brain Structure and Function. 2014;219(1):185-92.
32. Koolschijn PC, van Haren NE, Lensvelt-Mulders GJ, Hulshoff Pol HE, Kahn RS. Brain volume abnormalities in major depressive disorder: a meta-analysis of magnetic resonance imaging studies. Hum Brain Mapp. 2009;30(11):3719-35.
33. Lim HK, Jung WS, Ahn KJ, Won WY, Hahn C, Lee SY, et al. Regional cortical thickness and subcortical volume changes are associated with cognitive impairments in the drug-naive patients with late-onset depression. Neuropsychopharmacology. 2012;37(3):838-49.
34. Bissiere S, McAllister KH, Olpe HR, Cryan JF. The rostral anterior cingulate cortex modulates depression but not anxiety-related behaviour in the rat. Behavioural Brain Research. 2006;175(1):195-9.
35. Devinsky O, Morrell M, Vogt BA. Contributions of anterior cingulate cortex to behavior1995. 279-306 p.
36. Talairach J, Bancaud J, Geier S, Bordas-Ferrer M, Bonis A, Szikla G, et al. The cingulate gyrus and human behaviour. Electroencephalography and Clinical Neurophysiology. 1973;34(1):45-52.
37. Agarwal N, Choi PA, Shin SS, Hansberry DR, Mammis A. Anterior cingulotomy for intractable pain. Interdisciplinary Neurosurgery. 2016;6:80-3.
38. Tow PM, Whitty CWM. PERSONALITY CHANGES AFTER OPERATIONS ON THE CINGULATE GYRUS IN MAN. Journal of Neurology, Neurosurgery & Psychiatry. 1953;16(3):186.
39. Murphy FC, Rubinsztein JS, Michael A, Rogers RD, Robbins TW, Paykel ES, et al. Decision-making cognition in mania and depression. Psychological medicine. 2001;31(4):679-93.
40. Bush G, Vogt BA, Holmes J, Dale AM, Greve D, Jenike MA, et al. Dorsal anterior cingulate cortex: A role in reward-based decision making. Proceedings of the National Academy of Sciences of the United States of America. 2002;99(1):523-8.
41. Walton ME, Bannerman DM, Rushworth MFS. The Role of Rat Medial Frontal Cortex in Effort-Based Decision Making. The Journal of Neuroscience. 2002;22(24):10996-1003.

42. Shima K, Tanji J. Role for Cingulate Motor Area Cells in Voluntary Movement Selection Based on Reward. Science (New York, NY). 1998;282(5392):1335-8.
43. Gabbott PLA, Warner TA, Jays PRL, Salway P, Busby SJ. Prefrontal cortex in the rat: Projections to subcortical autonomic, motor, and limbic centers. Journal of Comparative Neurology. 2005;492(2):145-77.
44. Hoover WB, Vertes RP. Anatomical analysis of afferent projections to the medial prefrontal cortex in the rat. Brain Structure and Function. 2007;212(2):149-79.
45. Wang Y, Matsuzaka Y, Mushiake H, Shima K. Spatial distribution of cingulate cortical cells projecting to the primary motor cortex in the rat. Neuroscience Research. 2008;60(4):406-11.
46. Jones BF, Witter MP. Cingulate cortex projections to the parahippocampal region and hippocampal formation in the rat. Hippocampus. 2007;17(10):957-76.
47. Jones BF, Groenewegen HJ, Witter MP. Intrinsic connections of the cingulate cortex in the rat suggest the existence of multiple functionally segregated networks. Neuroscience. 2005;133(1):193-207.
48. Posner M, Digirolamo G. Executive attention: Conflict, target detection, and cognitive control1998.
49. Vollmayr B, Henn FA. Learned helplessness in the rat: improvements in validity and reliability. Brain research Brain research protocols. 2001;8(1):1.
50. Henn FA, Vollmayr B. Stress models of depression: Forming genetically vulnerable strains. Neuroscience and biobehavioral reviews. 2005;29(4):799-804.
51. Vollmayr B, Bachteler D, Vengeliene V, Gass P, Spanagel R, Henn F. Rats with congenital learned helplessness respond less to sucrose but show no deficits in activity or learning. Behav Brain Res. 2004;150(1-2):217-21.
52. Hatcher JP, Bell DJ, Reed TJ, Hagan JJ. Chronic mild stress-induced reductions in saccharin intake depend upon feeding status. Journal of Psychopharmacology. 1997;11(4):331-8.
53. Willner P, Mitchell PJ. The validity of animal models of predisposition to depression. Behavioural pharmacology. 2002;13(3):169-88.
54. Posner J, Hellerstein DJ, Gat I, Mechling A, Klahr K, Wang Z, et al. Antidepressants normalize the default mode network in patients with dysthymia. JAMA Psychiatry. 2013;70(4):373-82.
55. Lu H, Zou Q, Gu H, Raichle ME, Stein EA, Yang Y. Rat brains also have a default mode network. Proceedings of the National Academy of Sciences. 2012;109(10):3979-84.
56. Upadhyay J, Baker SJ, Chandran P, Miller L, Lee Y, Marek GJ, et al. Default-Mode-Like Network Activation in Awake Rodents. PLoS ONE. 2011;6(11).
57. Williams KA, Mehta NS, Redei EE, Wang L, Procissi D. Aberrant resting-state functional connectivity in a genetic rat model of depression. Psychiatry research. 2014;222(1-2):111-3.
58. Gass N, Cleppien D, Zheng L, Schwarz AJ, Meyer-Lindenberg A, Vollmayr B, et al. Functionally altered neurocircuits in a rat model of treatment-resistant depression show prominent role of the habenula. European neuropsychopharmacology : the journal of the European College of Neuropsychopharmacology. 2014;24(3):381-90.
59. Berton O, Nestler EJ. New approaches to antidepressant drug discovery: beyond monoamines. Nature reviews Neuroscience. 2006;7(2):137-51.
60. Pittenger C, Duman RS. Stress, Depression, and Neuroplasticity: A Convergence of Mechanisms. Neuropsychopharmacology. 2007;33(1):88-109.
61. Duric V, Banasr M, Stockmeier CA, Simen AA, Newton SS, Overholser JC, et al. Altered expression of synapse and glutamate related genes in post-mortem hippocampus of depressed subjects. The international journal of neuropsychopharmacology. 2013;16(1):69-82.
62. Medina A, Burke S, Thompson RC, Bunney W, Jr., Myers RM, Schatzberg A, et al. Glutamate transporters: a key piece in the glutamate puzzle of major depressive disorder. Journal of psychiatric research. 2013;47(9):1150-6.
63. Kim JS, Schmid-Burgk W, Claus D, Kornhuber HH. Increased serum glutamate in depressed patients. Archiv fur Psychiatrie und Nervenkrankheiten. 1982;232(4):299-304.

64. Altamura CA, Mauri MC, Ferrara A, Moro AR, D'Andrea G, Zamberlan F. Plasma and platelet excitatory amino acids in psychiatric disorders. Am J Psychiatry. 1993;150(11):1731-3.
65. Kucukibrahimoglu E, Saygin MZ, Caliskan M, Kaplan OK, Unsal C, Goren MZ. The change in plasma GABA, glutamine and glutamate levels in fluoxetine- or S-citalopram-treated female patients with major depression. European journal of clinical pharmacology. 2009;65(6):571-7.
66. Mirza Y, Tang J, Russell A, Banerjee SP, Bhandari R, Ivey J, et al. Reduced anterior cingulate cortex glutamatergic concentrations in childhood major depression. Journal of the American Academy of Child and Adolescent Psychiatry. 2004;43(3):341-8.
67. Auer DP, Putz B, Kraft E, Lipinski B, Schill J, Holsboer F. Reduced glutamate in the anterior cingulate cortex in depression: an in vivo proton magnetic resonance spectroscopy study. Biol Psychiatry. 2000;47(4):305-13.
68. Zhao J, Bao AM, Qi XR, Kamphuis W, Luchetti S, Lou JS, et al. Gene expression of GABA and glutamate pathway markers in the prefrontal cortex of non-suicidal elderly depressed patients. Journal of affective disorders. 2012;138(3):494-502.
69. Gittins RA, Harrison PJ. A morphometric study of glia and neurons in the anterior cingulate cortex in mood disorder. Journal of affective disorders. 2011;133(1-2):328-32.
70. Chana G, Landau S, Beasley C, Everall IP, Cotter D. Two-dimensional assessment of cytoarchitecture in the anterior cingulate cortex in major depressive disorder, bipolar disorder, and schizophrenia: evidence for decreased neuronal somal size and increased neuronal density. Biol Psychiatry. 2003;53(12):1086-98.
71. Ongur D, Drevets WC, Price JL. Glial reduction in the subgenual prefrontal cortex in mood disorders. Proceedings of the National Academy of Sciences of the United States of America. 1998;95(22):13290-5.
72. McOmish CE, Pavey G, Gibbons A, Hopper S, Udawela M, Scarr E, et al. Lower [3H]LY341495 binding to mGlu2/3 receptors in the anterior cingulate of subjects with major depressive disorder but not bipolar disorder or schizophrenia. Journal of affective disorders. 2016;190:241-8.
73. Block W, Traber F, von Widdern O, Metten M, Schild H, Maier W, et al. Proton MR spectroscopy of the hippocampus at 3 T in patients with unipolar major depressive disorder: correlates and predictors of treatment response. The international journal of neuropsychopharmacology. 2009;12(3):415-22.
74. Milak MS, Proper CJ, Mulhern ST, Parter AL, Kegeles LS, Ogden RT, et al. A Pilot In Vivo Proton Magnetic Resonance Spectroscopy Study of Amino Acid Neurotransmitter Response to Ketamine Treatment of Major Depressive Disorder. Molecular psychiatry. 2016;21(3):320-7.
75. Sollner T, Bennett MK, Whiteheart SW, Scheller RH, Rothman JE. A protein assembly-disassembly pathway in vitro that may correspond to sequential steps of synaptic vesicle docking, activation, and fusion. Cell. 1993;75(3):409-18.
76. Kaut O, Schmitt I, Hofmann A, Hoffmann P, Schlaepfer TE, Wullner U, et al. Aberrant NMDA receptor DNA methylation detected by epigenome-wide analysis of hippocampus and prefrontal cortex in major depression. European archives of psychiatry and clinical neuroscience. 2015;265(4):331-41.
77. Hellman A, Chess A. Gene body-specific methylation on the active X chromosome. Science (New York, NY). 2007;315(5815):1141-3.
78. Chen N, Luo T, Raymond LA. Subtype-Dependence of NMDA Receptor Channel Open Probability. The Journal of Neuroscience. 1999;19(16):6844-54.
79. Schulz D, Smith D, Yu M, Lee H, Henn FA. Selective breeding for helplessness in rats alters the metabolic profile of the hippocampus and frontal cortex: a 1H-MRS study at 9.4 T. The international journal of neuropsychopharmacology. 2013;16(1):199-212.
80. Zink M, Vollmayr B, Gebicke-Haerter PJ, Henn FA, Thome J. Reduced expression of complexins I and II in rats bred for learned helplessness. Brain Res. 2007;1144:202-8.
81. Zink M, Vollmayr B, Gebicke-Haerter PJ, Henn FA. Reduced expression of glutamate transporters vGluT1, EAAT2 and EAAT4 in learned helpless rats, an animal model of depression. Neuropharmacology. 2010;58(2):465-73.

82. Almeida RF, Thomazi AP, Godinho GF, Saute JA, Wofchuk ST, Souza DO, et al. Effects of depressive-like behavior of rats on brain glutamate uptake. Neurochemical research. 2010;35(8):1164-71.
83. Zhu X, Ye G, Wang Z, Luo J, Hao X. Sub-anesthetic doses of ketamine exert antidepressant-like effects and upregulate the expression of glutamate transporters in the hippocampus of rats. Neurosci Lett. 2017;639:132-7.
84. Treccani G, Gaarn du Jardin K, Wegener G, Muller HK. Differential expression of postsynaptic NMDA and AMPA receptor subunits in the hippocampus and prefrontal cortex of the flinders sensitive line rat model of depression. Synapse (New York, NY). 2016;70(11):471-4.
85. Conti F, Minelli A, Brecha NC. Cellular localization and laminar distribution of AMPA glutamate receptor subunits mRNAs and proteins in the rat cerebral cortex. The Journal of comparative neurology. 1994;350(2):241-59.
86. Man H-Y. GluA2-lacking, calcium-permeable AMPA receptors — inducers of plasticity? Current Opinion in Neurobiology. 2011;21(2):291-8.
87. Pellegrini-Giampietro DE, Bennett MVL, Zukin RS. Are Ca2+-permeable kainate/AMPA receptors more abundant in immature brain? Neuroscience Letters. 1992;144(1):65-9.
88. MacDermott AB, Mayer ML, Westbrook GL, Smith SJ, Barker JL. NMDA-receptor activation increases cytoplasmic calcium concentration in cultured spinal cord neurones. Nature. 1986;321(6069):519-22.
89. Das S, Sasaki YF, Rothe T, Premkumar LS, Takasu M, Crandall JE, et al. Increased NMDA current and spine density in mice lacking the NMDA receptor subunit NR3A. Nature. 1998;393(6683):377-81.
90. Zhang Z, Sun Q-Q. Development of NMDA NR2 Subunits and Their Roles in Critical Period Maturation of Neocortical GABAergic Interneurons. Developmental neurobiology. 2011;71(3):221-45.
91. Laube B, Kuhse J, Betz H. Evidence for a tetrameric structure of recombinant NMDA receptors. The Journal of neuroscience : the official journal of the Society for Neuroscience. 1998;18(8):2954-61.
92. Monyer H, Burnashev N, Laurie DJ, Sakmann B, Seeburg PH. Developmental and regional expression in the rat brain and functional properties of four NMDA receptors. Neuron. 1994;12(3):529-40.
93. Herkert M, Rottger S, Becker CM. The NMDA receptor subunit NR2B of neonatal rat brain: complex formation and enrichment in axonal growth cones. The European journal of neuroscience. 1998;10(5):1553-62.
94. Goebel DJ, Poosch MS. NMDA receptor subunit gene expression in the rat brain: a quantitative analysis of endogenous mRNA levels of NR1Com, NR2A, NR2B, NR2C, NR2D and NR3A. Molecular Brain Research. 1999;69(2):164-70.
95. Monyer H, Sprengel R, Schoepfer R, Herb A, Higuchi M, Lomeli H, et al. Heteromeric NMDA Receptors: Molecular and Functional Distinction of Subtypes. Science (New York, NY). 1992;256(5060):1217-21.
96. Ishii T, Moriyoshi K, Sugihara H, Sakurada K, Kadotani H, Yokoi M, et al. Molecular characterization of the family of the N-methyl-D-aspartate receptor subunits. The Journal of biological chemistry. 1993;268(4):2836-43.
97. Flint AC, Maisch US, Weishaupt JH, Kriegstein AR, Monyer H. NR2A Subunit Expression Shortens NMDA Receptor Synaptic Currents in Developing Neocortex. The Journal of Neuroscience. 1997;17(7):2469-76.
98. Yashiro K, Philpot BD. Regulation of NMDA Receptor Subunit Expression and Its Implications for LTD, LTP, and Metaplasticity. Neuropharmacology. 2008;55(7):1081-94.
99. Kim E, Niethammer M, Rothschild A, Nung Jan Y, Sheng M. Clustering of Shaker-type K+ channels by interaction with a family of membrane-associated guanylate kinases. Nature. 1995;378(6552):85-8.
100. Niethammer M, Kim E, Sheng M. Interaction between the C terminus of NMDA receptor subunits and multiple members of the PSD-95 family of membrane-associated guanylate kinases. The Journal of neuroscience : the official journal of the Society for Neuroscience. 1996;16(7):2157-63.

101. Kornau H, Schenker L, Kennedy M, Seeburg P. Domain interaction between NMDA receptor subunits and the postsynaptic density protein PSD-95. Science (New York, NY). 1995;269(5231):1737-40.
102. Ehrlich I, Malinow R. Postsynaptic Density 95 controls AMPA Receptor Incorporation during Long-Term Potentiation and Experience-Driven Synaptic Plasticity. The Journal of Neuroscience. 2004;24(4):916-27.
103. Schnell E, Sizemore M, Karimzadegan S, Chen L, Bredt DS, Nicoll RA. Direct interactions between PSD-95 and stargazin control synaptic AMPA receptor number. Proceedings of the National Academy of Sciences. 2002;99(21):13902-7.
104. Gomperts SN. Clustering Membrane Proteins: It's All Coming Together with the PSD-95/SAP90 Protein Family. Cell. 1996;84(5):659-62.
105. Migaud M, Charlesworth P, Dempster M, Webster LC, Watabe AM, Makhinson M, et al. Enhanced long-term potentiation and impaired learning in mice with mutant postsynaptic density-95 protein. Nature. 1998;396(6710):433-9.
106. Jahn R, Scheller RH. SNAREs [mdash] engines for membrane fusion. Nat Rev Mol Cell Biol. 2006;7(9):631-43.
107. Hussain S, Davanger S. Postsynaptic VAMP/Synaptobrevin Facilitates Differential Vesicle Trafficking of GluA1 and GluA2 AMPA Receptor Subunits. PLOS ONE. 2015;10(10):e0140868.
108. Kimura K, Mizoguchi A, Ide C. Regulation of growth cone extension by SNARE proteins. The journal of histochemistry and cytochemistry : official journal of the Histochemistry Society. 2003;51(4):429-33.
109. Papp EA, Leergaard TB, Calabrese E, Johnson GA, Bjaalie JG. Waxholm Space atlas of the Sprague Dawley rat brain. NeuroImage. 2014;97:374-86.
110. Pesqueira LMV, Davanger S. Quantification of Spine Density in the Rat Default Mode Network. NTNU; 2015.
111. Azzinnari D, Sigrist H, Staehli S, Palme R, Hildebrandt T, Leparc G, et al. Mouse social stress induces increased fear conditioning, helplessness and fatigue to physical challenge together with markers of altered immune and dopamine function. Neuropharmacology. 2014;85:328-41.
112. Zhang Y-F, Li Q-Q, Qu J, Sun C-M, Wang Y. Alterations of motor cortical microcircuit in a depressive-like mouse model produced by light deprivation. Neuroscience. 2017;341:79-94.
113. Nagura H, Ishikawa Y, Kobayashi K, Takao K, Tanaka T, Nishikawa K, et al. Impaired synaptic clustering of postsynaptic density proteins and altered signal transmission in hippocampal neurons, and disrupted learning behavior in PDZ1 and PDZ2 ligand binding-deficient PSD-95 knockin mice. Molecular brain. 2012;5:43.
114. Béïque J-C, Andrade R. PSD-95 regulates synaptic transmission and plasticity in rat cerebral cortex. The Journal of Physiology. 2003;546(3):859-67.
115. Prange O, Wong TP, Gerrow K, Wang YT, El-Husseini A. A balance between excitatory and inhibitory synapses is controlled by PSD-95 and neuroligin. Proceedings of the National Academy of Sciences of the United States of America. 2004;101(38):13915-20.
116. Xu T, Yu X, Perlik AJ, Tobin WF, Zweig JA, Tennant K, et al. Rapid formation and selective stabilization of synapses for enduring motor memories. Nature. 2009;462(7275):915-9.
117. Rioult-Pedotti MS, Friedman D, Hess G, Donoghue JP. Strengthening of horizontal cortical connections following skill learning. Nat Neurosci. 1998;1(3):230-4.
118. Maeda F, Keenan JP, Pascual-Leone A. Interhemispheric asymmetry of motor cortical excitability in major depression as measured by transcranial magnetic stimulation. The British journal of psychiatry : the journal of mental science. 2000;177:169-73.
119. Bajwa S, Bermpohl F, Rigonatti SP, Pascual-Leone A, Boggio PS, Fregni F. Impaired interhemispheric interactions in patients with major depression. The Journal of nervous and mental disease. 2008;196(9):671-7.
120. Reid PD, Daniels B, Rybak M, Turnier-Shea Y, Pridmore S. Cortical excitability of psychiatric disorders: reduced post-exercise facilitation in depression compared to schizophrenia and controls. The Australian and New Zealand journal of psychiatry. 2002;36(5):669-73.

121. Montgomery JM, Madison DV. State-dependent heterogeneity in synaptic depression between pyramidal cell pairs. Neuron. 2002;33(5):765-77.
122. Kuhn M, Mainberger F, Feige B, Maier JG, Mall V, Jung NH, et al. State-Dependent Partial Occlusion of Cortical LTP-Like Plasticity in Major Depression. Neuropsychopharmacology. 2016;41(6):1521-9.
123. Player MJ, Taylor JL, Weickert CS, Alonzo A, Sachdev P, Martin D, et al. Neuroplasticity in Depressed Individuals Compared with Healthy Controls. Neuropsychopharmacology. 2013;38(11):2101-8.
124. Levinson AJ, Fitzgerald PB, Favalli G, Blumberger DM, Daigle M, Daskalakis ZJ. Evidence of Cortical Inhibitory Deficits in Major Depressive Disorder. Biological Psychiatry. 2010;67(5):458-64.
125. Veronezi BP, Moffa AH, Carvalho AF, Galhardoni R, Simis M, Bensenor IM, et al. Evidence for increased motor cortical facilitation and decreased inhibition in atypical depression. Acta psychiatrica Scandinavica. 2016;134(2):172-82.
126. Bader J-P, Bühler J, Endrass J, Klipstein A, Hell D. Muskelkraft und Gangcharakteristika depressiver Menschen. Der Nervenarzt. 1999;70(7):613-9.
127. Treadway MT, Buckholtz JW, Schwartzman AN, Lambert WE, Zald DH. Worth the 'EEfRT'? The Effort Expenditure for Rewards Task as an Objective Measure of Motivation and Anhedonia. PLOS ONE. 2009;4(8):e6598.
128. Parker G, Hadzi-Pavlovic D, Brodaty H, Boyce P, Mitchell P, Wilhelm K, et al. Psychomotor disturbance in depression: defining the constructs. Journal of affective disorders. 1993;27(4):255-65.
129. Lemke MR, Puhl P, Koethe N, Winkler T. Psychomotor retardation and anhedonia in depression. Acta psychiatrica Scandinavica. 1999;99(4):252-6.
130. Cantisani A, Koenig T, Horn H, Müller T, Strik W, Walther S. Psychomotor retardation is linked to frontal alpha asymmetry in major depression. Journal of affective disorders. 2015;188:167-72.
131. Huang H, Harlé K, Movellan J, Paulus M. Using Optimal Control to Disambiguate the Effect of Depression on Sensorimotor, Motivational and Goal-Setting Functions. PLoS One. 2016;11(12).
132. Nam H, Clinton SM, Jackson NL, Kerman IA. Learned helplessness and social avoidance in the Wistar-Kyoto rat. Frontiers in Behavioral Neuroscience. 2014;8:109.
133. Irie M, Hata Y, Takeuchi M, Ichtchenko K, Toyoda A, Hirao K, et al. Binding of neuroligins to PSD-95. Science (New York, NY). 1997;277(5331):1511-5.
134. Feng P, Akladious AA, Hu Y. Hippocampal and motor fronto-cortical neuroligin1 is increased in an animal model of depression. Psychiatry research. 2016;243:210-8.
135. Henderson AK, Pittman QJ, Teskey GC. High frequency stimulation alters motor maps, impairs skilled reaching performance and is accompanied by an upregulation of specific GABA, glutamate and NMDA receptor subunits. Neuroscience. 2012;215:98-113.
136. Munoz A, Woods TM, Jones EG. Laminar and cellular distribution of AMPA, kainate, and NMDA receptor subunits in monkey sensory-motor cortex. The Journal of comparative neurology. 1999;407(4):472-90.
137. Gerlai R, Henderson JT, Roder JC, Jia Z. Multiple behavioral anomalies in GluR2 mutant mice exhibiting enhanced LTP. Behavioural Brain Research. 1998;95(1):37-45.
138. Passafaro M, Nakagawa T, Sala C, Sheng M. Induction of dendritic spines by an extracellular domain of AMPA receptor subunit GluR2. Nature. 2003;424(6949):677-81.
139. Gibbons AS, Brooks L, Scarr E, Dean B. AMPA receptor expression is increased post-mortem samples of the anterior cingulate from subjects with major depressive disorder. Journal of affective disorders. 2012;136(3):1232-7.
140. Schmidt MV, Trumbach D, Weber P, Wagner K, Scharf SH, Liebl C, et al. Individual stress vulnerability is predicted by short-term memory and AMPA receptor subunit ratio in the hippocampus. The Journal of neuroscience : the official journal of the Society for Neuroscience. 2010;30(50):16949-58.
141. Chourbaji S, Vogt MA, Fumagalli F, Sohr R, Frasca A, Brandwein C, et al. AMPA receptor subunit 1 (GluR-A) knockout mice model the glutamate hypothesis of depression. FASEB journal : official publication of the Federation of American Societies for Experimental Biology. 2008;22(9):3129-34.

142. Austen JM, Sprengel R, Sanderson DJ. GluA1 AMPAR subunit deletion reduces the hedonic response to sucrose but leaves satiety and conditioned responses intact. Scientific reports. 2017;7(1):7424.
143. Vekovischeva OY, Aitta-aho T, Echenko O, Kankaanpää A, Seppälä T, Honkanen A, et al. Reduced aggression in AMPA-type glutamate receptor GluR-A subunit-deficient mice. Genes, Brain and Behavior. 2004;3(5):253-65.
144. Barbon A, Caracciolo L, Orlandi C, Musazzi L, Mallei A, La Via L, et al. Chronic antidepressant treatments induce a time-dependent up-regulation of AMPA receptor subunit protein levels. Neurochem Int. 2011;59(6):896-905.
145. Jonas P, Burnashev N. Molecular mechanisms controlling calcium entry through AMPA-type glutamate receptor channels. Neuron. 1995;15(5):987-90.
146. Jia Z, Agopyan N, Miu P, Xiong Z, Henderson J, Gerlai R, et al. Enhanced LTP in Mice Deficient in the AMPA Receptor GluR2. Neuron. 1996;17(5):945-56.
147. Seese RR, Chen LY, Cox CD, Schulz D, Babayan AH, Bunney WE, et al. Synaptic Abnormalities in the Infralimbic Cortex of a Model of Congenital Depression. The Journal of Neuroscience. 2013;33(33):13441-8.
148. Cieri F, Esposito R, Cera N, Pieramico V, Tartaro A, di Giannantonio M. Late-Life Depression: Modifications of Brain Resting State Activity. Journal of geriatric psychiatry and neurology. 2017;30(3):140-50.
149. Ben-Shimol E, Gass N, Vollmayr B, Sartorius A, Goelman G. Reduced connectivity and inter-hemispheric symmetry of the sensory system in a rat model of vulnerability to developing depression. Neuroscience. 2015;310:742-50.
150. Qi H, Ning Y, Li J, Guo S, Chi M, Gao M, et al. Gray matter volume abnormalities in depressive patients with and without anxiety disorders. Medicine. 2014;93(29):e345.
151. Boyce-Rustay JM, Holmes A. Genetic Inactivation of the NMDA Receptor NR2A Subunit has Anxiolytic- and Antidepressant-Like Effects in Mice. Neuropsychopharmacology. 2006;31(11):2405-14.
152. Ganguly P, Holland FH, Brenhouse HC. Functional Uncoupling NMDAR NR2A Subunit from PSD-95 in the Prefrontal Cortex: Effects on Behavioral Dysfunction and Parvalbumin Loss after Early-Life Stress. Neuropsychopharmacology. 2015;40(12):2666-75.
153. Sun H, Jia N, Guan L, Su Q, Wang D, Li H, et al. Involvement of NR1, NR2A different expression in brain regions in anxiety-like behavior of prenatally stressed offspring. Behavioural Brain Research. 2013;257:1-7.
154. Wieck A, Andersen SL, Brenhouse HC. Evidence for a neuroinflammatory mechanism in delayed effects of early life adversity in rats: Relationship to cortical NMDA receptor expression. Brain, Behavior, and Immunity. 2013;28:218-26.
155. Jacobs SA, Tsien JZ. Overexpression of the NR2A subunit in the forebrain impairs long-term social recognition and non-social olfactory memory. Genes, Brain & Behavior. 2014;13(4):376-84.
156. Cui Z, Feng R, Jacobs S, Duan Y, Wang H, Cao X, et al. Increased NR2A:NR2B ratio compresses long-term depression range and constrains long-term memory. Scientific reports. 2013;3:1036.
157. Marazziti D, Consoli G, Picchetti M, Carlini M, Faravelli L. Cognitive impairment in major depression. European journal of pharmacology. 2010;626(1):83-6.
158. Fritts ME, Asbury ET, Horton JE, Isaac WL. Medial prefrontal lesion deficits involving or sparing the prelimbic area in the rat. Physiology & Behavior. 1998;64(3):373-80.
159. Li L, Shao J. Restricted lesions to ventral prefrontal subareas block reversal learning but not visual discrimination learning in rats. Physiology & Behavior. 1998;65(2):371-9.
160. Magee JC. Dendritic integration of excitatory synaptic input. Nature reviews Neuroscience. 2000;1(3):181-90.
161. Selemon LD, Goldman-Rakic PS. Common cortical and subcortical targets of the dorsolateral prefrontal and posterior parietal cortices in the rhesus monkey: evidence for a distributed neural network subserving spatially guided behavior. The Journal of neuroscience : the official journal of the Society for Neuroscience. 1988;8(11):4049-68.

162. Cotrena C, Branco LD, Shansis FM, Fonseca RP. Executive function impairments in depression and bipolar disorder: association with functional impairment and quality of life. Journal of affective disorders. 2016;190:744-53.
163. Srinivasan L, Asaad WF, Ginat DT, Gale JT, Dougherty DD, Williams ZM, et al. Action Initiation in the Human Dorsal Anterior Cingulate Cortex. PLoS ONE. 2013;8(2):e55247.
164. Brody AL, Saxena S, Mandelkern MA, Fairbanks LA, Ho ML, Baxter LR. Brain metabolic changes associated with symptom factor improvement in major depressive disorder. Biol Psychiatry. 2001;50(3):171-8.
165. Sala N, Musazzi L, Di Grigoli G, Tornese P, Sala F, Valtorta S, et al. Acute stress induces rapid region-specific changes in brain energy consumption and synaptic glucose metabolism. Eur Neuropsychopharmacol. 2016;26(s2):S624-S5.
166. Lee J, Yan Z. REGULATION OF STRESS-INDUCED CHANGES IN PFC SYNAPTIC FUNCTION BY HDAC6. J Invest Med. 2011;59(4):724-.
167. Campioni MR, Xu M, McGehee DS. Stress-induced changes in nucleus accumbens glutamate synaptic plasticity. Journal of Neurophysiology. 2009;101(6):3192-8.
168. Gos T, Bock J, Poeggel G, Braun K. Stress-induced synaptic changes in the rat anterior cingulate cortex are dependent on endocrine developmental time windows. Synapse (New York, NY). 2008;62(3):229-32.
169. Ren JQ, Aika Y, Heizmann CW, Kosaka T. Quantitative analysis of neurons and glial cells in the rat somatosensory cortex, with special reference to GABAergic neurons and parvalbumin-containing neurons. Experimental Brain Research. 1992;92(1):1-14.
170. Timmermans W, Xiong H, Hoogenraad CC, Krugers HJ. Stress and excitatory synapses: From health to disease. Neuroscience. 2013;248:626-36.
171. Ericsson C, Peredo I, Nister M. Optimized protein extraction from cryopreserved brain tissue samples. Acta oncologica (Stockholm, Sweden). 2007;46(1):10-20.
172. Lee H-G, Jo J, Hong H-H, Kim KK, Park J-K, Cho S-J, et al. State-of-the-art housekeeping proteins for quantitative western blotting: Revisiting the first draft of the human proteome. PROTEOMICS. 2016;16(13):1863-7.
173. Goasdoue K, Awabdy D, Bjorkman ST, Miller S. Standard loading controls are not reliable for Western blot quantification across brain development or in pathological conditions. ELECTROPHORESIS. 2016;37(4):630-4.
174. Moehle MS, Luduena RF, Haroutunian V, Meador-Woodruff JH, McCullumsmith RE. Regional differences in expression of β-tubulin isoforms in schizophrenia. Schizophrenia Research. 2012;135(1):181-6.
175. Bauer DE, Haroutunian V, McCullumsmith RE, Meador-Woodruff JH. Expression of four housekeeping proteins in elderly patients with schizophrenia. Journal of neural transmission. 2009;116(4):487-91.
176. Zhang R, Yang D, Zhou C, Cheng K, Liu Z, Chen L, et al. β-Actin as a loading control for plasma-based Western blot analysis of major depressive disorder patients. Analytical biochemistry. 2012;427(2):116-20.
177. Tanic N, Perovic M, Mladenovic A, Ruzdijic S, Kanazir S. Effects of aging, dietary restriction and glucocorticoid treatment on housekeeping gene expression in rat cortex and hippocampus-evaluation by real time RT-PCR. Journal of molecular neuroscience : MN. 2007;32(1):38-46.
178. Moura AC, Lazzari VM, Agnes G, Almeida S, Giovenardi M, Veiga AB. Transcriptional expression study in the central nervous system of rats: what gene should be used as internal control? Einstein (Sao Paulo, Brazil). 2014;12(3):336-41.
179. Bonefeld BE, Elfving B, Wegener G. Reference genes for normalization: a study of rat brain tissue. Synapse (New York, NY). 2008;62(4):302-9.
180. Aldridge GM, Podrebarac DM, Greenough WT, Weiler IJ. The use of total protein stains as loading controls: An alternative to high-abundance single-protein controls in semi-quantitative immunoblotting. Journal of Neuroscience Methods. 2008;172(2):250-4.

181. Chen W, Xu W-H. β-Actin as a loading control: Less than 2 μg of total protein should be loaded. ELECTROPHORESIS. 2015;36(17):2046-9.
182. Dittmer A, Dittmer J. Beta-actin is not a reliable loading control in Western blot analysis. Electrophoresis. 2006;27(14):2844-5.
183. Degasperi A, Birtwistle MR, Volinsky N, Rauch J, Kolch W, Kholodenko BN. Evaluating strategies to normalise biological replicates of Western blot data. PLoS One. 2014;9(1):e87293.